

UNIVERSITY OF BELGRADE
SCHOOL OF ELECTRICAL ENGINEERING

Jiana Jarrouj

**PERFORMANCE ANALYSIS OF
COGNITIVE TELECOMMUNICATION
SYSTEMS WITH CONTROLLED
INTERFERENCE LEVEL AND
IMPERFECT CHANNEL KNOWLEDGE**

Doctoral Dissertation

Belgrade, 2016

UNIVERZITET U BEOGRADU
ELEKTROTEHNIČKI FAKULTET

Jiana Jarrouj

**ANALIZA PERFORMANSI
KOGNITIVNIH
TELEKOMUNIKACIONIH SISTEMA
SA KONTROLISANIM NIVOOM
INTERFERENCIJE I NESAVRŠENOM
PROCENOM STANJA U KANALU**

Doktorska disertacija

Beograd, 2016

Mentor disertacije

dr Predrag N. Ivaniš, vanredni profesor,
Univerzitet u Beogradu, Elektrotehnički fakultet

Članovi komisije

dr Vesna Blagojević, docent
Univerzitet u Beogradu - Elektrotehnički fakultet

dr Marija Malnar, docent
Univerzitet u Beogradu - Saobraćajni fakultet

dr Nenad Cakić, redovni profesor
Univerzitet u Beogradu - Elektrotehnički fakultet

Datum odbrane

PERFORMANCE ANALYSIS OF COGNITIVE TELECOMMUNICATION SYSTEMS WITH CONTROLLED INTERFERENCE LEVEL AND IMPERFECT CHANNEL KNOWLEDGE

Abstract:

Cognitive Radio (CR) is an optimal solution for the scarcity that the limited spectrum resource faces due to the high demand for available spectrum bands for new wireless technologies. Cognitive radio enhances the use of the spectrum by allowing unlicensed users (secondary users) to coexist with the licensed users (primary users) under the condition that the secondary users' interference at the primary receiver is under a pre-defined threshold.

In this thesis, underlay cognitive radio system with controlled interference level is analysed when the transmit power of the secondary transmitter is also constrained. In this dissertation, the interference power generated from primary transmission and its effect on the performance of the secondary user has been studied in the form of signal to interference and noise ratio (SINR) at the secondary receiver.

Different cases of available channel state information (CSI) of the link from secondary transmitter to primary receiver have been discussed in this thesis. Perfect knowledge of CSI which is the difficult to be achieved in practical system, outdated and the worst case only statistical characteristics of the channel is available at the transmitter have been analysed when the system is under Nakagami fading distribution.

Maximal Ratio Combining (MRC) diversity technique employment at the secondary receiver is studied and compared in some special cases with the application of the orthogonal space time block codes (OSTBC) at the secondary link.

Closed form expressions of the probability density function (PDF) of SINR at the secondary receiver, outage probability in addition to the moments of SINR have been

derived for the case of no diversity and when the secondary transmitter has full and outdated knowledge of CSI, as well as for the case when MRC is applied when the available CSI is perfect, outdated and statistical. Furthermore, ergodic capacity analytical expression of the SU link is derived when MRC is applied for the case of outdated CSI as well as for the case of statistical CSI. Two limiting cases have been analysed, one when the noise at the secondary receiver is dominant as noise-limited case and the other when the interference from primary transmission is dominant as interference-limited case. It has been shown that the noise-limited system has a lower performance compared to the interference-limited one.

Performance of the primary user in the form of bit error rate (BER) has been studied practically through an experiment using two computers and two universal software radio peripherals (USRP). In this experiment, the effect of the secondary interference on the signal quality at the primary receiver has been analysed for different values of signal to noise ratio (SNR), where both the primary and secondary links use orthogonal frequency division multiplexing (OFDM) modulation.

Keywords: Bit error rate, co-channel interference, cognitive radio, ergodic capacity, imperfect channel state information, MRC, Nakagami fading, OFDM, outage probability, signal to interference and noise ratio.

Scientific field: Telecommunications.

Special topic: Cognitive radio.

ANALIZA PERFORMANSI KOGNITIVNIH TELEKOMUNIKACIONIH SISTEMA SA KONTROLISANIM NIVOOM INTERFERENCIJE I NESAVRŠENOM PROCENOM STANJA U KANALU

Rezime

Kognitivni radio (*Cognitive Radio*, CR) predstavlja optimalno rešenje za danas prisutan problem nedostatka slobodnih spektralnih resursa, nastalih usled visokih zahteva korisnika za korišćenjem novih bežičnih tehnologija i dostupnim novim opsezima učestanosti. Kognitivni radio omogućava efikasnije korišćenje opsega tako što dopušta nelicenciranim korisnicima (sekundarnim korisnicima) da koegzistiraju sa licenciranim korisnicima (primarnim korisnicima), pod uslovom da je interferencija koju stvara sekundarni korisnik na strani primarnog prijemnika niža od unapred definisanog praga.

U okviru ove disertacije analiziran je kognitivni radio sistem sa kontrolisanim nivoom interferencije, kod koga je emitovana snaga sekundarnog predajnika takodje ograničena. Snaga interferencije generisana od strane primarnog predajnika i njen efekat na performanse sekundarnog korisnika proučavana je kroz analizu odnosa snage signala, i ukupne snage interferencije i šuma (SINR, *Signal to Interference and Noise Ratio*) na strani sekundarnog prijemnika.

Razmatrani su različiti slučajevi raspoloživih informacija o stanju kanala od sekundarnog predajnika do primarnog prijemnika. Analiziran je slučaj kada je dostupna savršena informacija o stanju u kanalu, koju je teško postići u praktičnim sistemima, zatim slučaj kada je informacija o stanju u kanalu zastarela, kao i najgori slučaj kada su predajniku dostupne samo statističke karakteristike kanala. Svi navedeni slučajevi analizirani su za slučaj Nakagami fedinga u propagacionom okruženju.

Proučavana je primena tehnike kombinovanja sa maksimalnim odnosom (*Maximal Ratio Combining*, MRC) na sekundarnom prijemniku i izvršeno je poređenje

sa nekim posebnim slučajevima primene ortogonalnih prostorno-vremenskih blok kodova (*Orthogonal Space Time Block Codes*, OSTBC) na sekundarnom linku.

Izvedeni su izrazi u zatvorenom obliku za funkciju gustine verovatnoće (*Probability Density Function*, PDF), verovatnoću otkaza, kao i momente odnosa SINR na sekundarnom prijemniku. Navedeni izrazi izvedeni su za slučaj kada diverzitet nije primenjen i sekundarnom predajniku je dostupno savršena ili zastarela CSI. Osim toga, izrazi su izvedeni i za slučaj kada je primenjena MRC tehnika kombinovanja na sekundarnom prijemniku i slučajeve kada je dostupna savršena, zastarela ili statistička informacija o stanju u kanalu. Dalje, analitički izraz za ergodični kapacitet sekundarnog linka na kojem je primenjena MRC tehnika izveden je za slučajeve dostupne zastarele, kao i slučaj dostupne statističke informacije o stanju u kanalu. Takođe, analizirana su i dva granična slučaja: prvi kada je na ulazu u sekundarni prijemnik dominantan uticaj šuma i drugi slučaj kada je na ulazu u sekundarni prijemnik dominantan uticaj interferencije koja potiče od strane primarnog predajnika. Pokazano je da sistem kod kojeg je dominantan uticaj šuma postiže lošije performanse u poredjenju sa sistemom kod kojeg je dominantan uticaj interferencije.

Korišćenjem USRP (*Universal Software Radio Peripherals*) platforme i računara izvršena je i praktična analiza performansi primarnog korisnika. Razmatran je slučaj kada i primarni i sekundarni korisnik primenjuju modulaciju sa većim brojem ortogonalnih podnosilaca (*Orthogonal Frequency Division Multiplexing*, OFDM). Kroz praktičnu primenu eksperimenta analiziran je uticaj interferencije od strane sekundarnog predajnika na kvalitet signala primarnog prijemnika i određena je odgovarajuća verovatnoća greške po bitu (*Bit Error Rate*, BER) za različite vrednosti odnosa snage signala i snage šuma.

Ključne reči: Ergodični kapacitet, kanalna interferencija, kognitivni radio, MRC, Nakagamijev fading, nesavršena informacija o stanju u kanalu, odnos snage signala i snage interferencije i šuma, OFDM, verovatnoća greške po bitu, verovatnoća otkaza.

Naučna oblast: Telekomunikacije.

Uža naučna oblast: Kognitivni radio.

Contents

1. Introduction	1
<i>1.1 Cognitive Radio Concept.....</i>	<i>4</i>
<i>1.2 Main Functions of Cognitive Radio.....</i>	<i>7</i>
1.2.1 Spectrum Sensing	7
1.2.2 Spectrum Decision.....	7
1.2.3 Spectrum Mobility	8
1.2.4 Spectrum Sharing	8
<i>1.3 Spectrum Access Technique.....</i>	<i>9</i>
1.3.1 Interweave Spectrum Sharing (Interference Avoidance):	9
1.3.2 Overlay Spectrum Sharing (Interference Mitigating Behaviour):	11
1.3.3 Underlay Spectrum Sharing (Interference Controlling Behaviour): ..	12
<i>1.4 Applications of Cognitive Radio.....</i>	<i>13</i>
1.4.1 Military Usage	13
1.4.2 IEEE 802.22, WRAN	14
1.4.3 Cognitive Cellular Relays.....	14
1.4.4 Cognitive Femtocell	15
1.4.5 Emergency Networks	16
2. Fundamentals in wireless communication systems and diversity techniques	17

2.1	<i>Channel</i>	18
2.1.1	Fading Channel Models.....	19
2.1.2	Channel State Information.....	21
2.2	<i>Channel Capacity</i>	22
2.2.1	Ergodic Capacity.....	24
2.2.2	Outage Capacity and Outage Probability.....	25
2.3	<i>Resource Allocation and Power Control</i>	26
2.4	<i>Diversity Techniques</i>	28
2.4.1	Maximal Ratio Combining (MRC).....	29
2.4.2	Alamouti Orthogonal Space Time Block Codes (OSTBC).....	31
3.	Statistical properties of spectrum sharing systems with co-channel interference	34
3.1	<i>Cognitive Radio System Model with Perfect CSI</i>	37
3.1.1	Probability Density Function of SINR.....	40
3.1.2	Outage Probability of SINR.....	43
3.1.3	Moments of SINR.....	49
3.2	<i>Cognitive Radio System Model with Outdated CSI</i>	50
3.2.1	Probability Density Function of SINR.....	53
3.2.2	Outage Probability of SINR.....	55
3.2.3	Moments of SINR at the SU-Rx.....	59
	<i>Appendix 3 – A</i>	63
	<i>Appendix 3 – B</i>	64
	<i>Appendix 3 – C</i>	65
4.	Spectrum sharing systems with co-channel interference and MRC diversity technique	66
4.1	<i>Cognitive Radio System with MRC Diversity for Perfect CSI</i>	68
4.1.1	Statistical Characterizations of SINR with MRC.....	69
4.1.2	Statistical Characterizations of SIR with OSTBC.....	71

4.2	<i>Cognitive Radio System with MRC Diversity for Outdated CSI</i>	76
4.2.1	Statistical Characterizations of SINR with MRC and Outdated CSI .	76
4.3	<i>Cognitive Radio System with MRC Diversity for Statistical CSI</i>	81
4.3.1	Statistical Characterizations of SINR with MRC with Statistical CSI	83
5.	Ergodic Capacity of cognitive radio system with co-channel interference and MRC diversity for imperfect CSI	89
5.1	<i>Ergodic Capacity of Cognitive Radio System with MRC Diversity for outdated CSI</i>	91
5.1.1	Ergodic Capacity for Interference-limited System with OSTBC for Perfect CSI	99
5.2	<i>Ergodic Capacity of Cognitive Radio System with MRC Diversity for Statistical CSI</i>	100
	<i>Appendix 5 – A</i>	103
	<i>Appendix 5 – B</i>	105
6.	Experimental results for OFDM-based cognitive radio	107
6.1	<i>OFDM Characteristics</i>	109
6.2	<i>OFDM-based Cognitive Radio</i>	112
6.2.1	Hardware: Characteristics of USRP	114
6.2.2	System Model	115
6.2.3	Coexistence of Primary and Secondary Users (OFDM)	117
7.	Conclusion	122
	References	125

List of Figures

<i>Figure 1.1 – Ericsson report for outlook of connected devices.....</i>	<i>2</i>
<i>Figure 1.2 – Measurement of 0-6 GHz spectrum utilization at Berkeley Wireless Research Centre[9]</i>	<i>3</i>
<i>Figure 1.3 – Spectrum hole concept.</i>	<i>10</i>
<i>Figure 1.4 – Interweave spectrum sharing.....</i>	<i>10</i>
<i>Figure 1.5 – Overlay spectrum sharing.....</i>	<i>11</i>
<i>Figure 1.6 – Interference temperature concept.</i>	<i>12</i>
<i>Figure 1.7 – Underlay spectrum sharing.</i>	<i>13</i>
<i>Figure 1.8 – IEEE 802.22, WRAN architecture.</i>	<i>14</i>
<i>Figure 1.9 – Proposed cognitive cellular relays network [36].</i>	<i>15</i>
<i>Figure 1.10 – Proposed cognitive femtocell network [40].....</i>	<i>16</i>
<i>Figure 2.1 – Path loss, slow and fast fading versus distance [42]......</i>	<i>19</i>
<i>Figure 2.2 – Capacity of AWGN with Bandwidth and Power Limited Regimes.</i>	<i>24</i>
<i>Figure 2.3 – MRC structure.....</i>	<i>30</i>
<i>Figure 2.4 – Effect of MRC on the channel capacity.....</i>	<i>31</i>
<i>Figure 2.5 – Transmit diversity vs. receive diversity.</i>	<i>33</i>
<i>Figure 3.1 – Cognitive radio system model with co-channel interference.</i>	<i>37</i>

Figure 3.2 – Outage probability for noise and interference limited cases when $m_2=m_3=3$, $\lambda_i=1/m_i$ and $P_m=10$ for various values of SINR-threshold and m_1	46
Figure 3.3 – Outage probability in the presence and absence of noise when $m_1=m_2=2$, $\lambda_i=1/m_i$, $P_m=10$, $\rho=6\text{dB}$ for different values of co-channel interference and m_3	47
Figure 3.4 – Outage probability for different values of P_m and m_2 , when $m_1=m_3=2$, $\lambda_i=1/m_i$, $P_{PU}=1$ and $\rho=0\text{dB}$	48
Figure 3.5 – Outdated CSI concept.	50
Figure 3.6 – Dependence of protection coefficient for various values of m_2 and constraint Q_p when $\lambda_2=1/m_2$, $P_m=10\text{dB}$ and $P_o=0.01$	57
Figure 3.7 – Outage probability for outdated CSI when $m_i=5$, $\lambda_i=1/m_i$, $P_{PU}=\sigma^2=0.5$, $\rho=6\text{dB}$ and various values of R and P_o	58
Figure 3.8 – Mean value of SINR for various values of P_m and INR when $m_i=2$, $\lambda_i=1/m_i$, $k_o=1$, and $P_{PU}+\sigma^2=1$	61
Figure 3.9 – Amount of fading for SINR, $m_i=2$, $\lambda_i=1/m_i$, $P_m=5$, $P_{PU}+\sigma^2=1$	62
Figure 4.1 – Spectrum sharing system model with co-channel interference and receiving MRC diversity technique.....	68
Figure 4.2 – Spectrum sharing system model with co-channel interference with OSTBC.....	71
Figure 4.3 – PDF of SIR for Alamouti code scheme and MRC diversity at SU-Rx, $\lambda_1=1/6$, $\lambda_2=1/4$, $\lambda_3=1/2$	74
Figure 4.4 – PDF of SIR for Alamouti code scheme and MRC diversity at SU-Rx, $\lambda_i=1/m_i$	74
Figure 4.5 – Comparison between Alamouti and MRC.	75
Figure 4.6 – Outage probability for the case of outdated CSI, MRC diversity with $n_R=1$ or $n_R=2$ antennas, $P_m=20$, $\rho=0\text{dB}$, and various values of P_{PU} , with and without noise.....	80
Figure 4.7 – Outage probability vs. protection coefficient, outdated CSI, $P_m=10$, $\rho=0\text{dB}$, $P_{PU}=4$, $Q_p=2\text{dB}$ or 4dB , $\sigma^2=1$ and $m_i=5$ ($i=1, 2, 3$) for different number of receive antennas n_R . 81	

Figure 4.8 – Outage probability for the case of statistical CSI, MRC diversity with $n_R=2$, $m_1=m_3=2$, $P_{PU}=4$ and different values of permitted interference probability.....	85
Figure 4.9 – Protection factor for various values of m_2 and interference outage probability at the link from SU-Tx to PU-Rx.	85
Figure 4.10 – Outage Probability for the case of statistical CSI, $P_o^{th}=10^{-2}$, MRC diversity with $n_R=1$ or $n_R=2$ antennas, $P_m=5$, $m_3=m_2=3$ and $m_1=2$ or $m_1=3$	86
Figure 4.11 – Outage capacity vs. peak interference power Q_p for the case of the perfect CSI, MRC diversity with $n_R=2$ antennas, $P_m=20$, $P_{PU}=5$, $m_1=m_3=2$, $m_2=5$, and different values of the interference probability.....	87
Figure 5.1 – Ergodic capacity vs. Q_p for the case of outdated CSI, MRC diversity with $n_R=1$ or $n_R=4$ antennas, $P_m=5$, $P_{PU}=1$, and $m_2=2$	96
Figure 5.2 – Impact of noise on ergodic capacity for outdated CSI with MRC diversity $n_R=1$, and $n_R=5$, when $P_{PU}=1$, $P_m=5$, $m_1=2$, $m_2=3$, and $m_3=5$	97
Figure 5.3 – Comparison of ergodic capacities for noise-limited and interference-limited cases with MRC diversity with $n_R=1, 2, 4$ receive antennas for the case of outdated CSI.	98
Figure 5.4 – Comparison of ergodic capacity for Alamouti and MRC for interference-limited case.....	100
Figure 5.5 – Impact of statistical CSI on the ergodic capacity of the spectrum sharing system, $n_R=2$, $P_m=10$, $P_{PU}=1$ when $\sigma^2=0$, and $P_{PU}=5$ for both cases of presence and absence of noise, $m_1=m_3=2$ and $m_2=10$	102
Figure 6.1 – multi-carrier signal spectrum.	109
Figure 6.2 – OFDM modulation and demodulation scheme.	110
Figure 6.3 – Bandwidth saving in OFDM.	110
Figure 6.4 – Orthogonality concept in OFDM.....	111
Figure 6.5 – OFDM symbol with guard interval.	112

<i>Figure 6.6 – USRP block diagram.</i>	<i>114</i>
<i>Figure 6.7 – System environment.</i>	<i>115</i>
<i>Figure 6.8 – Primary transmission data, 256 gray-scale bitmap image.....</i>	<i>116</i>
<i>Figure 6.9 – Coexistence between primary and secondary users.....</i>	<i>117</i>
<i>Figure 6.10 – Bit error rate of primary signal for the wireless channel.....</i>	<i>119</i>
<i>Figure 6.11 – Bit error rate of primary signal for the cable case.</i>	<i>120</i>

List of Tables

<i>Table 6.1 – Primary and secondary signals' (OFDM) parameters.....</i>	<i>1189</i>
<i>Table 6.2 – USRP-Tx parameters.....</i>	<i>1189</i>
<i>Table 6.3 – USRP-Rx parameters.....</i>	<i>11920</i>

List of Abbreviations

ADSL	<i>Asymmetric Digital Subscriber Line</i>
AF	<i>Amount of Fading</i>
AWGN	<i>Additive White Gaussian Noise</i>
BER	<i>Bit Error Rate</i>
CCI	<i>Co-Channel Interference</i>
CDF	<i>Cumulative Distribution Function</i>
CDMA	<i>Code Division Multiple Access</i>
CP	<i>Cyclic Prefix</i>
CSI	<i>Channel State Information</i>
DAB	<i>Digital Audio Broadcasting</i>
DoD	<i>Department of Defence</i>
DVB-T	<i>Digital Video Broadcasting TV</i>
EG	<i>Equal Gain</i>
FCC	<i>Federal Communication Commission</i>
FDF	<i>Finnish Defence Force</i>
FDMA	<i>Frequency Division Multiple Access</i>
FFT	<i>Fast Fourier Transform</i>
FICORA	<i>Finnish Communication Regulatory Authority</i>
IEEE	<i>Institute of Electrical and Electronic Engineers</i>
ISI	<i>Inter Symbol Interference</i>

ISM	<i>Industrial, Scientific and Medical</i>
ITU	<i>International Telecommunication Union</i>
LOS	<i>Line of Sight</i>
MIMO	<i>Multi-Input Multi-Output</i>
MRC	<i>Maximal Ratio Combining</i>
NTIA	<i>National Telecommunication and Information Administration</i>
Ofcom	<i>Office of Communications</i>
OFDM	<i>Orthogonal Frequency Division Multiplexing</i>
OSTBC	<i>Orthogonal Space Time Block Codes</i>
PDF	<i>Probability Density Function</i>
PSK	<i>Phase Shift Keying</i>
QoS	<i>Quality of Service</i>
SC	<i>Selective Combining</i>
SINR	<i>Signal to Interference and Noise Ratio</i>
TDD	<i>Time Division Duplexing</i>
TDMA	<i>Time Division Multiple Access</i>
UDP	<i>User Datagram Protocol</i>
UHF	<i>Ultra High Frequency</i>
USRP	<i>Universal Software Radio Peripherals</i>
UWB	<i>Ultra Wide Band</i>
VHF	<i>Very High Frequency</i>
WiMax	<i>Worldwide Interoperability for Microwave Access</i>
WLAN	<i>Wireless Local Area Networks</i>
WRAN	<i>Wireless Regional Area Network</i>

1. Introduction

Wireless Communication technology has changed the human life in a big level since it has been an essential part of the daily activities, like the social networks, instant communication, online shopping and the access to any data worldwide at any time. According to an update market forecast from ABI research, the number of the connected wireless devices (like cell phones and mobile computers) is over than 16 billion in use today, and it is expected to be over 21 billion by the year 2020 [1]. Figure 1.1 shows the growth in the number of connected devices [2], where it shows that the mobile phones are the largest growing segment among devices. In total 26 billion connected devices are expected by 2020 of which 15 billion will be phones, tablets and PCs. With this phenomenal growth of the wireless devices, wireless communication technologies and their applications are becoming more and more advanced [3], and this will create an increasing demand for radio spectrum. Unfortunately, spectrum is a finite resource which its use is carefully managed at the international and national level due to its great importance.

The use of the radio spectrum in each country is regulated by the corresponding governmental agencies such as the International Telecommunication Union (ITU) [4], which license the spectrum to individuals or organizations based on geographical regions and applications. In 1934, Federal Communication Commission (FCC) was created by US congress to manage the non-federal use of spectrum, while the National Telecommunication and Information Administration (NTIA) organization governs the federal use in USA. Moreover, the decision-making body in Finland is the Finnish Communication Regulatory Authority (FICORA) and the Office of Communications (Ofcom) is in United Kingdom.

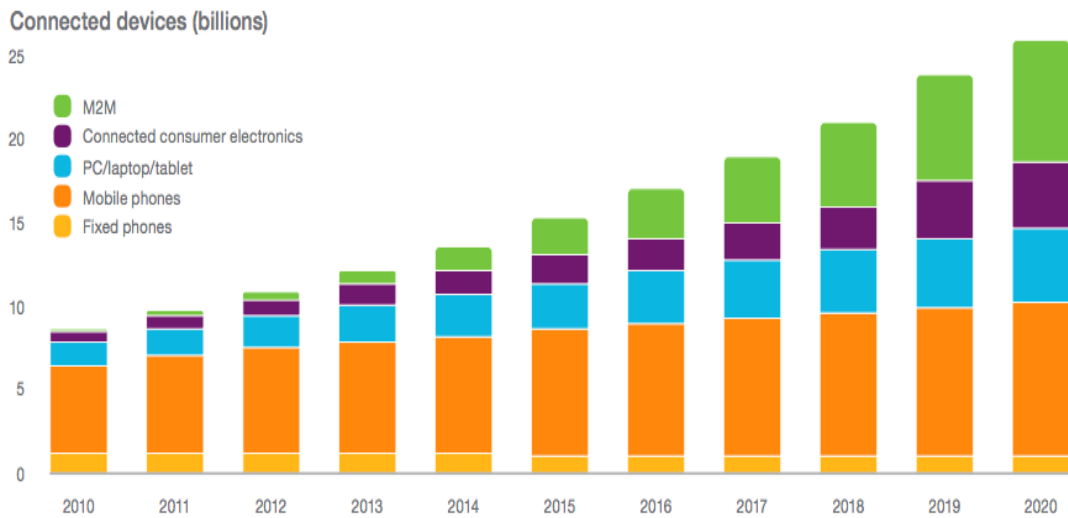


Figure 1.1 – Ericsson report for outlook of connected devices.

According to the regulations by the agencies, spectrum bands are assigned in three types:

1. No one can transmit: In this type the frequencies are reserved for radio astronomy to avoid any interference at radio telescopes.
2. Open spectrum bands: In this type anyone can transmit as long as they respect certain transmission power and other limits, such as the unlicensed Industrial, Scientific and Medical (ISM) bands. Protocol “listen before talk” is mostly used in this case.
3. Licensed bands: Only the licensed users of that band may transmit, they have exclusive rights to utilize their spectrum and no other parties can access it in order to protect them from interference.

The static allocation of frequency bands in the spectrum and attaching those to specific licensed services has many benefits, such as the simplicity and as the allocations have been made once; there is no confusion about who can use this spectrum. Furthermore, dedicating frequencies to specific uses simplifies the equipment and often leads to a better service quality.

While these allocations have many advantages, they lead to a considerable inefficiency in the spectrum utilization and generating a spectrum shortage. New wireless technologies aim to improve the data rate and the quality of service (QoS)

requirements; therefore, more and more spectrum resources are needed. While radio spectrum is theoretically unlimited, the frequency ranges that suit the commercial applications and the wireless communication technology transmission are limited. Therefore, how to utilize the spectrum in an efficient way is becoming a basic task, and attracts the attention from both industry and academy body.

Studies and researches were performed by different organizations around the world, measured the activity of the wireless technology over various allocated spectrum bands to come up with important results [5] – [9]. The Federal Communication Commission in USA [10] and the communications regulator in United Kingdom [11] have found by their researches that the average utilization of frequency bands is as low as 5%. The majority of the allocated spectrum is occupied for frequency ranges lower than 3GHZ, compared to reduced occupancy for higher frequencies (3-6 GHZ), as it is shown in Figure 1.2.

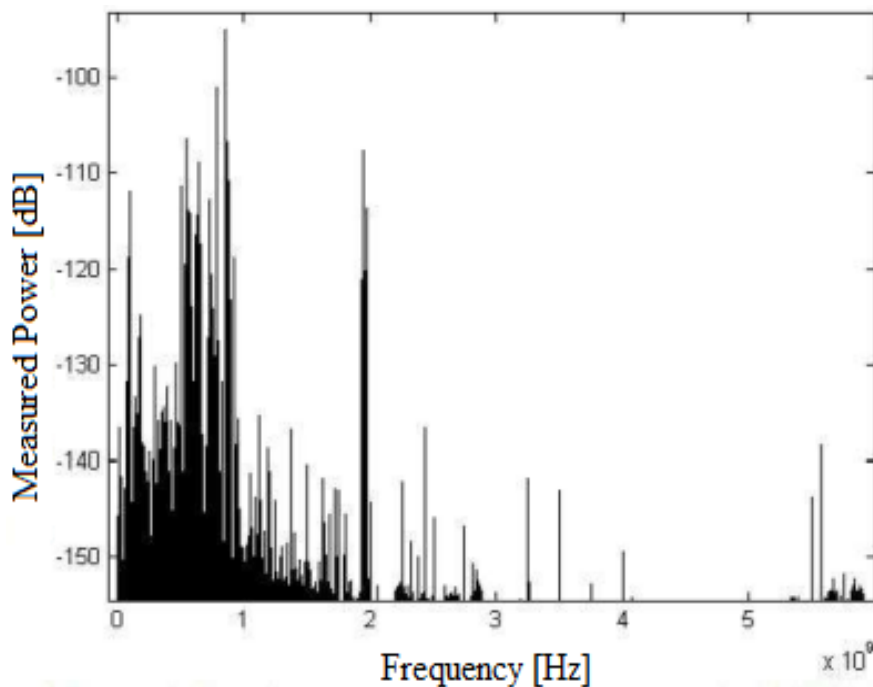


Figure 1.2 – Measurement of 0-6 GHz spectrum utilization at Berkeley Wireless Research Centre [9].

As a conclusion, these studies declared that the spectrum scarcity problem is not limited to that the available spectrum being insufficient, but that the most of the allocated spectrum is poorly utilized [8]. Some portions of the spectrum is overcrowded

(like GSM, UMTS), while other portions are almost unused (Military and amateur bands) or underutilized.

It can be seen that many frequency bands are underutilized as a result of the static spectrum allocation use which cannot manage the spectrum in an effective way. which leads to an observation that the spectrum is scarce. This emphasizes that the regulation communities need to a new dynamic spectrum allocation, which in turn leads to a better spectrum management. Such a scheme would define two types of spectrum users, the licensed user which already has a license from the agency to use a particular frequency, and the unlicensed user which could utilize the spectrum bands allocated to the licensed ones when it would not interfere with them.

Here comes the role of Cognitive Radio (CR) [12] in leading this revolution in the wireless communication technology, since it is the key for applying Dynamic Spectrum Access (DSA) instead of the existing fixed spectrum access. Dynamic spectrum access improves the spectrum utilization in three dimensions: frequency, location and time. It enables a network to opportunistically use a wide range of frequencies at points in time and space when and where they are authorized and available [13].

1.1 Cognitive Radio Concept

Cognitive radio approach is a promising solution in improving the spectrum underutilization efficiently, which will make a significant impact on the way spectrum will be managed in the future. The word “cognitive” is derived from “cognition”, which means an act or process of knowing including various processes like recognizing and analysing. While the term “radio” indicates any system communicates with other one by a modulated signal through the radio spectrum. In general, a CR system is an intelligent system that can observe data, analyse, learn and act according to that process with its environment.

The concept of cognitive radio was firstly presented by Joseph Mitola in a seminar in 1998, and then in an article by Mitola and Maguire in 1999 [12]. According to Mitola, cognitive radio is defined as “the point in which wireless personal digital assistants (PDAs) and the related networks are sufficiently computationally intelligent

about radio resources and related computer-to-computer communication to: (a) detect user communication needs as a function of user context and (b) provide radio resources and wireless services most appropriate to those needs”. However, Simon Haykin has defined cognitive radio in his paper [15] as “Cognitive radio is an intelligent wireless communication system that is aware of its surrounding environment (i.e., outside world), and uses the methodology of understanding-by-building to learn from the environment and adapt its internal states to statistical variations in the incoming radio frequency stimuli by making corresponding changes in certain operating parameters (e.g., transmit power; carrier-frequency, and modulation strategy) in real-time, with two primary objectives in mind: (a) highly reliable communication whenever and wherever needed and (b) efficient utilization of the radio spectrum”.

Besides that, CR has various definitions given by different regulation agencies. Such as the international telecommunication union which defined it as “A radio or system that senses and is aware of its operational environment and dynamically and autonomously adjust its radio operating parameters accordingly”. Formally, federal communication commission in [8] has defined the term cognitive radio as “A cognitive radio is a radio that can change its transmitter parameters based on interaction with the environment in which it operates”.

No matter how the definitions were made specific, the essential thing that the cognitive radio can obtain the best available spectrum through two main characteristics: capability and re-configurability, which can be explained as:

- Cognitive capability enables the cognitive radio to identify the unused portions of the spectrum at a specific time or location. Then, the best unused spectrum will be selected to be shared with other users without causing any harmful interference to the licensed users [13].
- Re-configurability refers to that the cognitive radio can dynamically change some parameters according to the surrounding, like radio frequency, transmission power and modulation scheme, without any modification of the hardware design [16].

Since the first mentioning of cognitive radio in [12], it has become the focus of the researches in industry, research centers as well as universities. Showing the support for the cognitive radio idea, FCC allowed the usage of the unused television spectrum by unlicensed users whenever the spectrum is free [15] and [17].

Furthermore, FCC has defined four different scenarios about how to improve spectrum access and efficiency of spectrum using cognitive radio technologies [18]:

1. A holder of a license can employ cognitive radio technologies internally within its own network to increase the efficiency of use.
2. Cognitive radio technologies can facilitate secondary markets in spectrum use, implemented by voluntary agreements between license holders and third parties.
3. Cognitive radio technologies can facilitate automated frequency coordination among licensees of co-primary services.
4. Cognitive radio technologies can be used to enable non-voluntary third party access to spectrum, for instance as an unlicensed device operating at times or in locations where licensed spectrum is not in use.

Furthermore, IEEE (Institute of Electrical and Electronic Engineers) has also supported the cognitive radio paradigm by developing a standard based on cognitive radio technology, IEEE 802.22 standard, for wireless regional area network (WRAN), which works in unused UHF-VHF TV channels [19]- [21].

Two basic types of users share the same band in cognitive radio, primary user (PU) and secondary user (SU). Primary users are the licensed ones; they have the right to access the band whenever they want without any modification in their parameters. Therefore, additional functionalities are required from the secondary users (unlicensed) to coexist with the licensed ones, where each SU must sense the spectrum and determine the presence of primary user in the available spectrum bands. Then based on the sensing information it selects the best available channel, in order to coordinate the access to this channel with other users depending on a scheduling method made by the spectrum sharing in order to use the spectrum bands effectively and prevent any collision. Furthermore, the channel must be vacated and the secondary users should switch to use other available bands as soon as the licensed user is detected, this process is the so-called spectrum mobility.

These capabilities can be realized through spectrum management functions: spectrum sensing, spectrum decision, spectrum sharing, and spectrum mobility.

Depending on the knowledge of cognitive radio system and in order to protect the primary users, three modes of cognitive radio were introduced [22]: Underlay, Overlay and Interweave.

1.2 Main Functions of Cognitive Radio

1.2.1 Spectrum Sensing

Spectrum sensing is the most important task to the realization of cognitive radio; it enables the secondary users to detect the available spectrum bands without causing any interference to the primary users. In order to determine the presence or absence of the PU transmission, different sensing techniques have been used [18] and can be classified into:

- a. Primary Transmitter Detection: several approaches are used and the easiest one is the *energy detection* in which the detector compares the received signal with a threshold to determine the presence or absence of the primary signal. But this way cannot differentiate between the signal from PU and other interference signals. Another way is the *feature detection* which has robustness to uncertainty in noise power since the modulated signal is characterized by cyclostationary behaviour, while noise signals do not have this experience [23], but on the other hand it requires a long observation time.
- b. Primary Receiver Detection which it can be said that it is the most effective way in detecting the available free bands [24], but currently is only practical in detecting the television receivers.

1.2.2 Spectrum Decision

Through the spectrum decision function, secondary user decides the best spectrum band meets the quality of service (QoS) requirement of the applications over all the available spectrum bands [25]. According to the information about the channel characterization (like interference at the primary user which helps in deriving the power

of secondary user and estimating the channel capacity) and the statistical information from primary users, the decision is taken. Spectrum decision is an important topic in cognitive radio but till now is unexplored.

1.2.3 Spectrum Mobility

Spectrum mobility is the process of changing the operating spectrum band as soon as the primary user activity in that band has been detected. The continuous allocation of spectrum is a challenging, where spectrum mobility must ensure the smooth and easy transition leading to the minimum performance degradation during a spectrum handoff. So far, there is no research effort on this topic.

1.2.4 Spectrum Sharing

Depending on the parts of the available spectrum for secondary user, the schemes can be divided into two types, namely licensed spectrum and open spectrum [13]. In the licensed spectrum, primary users have higher priorities than the secondary users which need to adjust their parameters (such as transmit power and transmission strategy) to avoid the interruption to the PUs. While in the open spectrum access, all the users have an equal right to access the channels, such as the described system in IEEE 802.15 task group 2, which focuses on the coexistence of IEEE 802.11 and Bluetooth.

According to the relationship between the secondary users, spectrum sharing policies can be divided into *cooperative* and *non-cooperative* policies. In non-cooperative spectrum sharing, secondary users make spectrum access decisions by themselves without exchanging information with other users. Therefore, due to lacking in cooperation and ignoring the interference in other cognitive radio nodes, non-cooperative solutions cannot prevent the hidden terminal problem and may result in reduced spectrum utilization. Therefore, sensing information from other secondary users is required for more accurate detection, which is referred to as cooperative policy.

On the other hand, depending on the spectrum architecture, spectrum sharing can be managed by *centralized* or *distributed* approach [26]. In centralized approach, a central point exists which collects the information about available spectrums and

controls the spectrum access. While in distributed one, the spectrum allocation is performed by each node distributively. Many studies compared the centralized and distributed policies which showed that the distributed approach can provide similar QoS as a centralized algorithm using global information [27].

1.3 Spectrum Access Technique

In cognitive radio system, the primary and secondary users coexist with each other in one network architecture. The basic design principle is that the primary users are unaffected as much as possible. There are three possible modes [22]: overlay, underlay and interweave.

1.3.1 Interweave Spectrum Sharing (Interference Avoidance):

It is often referred to this scheme as Opportunistic Spectrum Access (OSA), and it was the original motivation for cognitive radio [28]. In the interweave model, the cognitive radio monitors the radio spectrum periodically and opportunistically communicates over the spectrum holes which are defined in [29] as “a band of frequencies allocated to a primary user, but at a particular time and specific geographical location, this band is not being utilized by that user”, Figure 1.3. The spectrum, in general, is comprised of frequency bands that are most of the time unoccupied (white spaces), other bands are underutilized (grey spaces), and heavily utilized bands (black spaces). By the opportunistic access to white and grey spaces at the right time and in the right location, the spectrum utilization can be improved.

The concurrent transmission of the primary and secondary user is not allowed, therefore SU must vacate the channel and its transmission is blocked as soon as the PU reappears (this phenomenon is called the forced termination). Accurate spectrum sensing is critical to the performance, especially when signal-to-noise ratio is low.

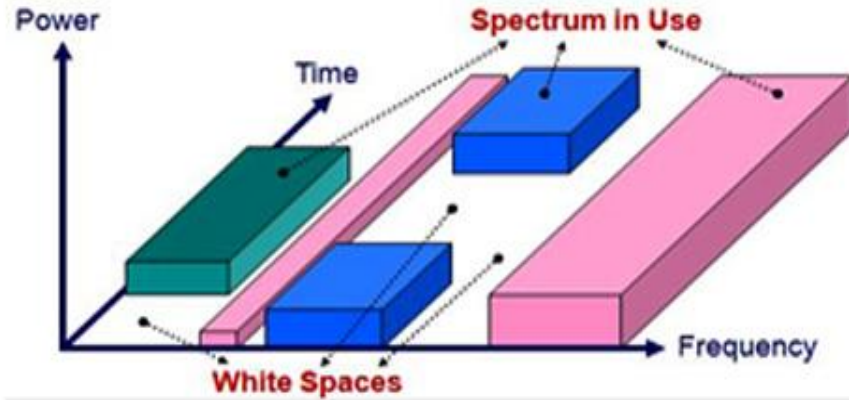


Figure 1.3 – Spectrum hole concept.

Although the interweave mode of operation results in a high spectrum efficiency, but the difficulty in timely detecting the spectrum holes limits its applicability [30]. Interweave approach is presented in Figure 1.4. Interweave systems can also be applied to networks where all users in a given band have equal priority, but existing users are treated as primary users, and new users become secondary users that cannot interfere with communications already taking place between the existing users.

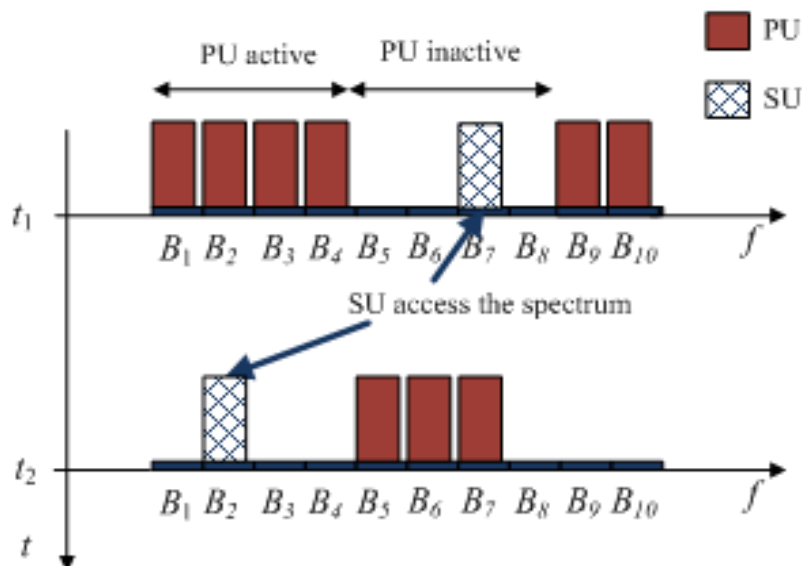


Figure 1.4 – Interweave spectrum sharing.

1.3.2 Overlay Spectrum Sharing (Interference Mitigating Behaviour):

In this mode, the cooperative transmissions between primary and secondary users are allowed, where secondary users access the unused spectrum bands by licensed users which minimize the interference to them. Beside to the channel state knowledge of the channel between primary and secondary users, additional information about the primary user and its transmission (PU's location, messages and codebook), which may be obtained through spectrum sensing, is required. Afterward, the SU uses an advanced signal processing and coding schemes (dirty paper coding [31] or Gelfand-Pinsker code [32]), where they Use part of their power for its own communication and the remainder for relying the data of primary user along with its own information to mitigate the interference. Figure 1.5 shows the concept of overlay spectrum sharing.

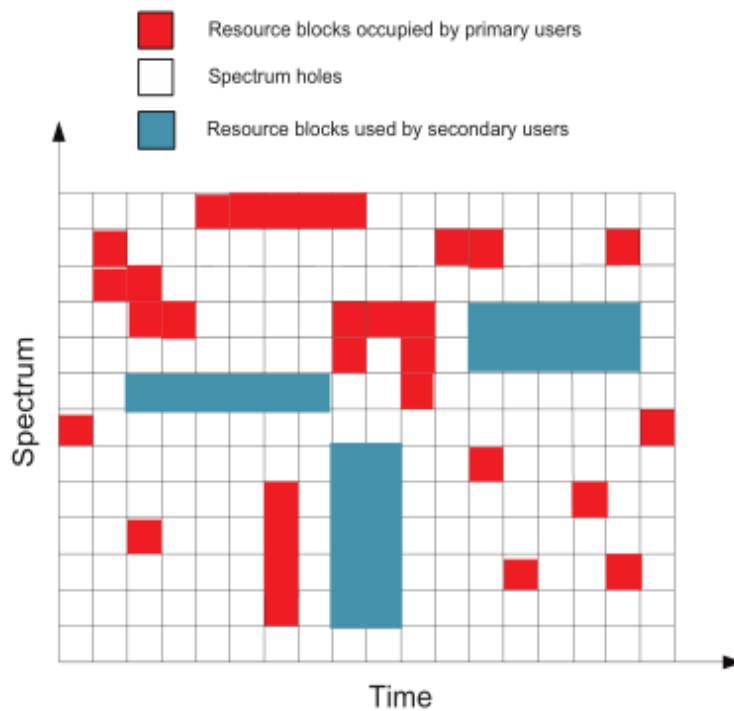


Figure 1.5 – Overlay spectrum sharing.

1.3.3 Underlay Spectrum Sharing (Interference Controlling Behaviour):

The underlay sharing refers to a simultaneous uncoordinated usage of spectrum in time and frequency domain depending on the primary receiver's acceptable interference limit. Actually, interference happens at the receiver but it can be controlled at the transmitter through the location and the radiated power. Therefore, FCC introduced a new model [33] limits the interference at the receiver by defining the interference limit that can be tolerated by the primary user, referred to it as "interference temperature", Figure 1.6. More information about using the interference temperature as a constraint to protect the primary user is given in later sections. The term *underlay* is that as secondary users spread their signals across the available bandwidth to insure that the interference caused to primary users can be treated as a wide-band background noise. However, underlay allows only short-range communication due to the power constraints. Underlay spectrum sharing concept is presented in Figure 1.7.

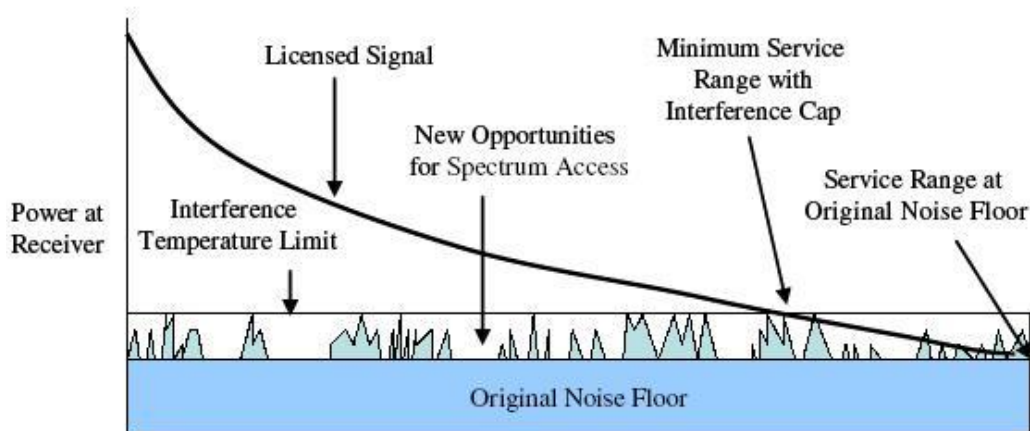


Figure 1.6 – Interference temperature concept.

While underlay, overlay and interweave are three distinct approaches to cognitive radio, hybrid schemes can also be constructed that combine the advantages of different approaches.

Although cognitive radio is a relatively new concept, there are already a number of applications proposed to implement dynamic spectrum access. The following section will highlight briefly some applications based on cognitive radio.

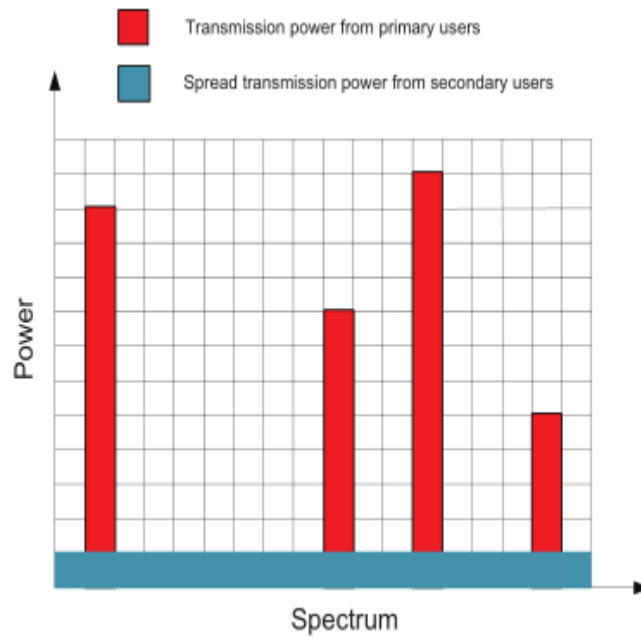


Figure 1.7 – Underlay spectrum sharing.

1.4 Applications of Cognitive Radio

1.4.1 Military Usage

Cognitive radio with its characteristics, from sensing its surrounding environment to controlling its own performances, is a must-have and appropriate technology in the defence domain in military. The military communications with cognitive radio use the available spectrum without causing any interference to the primary users and search for more transmission opportunities; moreover it can hide and avoid being interfered with any other transmission [34]. US Department of Defence (DoD) has established programs like SPEAK easy radio system to get the benefits of cognitive radio techniques. Furthermore, the Finnish Defence Force (FDF) has selected the tactical wireless IP network (TAC WIN), which includes the cognitive radio technologies, for the next generation of its wireless network.

1.4.2 IEEE 802.22, WRAN

Wireless Regional Area Network (WRAN) is a standard in development by IEEE working group 802.22 [20], which is based on Time Division Duplexing (TDD), Orthogonal Frequency Division Multiple Access (OFDMA), and opportunistic use of very high frequency/ultra-high frequency (VHF/UHF) TV bands. It implements dynamic spectrum access to deliver wireless connectivity to rural areas by utilizing the white spaces in UHF-VHF TV, which is from 54 to 862 MHz. WRAN is the first standard based on cognitive radio, many of its functionalities have been used to protect the primary users (which are here TV receivers) from the interference caused by the secondary users. The proposed WRAN architecture is given in Figure 1.8 [35], where only one base station (BS) serves multiple customer premise equipment (CPE). The coverage of each BS is typically 17 – 30 [km], with a maximum of 100 [km]. Both the customer and BS perform spectrum sensing, while customer returns sensing information to BS for central decision [36].

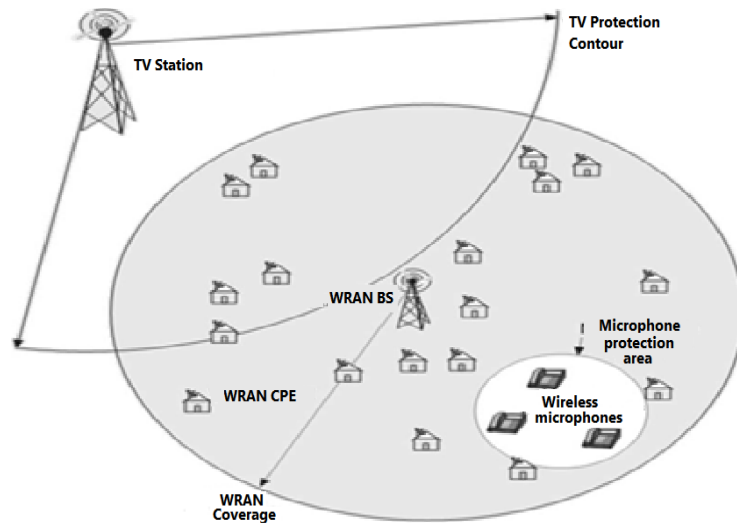


Figure 1.8 – IEEE 802.22, WRAN architecture.

1.4.3 Cognitive Cellular Relays

Cellular relay is one of the solutions which support the increasing number of subscribers per cell which leads to a difficulty in providing a sufficient signal-to-noise ratio to these users especially to those at the cell edge. Cellular relays network applies

multiple Relay Stations (RS), which forward traffic between base station (BS) and mobile station (MS), in each cell to improve the capacity and coverage area. Conventional cellular relay network utilise the licensed spectrum on the BS-RS link as well as the RS-MS link; the interference between these two links must be managed carefully. Cognitive cellular relays enhance the conventional cellular relays network applying cognitive radio [37], where implementing cognitive radio on one of the links can mitigate this interference. The link that implements cognitive radio operates on different frequency to the licensed hence causes no interference [38]. A proposed cognitive cellular relay network is presented in Figure 1.9.

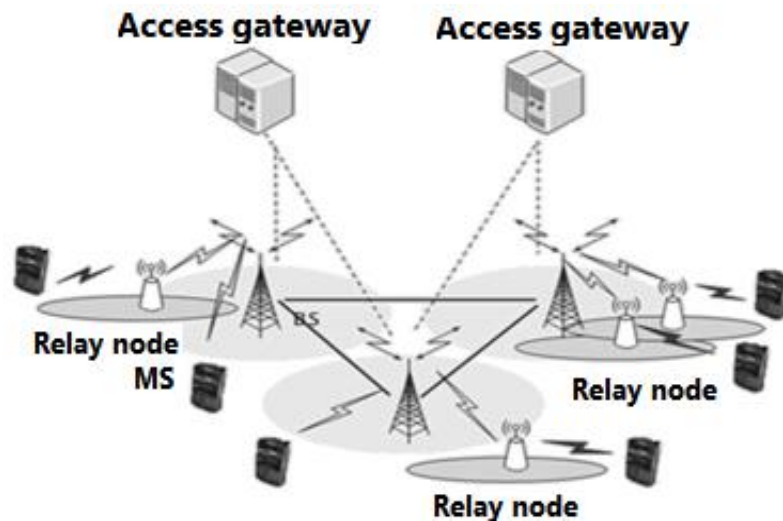


Figure 1.9 – Proposed cognitive cellular relays network [38].

1.4.4 Cognitive Femtocell

Femtocell is a small, low-power cellular base station, typically designed for enhancing the coverage of a cellular network at home or in small business office [39], which have been proposed in some companies like PicoChip driving femtocell resolution. Femtocell connects to the service provider's network by a fixed line connection (DSL, or cable), whereas it connects with the mobile station through a cellular licensed spectrum. Cognitive femtocells enhance the conventional femtocell network with cognitive radio capabilities [40]. Femtocell Base Station (FBS) performs a local sensing to find the unused spectrum by the primary users in its region and in the

neighbouring femtocells, in order to maintain the coverage and control the interference to the other macro-cells and nearby femtocells [41]. A proposed cognitive femtocell network is illustrated in Figure 1.10.

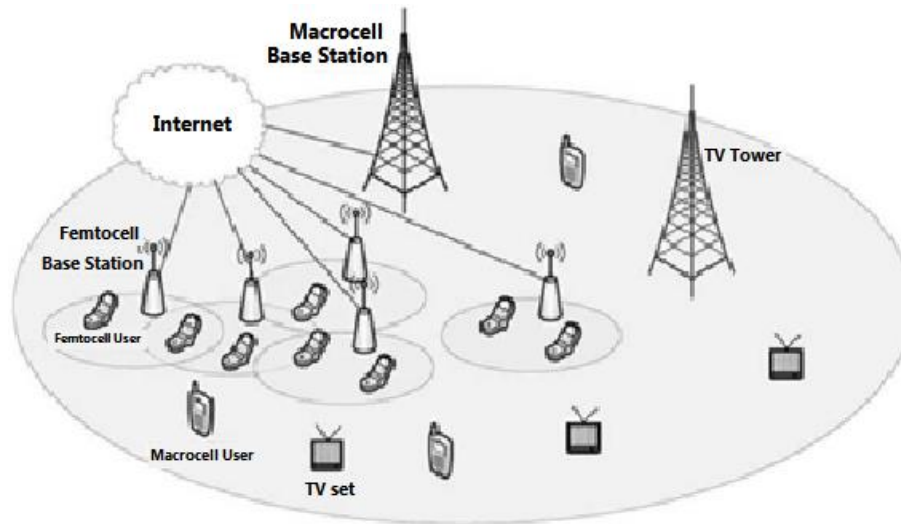


Figure 1.10 – Proposed cognitive femtocell network [42].

1.4.5 Emergency Networks

In the emerge situations, like natural disasters, accidents and wars, the important thing is the availability of a stable and clear communication between people and the safety agencies. Even though that the emergency systems have special channels to prevent the emergency services to be depended on the public network, but it is often get crowded in the sever situations because of its limited bandwidth. Cognitive Radio capabilities of sensing and detection of the unused bands in the existing networks can be put to the best use and establish an efficient emergency network. FCC has assigned a 700 [MHz] frequency band [42] for the emergency use. Moreover, mobile therapies and Wireless medical networks can be developed also with cognitive radio networks. Furthermore, applying cognitive radio with the integration of on-the-body sensors, patients can be monitored for vital signs such as temperature, pressure, blood oxygen and electrocardiogram (ECG). More about the emerging cognitive radio applications can be found in [43].

2. Fundamentals in wireless communication systems and diversity techniques

This chapter covers basic background materials, essential concepts and techniques that will be later employed in this dissertation. Fundamentals of wireless channels and fading channel models are presented, especially Nakagami fading model which is used in this study. The definition of Channel State Information (CSI) is provided with its various forms, since that one of the basic purposes of this study is analysing the performance of spectrum sharing system with controlling interference level for different cases of available CSI of the channel between the secondary transmitter and primary receiver. Furthermore, the performance of the system is evaluated by analysing the outage probability of SINR (signal to interference and noise ratio) at the secondary receiver, hence, outage probability definition is provided, in addition to the outage capacity. The basic concern in cognitive radio spectrum sharing is protecting the licensed users from any unfavourable interference; therefore resource allocation and power control under the controlled interference level is presented under different constraints applied at the transmitter and the receiver.

In the last part of this chapter, basics in diversity techniques and its importance are discussed, such as Maximum Ratio Combining (MRC) and Orthogonal Space Time Block Codes (OSTBC). In the dissertation, ergodic capacity of secondary link is studied when MRC is applied at the receiver.

2.1 Channel

In telecommunications, the channel refers to a pathway or a medium that is used to transfer information and data signal from one location to another, which in turn can use two types of media: cable (twisted-pair wire, cable and fiber-optic cable) and broadcast (microwave, satellite, radio and infrared). In order to have a better understanding of wireless channel, it is necessary to study its characteristics and variation over time and over frequency. In free-space channel, the signal follows one path and arrives at the receiver with a little attenuation, but it is not the same case for the practical channel, where the signal undergoes many changes through its travel: reflects, diffracts, and scatters from many obstacles presented in its way. The combination of the different signal pathways is termed as multipath fading or multipath propagation. These fading phenomena can be classified into two main groups known as large scale fading and small scale fading.

Large-scale fading concept is used to describe the signal level at the receiver after traveling over a large area, where the fading in this type is mainly caused by two effects: path loss where the loss in the signal power occurs because of the distance between the transmitter and receiver according to the type of the environment (rural, urban), and shadowing which occurs when large objects such as buildings block the signal and causes a permanent decrease in the power in that regions.

While the small-scale fading concept is used to describe the signal levels at the receiver after standing up to obstacles near the receiver. The common effect on the signal in this case is the Doppler shift, which is the change in the signal frequency when the receiver moves relatively to the transmitter (the received frequency is higher from the transmitted when the receiver approaches the transmitter), and according to this, the small-scale fading channels can be classified into *slow fading* where the symbol duration is smaller than the coherence time (where the coherence time is a statistical measure of the time duration in which the channel response is invariant, in other words, it is a parameter which measures the similarity of the channel response at different times) and *fast fading* where the symbol duration is larger than the coherence time, therefore, the signal changes dramatically within very small distance. In this study the channels are assumed to be in a slow fading environment.

Figure 2.1 shows the effects of path loss, shadowing and multipath fading phenomena on the received-to-transmitted power ratio as a function of the distance between the transmitter and the receiver [44].

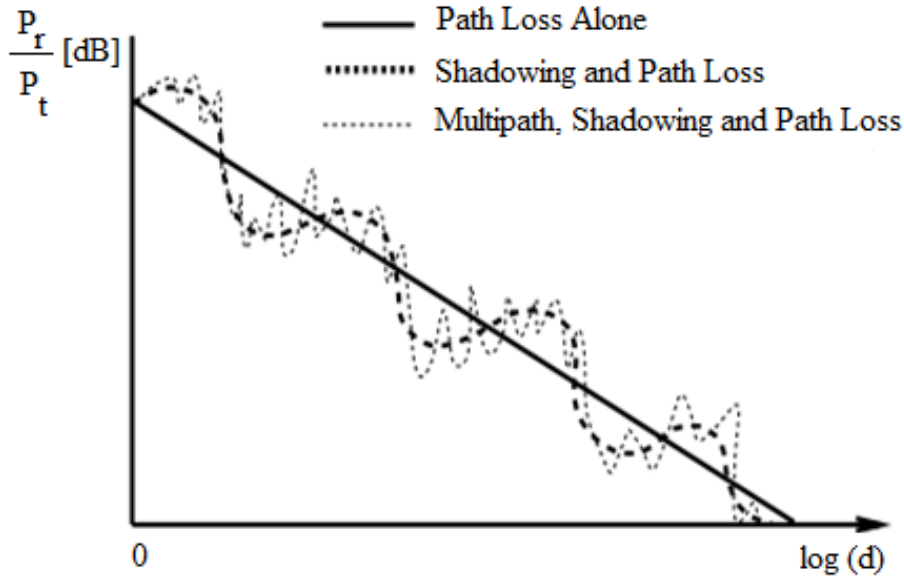


Figure 2.1 – Path loss, slow and fast fading versus distance [44].

2.1.1 Fading Channel Models

Modelling the channel propagation is as important as designing and analysing the performance of the system. As the radio-wave signal through channels undergoes many effects characterized by multipath fading and shadowing, these effects must be modelled in order to simulate the signal properly mathematically. Modelling of such fading channels is typically a complex process, many statistical models for fading channels described by their distributions are provided in [45]. In this section, a brief description about Rayleigh and Nakagami fading channel models are provided.

Rayleigh Fading Channel Model

It is used to model the channel when there is no dominant signal, which means that no line of sight (LOS) component of the signal from transmitter to receiver is existed. The received signal in this case consists of reflecting and scattering waves from different directions, which is modelled by Rayleigh distribution.

The probability density function (PDF) of Rayleigh fading distribution is given as

$$f_x(x) = \frac{x}{\Omega^2} e^{-x^2/2\Omega^2}, \quad x \geq 0, \quad (2.1)$$

where Ω is the average received signal envelop power. The envelop x is exponentially distributed with the PDF

$$f(x) = \lambda e^{-\lambda x}, \quad \lambda > 0, \quad (2.2)$$

where λ is the rate parameter.

When LOS component exists, the received signal can be expressed as random multipath components overlaying on the important signal and its PDF follows Rician distribution, which is known with its complexity. However, the long distance fading effects are described by Nakagami distribution.

Nakagami- m Fading Channel Model

Nakagami distribution describes the magnitude of the received envelope subject to a multipath propagation with a relatively larger time-delay spread. In [46], Nakagami distribution is presented as the appropriate statistical model for describing the mobile channel modelling. However, Nakagami fading model considered as the most appropriate channel modelling for several reasons, for example, Nakagami modelling is more universality as Rayleigh and Rician are special cases of it and can approximate them very well, even that it has a simpler probability density function. Furthermore, Nakagami distribution can model fading conditions more severe or less than that of Rayleigh. It is shown in [47] that Nakagami distribution the best fit for urban and indoor multipath propagation [48]. Furthermore, it offers closed form analytical expressions which are difficult to achieve otherwise [49]. In this dissertation, it is supposed that the power gains of the channels are Nakagami distributed.

The Probability density function of Nakagami distribution for a random variable channel gain α is given in [46, eq. (11)] as

$$f_\alpha(\alpha) = 2 \left(\frac{m}{\Omega} \right)^m \frac{\alpha^{2m-1}}{\Gamma(m)} e^{-\left(\frac{m}{\Omega} \alpha^2\right)}, \quad \alpha \geq 0, \quad (2.3)$$

where m is Nakagami fading parameter describes the fading degree of propagation field due to scattering and multipath interference process, which is inversely proportional to multipath fading severity, and Ω is the average received envelop power of multipath propagation, they are given in the following expressions

$$m = E^2(\alpha^2) / \text{var}(\alpha^2), \Omega = E(\alpha^2) \quad m \geq 1/2, \quad (2.4)$$

where $E(\cdot)$ is the expectation function. The function $\Gamma(\cdot)$ expresses the gamma function [50] and the squared envelop $\beta = \alpha^2$ represents the instantaneous power which is gamma distributed as follows

$$f(\beta) = \left(\frac{m}{\Omega}\right)^m \frac{\beta^{m-1}}{\Gamma(m)} e^{-\frac{m}{\Omega}\beta}, \quad \beta \geq 0. \quad (2.5)$$

Nakagami- m distribution formula represents the Rayleigh distribution with an exponentially distributed instantaneous power and one-sided Gaussian distribution as special cases of $m=1$ and $m=0.5$, respectively. For a better understanding of the Nakagami- m probability distribution function, it is important to understand the derivation of it, Nakagami- m formula is provided in more details in [48].

2.1.2 Channel State Information

Channel State Information (CSI) refers to the available knowledge of the channel properties that affect the propagation of the signal from the transmitter to the receiver and the propagation environment. The most important rule in spectrum sharing is adapting the secondary user parameters in order not to exceed the tolerable interference level at the primary user, and in order to fulfil this condition, information about the channel states especially the channel between the secondary transmitter and primary receiver are needed. The availability of CSI at the transmitter allows it to adapt its transmission signal according to the current channel conditions, which is crucial for achieving a reliable communication with high data rates. CSI can be estimated at the receiver, usually quantized, and fed back to the transmitter.

To estimate the channel condition, secondary user sends a probing signal to the primary receiver where in turn sends back the adaptations [51]. Another way in

estimation the channel state is the listening to the feedback control signals from the primary user; hence secondary user can obtain indirect information about the interference it generates and manage its parameters depending on it [52]. CSI could be in one of the following forms:

- Instantaneous CSI: the channel conditions are perfectly known and the transmission could be perfectly adapted.
- Statistical CSI: only channel statistics are available (type of fading and distribution parameters). Here the CSI can be estimated and the transmission power can be optimized.

Practically, obtaining CSI is limited by how fast the channel conditions are changing, where in fast fading systems only statistical CSI is reasonable. On the other hand, in slow fading systems instantaneous CSI can be estimated with reasonable accuracy and used for transmission adaptation for some time before being outdated to be used in estimating the system characteristics. In practical wireless communication systems, CSI is always somewhere between the two previous forms.

2.2 Channel Capacity

The channel capacity was first introduced by Shannon in 1949 [53] as the maximum data rate that could be supported by the channel without error or with a small probability of error (even with a noisy channel).

The channel inherently adds to the transmitted signal through some noise, which means an undesirable effect on the signal. This noise comes from variety of independent sources: the noise in the receiver equipment (which is known as thermal noise), atmospheric noise and random interference. Noise is independent of the signal information and the fading characterization of the channel, thus, it is usually known and modelled as Additive White Gaussian Noise (AWGN). The effect of the noise on the signal can be reduced by increasing the transmitting power, but this can lead to more power consumption, beside to that, the available channel bandwidth is limited. Based on Information Theory, the channel has a certain capacity for transmitting information; it is often measured by its bandwidth in Hertz [Hz] or its data rate in bits per second [bps].

The capacity of an AWGN channel is given as

$$C = B \log_2 (1 + SNR) \quad [\text{bits/s}], \quad (2.6)$$

where B is the transmission bandwidth and SNR is the signal-to-noise ratio. It could be normalized with unit bandwidth ($B = 1 \text{ Hz}$) and expressed by *bits/s/Hz* or bits per channel use (*bpcu*). However in some cases, the neperian logarithm (\log) is used in order to simplify calculations and avoid having the constant $\log(2)$ on the results. In this case, the capacity is expressed in nats per channel use (*npcu*).

The parameter SNR is a measure of the sensitivity performance and is usually taken at the receiver; it compares the level of the desired signal to the level of the background noise. The average transmitted signal power is denoted by \bar{P} , and the channel power gain by g , which follows a given distribution like Rayleigh or Nakagami. The availability of CSI knowledge at the transmitter and/or the receiver affects the value of the SNR as well as the capacity of the channel [54]. Let N_0 denotes the noise spectral density, and B the signal bandwidth then the average SNR, which is usually measured in decibels (dB), can be written as

$$SNR = \gamma = \bar{P}g / N_0 B \geq 0. \quad (2.7)$$

Then the capacity can be expressed as Shannon-Hartely theorem [55, eq. (15.7)]

$$C = B \log_2 \left(1 + \frac{\bar{P}}{N_0 B} \right). \quad (2.8)$$

Figure 2.2 shows the channel capacity with bandwidth and power limited regimes. When SNR is large ($SNR \gg 0\text{dB}$), the capacity is logarithmic in power and approximately linear in bandwidth and this is known as the bandwidth-limited regime. Whereas when SNR is small ($SNR \ll 0\text{dB}$, B goes to infinity), the capacity $C \approx (\bar{P}/N_0) \log_2(e)$ is linear in power but insensitive to bandwidth, this is known as the power-limited regime.

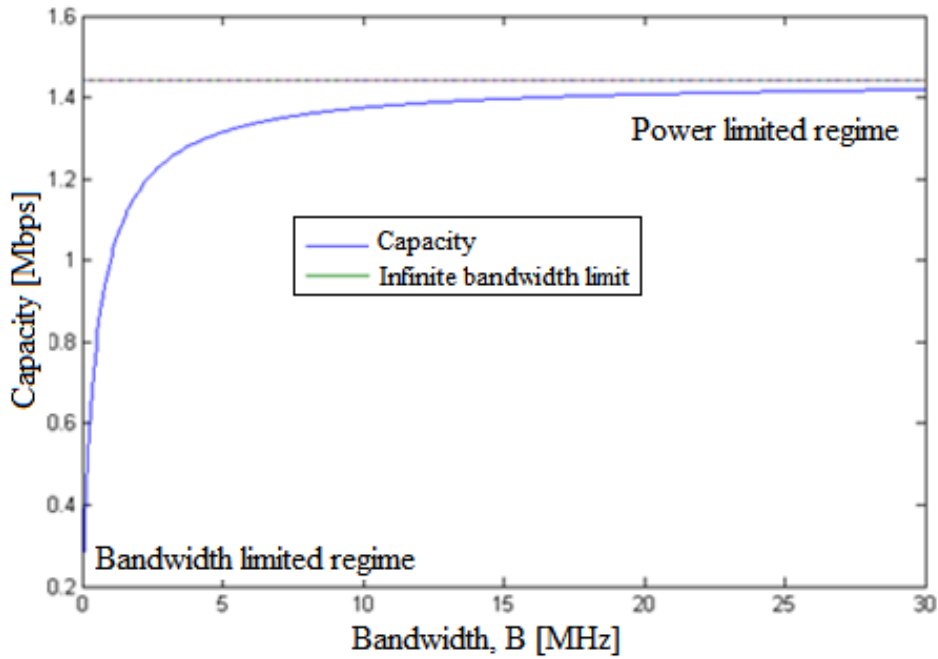


Figure 2.2 – Capacity of AWGN with Bandwidth and Power Limited Regimes.

2.2.1 Ergodic Capacity

The ergodicity aspect describes systems having the same behavior averaging over time and over space. Hence, ergodic channel is the channel where the randomness of the channel gain can be averaged out over time (like AWGN channels). In non-ergodic channel, the channel gain process is a random variable and does not change with the time (stationary) but not ergodic; the average is not very useful in non-ergodic channels since it will change with every new transmission.

Furthermore, in fading channel where its behaviour is changing dynamically and the transmission data takes place over all fading states (even in deep fades), ergodic capacity is computed. Shannon capacity of fading channel which is referred to it as ergodic capacity is given as

$$C_{erg} = \int_0^{\infty} B \log_2(1 + \gamma) p(\gamma) d\gamma, \quad (2.9)$$

where γ is the signal-to-noise ratio, and $p(\gamma)$ is the probability density function (PDF) of SNR which depends on the fading distribution in the channel. Since that in this

dissertation the basic point is analysing the effect of interference signal from primary user to the performance of secondary user in the presence of noise at the receiver, signal to interference and noise ratio (SINR) is computed instead of SNR. Ergodic capacity then will be computed using (2.9) when γ =SINR and $p(\gamma)$ is the PDF of SINR. More about analysing SINR and deriving its statistical characteristics is provided in the following chapters.

2.2.2 Outage Capacity and Outage Probability

When the channel is a slowly varying, the instantaneous signal-to-noise ratio (γ) is assumed to be constant for a large number of symbols, and then it is said that the channel is in outage. In other words, the channel goes in outage when the supported information rate falls below a threshold data rate, which is the minimum received signal-to-noise ratio γ_{\min} . Specifically, a design parameter P_{out} is selected to indicate the probability that the system cannot successfully decode the transmitted symbols. Hence the outage probability can be expressed as

$$P_{out} = p(\gamma < \gamma_{\min}). \quad (2.10)$$

For received SNRs below the threshold γ_{\min} , the received symbols cannot be successfully decoded with probability equals to 1, and the system declares an outage. As SNR increases, the outage probability decreases. In other words, the probability of outage characterizes the probability of the loss in data and it is expressed as the Cumulative Distribution Function (CDF) of the instantaneous signal-to-noise ratio or the instantaneous channel capacity.

When a system is in outage, the largest constant data rate at a certain outage probability is called outage capacity, which is the symbols that are successfully decoded with a probability equals to $(1 - P_{out})$. Outage capacity is given in the following expression

$$C_{out} = B \log_2 (1 + \gamma_{\min}). \quad (2.11)$$

2.3 Resource Allocation and Power Control

The idea of spectrum sharing systems is that secondary users can coexist with the primary users and transmit through the same spectrum, as long as their transmission does not affect the quality of the primary signal. In order to protect PU and limit the interference caused from SU and maintain an acceptable QoS of primary user, different constraints and power control schemes can be applied.

If the channel power gain for the links from SU transmitter to SU receiver and from SU-Tx to the primary receiver are denoted by y_1 , y_2 , respectively. For a given transmit power at the secondary transmitter P_{SU-Tx} , the most common ways to protect PU are by applying peak or average interference power constraints at the primary receiver. This concept has been proposed by FCC under the interference temperature model [33]. where in this model each primary user has its interference limit, which defines how much interference and noise can be tolerated in order to guarantee a certain quality of service. Interference threshold Q_p , or equivalently interference temperature T_p (where $Q_p = kBT_p$ and k is Boltzmann constant, B available bandwidth) is the direct measure of the maximal level of the interference that is primary user willing to tolerate at the input of its receiver. Interference threshold Q_p is a parameter that should usually be set by regulatory agency or other body that monitors the spectral use in the given area. Some practical implementations of considered interference temperature model are discussed in details in [56] and [57].

However, the most difficulty in the interference temperature model is to major the value of the interference limit at PU-Rx. In general the interference power constraint value depends on various parameters of PU transmission such as the type of primary receiver and characteristics of the service that PU network provides, and usually it is set by the regulatory agency or the responsible station in that given spectrum band.

Under the *peak interference power constraint* Q_p , the interference at the input of the primary receiver must be below the threshold Q_p and is given by

$$I_{PU-Rx} = P_{SU-Tx} y_2 \leq Q_p, \quad (2.12)$$

and for the average interference power constraint can be expressed as

$$E [P_{SU-Tx} y_2] \leq Q_{av}. \quad (2.13)$$

In various papers that analyse the performances of spectrum sharing systems for different system scenarios and propagation environments the maximal peak interference power threshold limits is mostly set to 20dB, while the minimum threshold value is usually set within between -20dB and 0dB [58] and [59]. Motivated by these important analyses, in this dissertation, the analysis are conducted for the same interference power limits. Furthermore, with the aim of maximizing the clarity and the visibility of important effects in the figures, the results are presented for the range [-10, 20] dB as the outage probability values are unacceptably high for the lower values of Q_p .

The effect of secondary user power transmission on primary user and how the value of peak interference power constraint can be decided depending on it is discussed in the final chapter practically using USRP platforms.

Moreover, a constraint on the transmit power of the secondary transmitter can be taken into account in its peak and average version. The *peak transmit power constraint* and the *average transmit power constraint* can be expressed in (2.14) and (2.15), respectively.

$$P_{SU-Tx} \leq P_{pk}, \quad (2.14)$$

$$E [P_{SU-Tx}] \leq P_{av}. \quad (2.15)$$

Different papers have analysed the performances of cognitive radio system for different power control schemes. In [55], the capacity of the secondary link for different fading distributions under peak and average interference power constraints was derived. The analysis has been extended to the case of average and peak transmission power constraints in [59]. Different types of capacities and outage probability were studied subject to different combinations of peak/average transmit and/or peak/average receive (interference) power constraints, where it was noticed that the SU capacity is maximized under the average over the peak transmit/interference power constraint. On the other hand, [60] has studied the performance of primary system under average and peak interference power constraints, where it has been shown that the average interference power constraints can be more advantageous than the peak constraints for

minimizing the losses in PU link capacity as well as for maximizing the cognitive radio throughput.

Another constraint can be used beside to the interference and transmit power constraints is the *outage probability constraint* [61]. In order to protect the primary user transmission, the outage probability at primary receiver should not fall below a given threshold. Subject to the outage probability constraint and average/peak transmit power constraint, new optimal power allocation strategies have been developed to maximize the outage capacity in the secondary link.

Another method for protecting the PU transmission was applied in [62], where a minimum value for *signal-to-interference and noise ratio* (SINR) at PU-Rx has been considered and any value below γ_{th} is not accepted. If the transmit power of the primary user is denoted by P_{PU-Tx} , the channel power gain of PU link is denoted by y_p and the additive white Gaussian noise variance at primary receiver is expressed by σ_p^2 , then the SINR at PU-Rx must be

$$\gamma_{PU-Rx} = \frac{P_{PU-Tx} y_p}{P_{SU-Tx} y_2 + \sigma_p^2} \geq \gamma_{th}. \quad (2.16)$$

Applying SINR constraint in order to protect PU, no need for a fixed interference constraint at PU, which could be a benefit to secondary link when the channel between PU-Tx and PU-Rx is strong enough to provide a good SINR. However, this type of constraint and what provides from relaxing in the tolerable interference constraint, in addition to a various possibilities of CSI availability for primary and secondary links at the secondary transmitter were well discussed in [62].

2.4 Diversity Techniques

In order to improve the system performance in flat fading channels, diversity is usually employed to reduce the fading depth effect on the received signal compared to the single antenna system. It is based on the fact that an individual channel experience different levels of fading and interference, where one path may undergo a deep fade, the other independent path has a strong signal. Multiple versions of the same signal may be

transmitted and/or received and combined in the receiver. Many diversity techniques are employed in wireless communication systems, like frequency diversity, time diversity, and spatial diversity. Spatial diversity is the most widely used diversity technique because it is easy to implement and it's cost effective and very simple [63] Spatial diversity can be applied at the receiver (SIMO, Receiver diversity), or at the transmitter (MISO transmit diversity), or at both transmitter and receiver to obtain multi-input multi-output (MIMO) system. The antennas should be at enough distance, ideally separated by one half or more wavelengths so that the received signals undergo independent fading. Although, wide distance is required between antennas for obtaining low correlation between channels but close distance is also required to synthesize to make a narrow beam not generating grating lobes which prevent introducing interference.

Furthermore, wireless channels suffer of co-channel interference (CCI) from other cells that share the same frequency channel, leading to distortion of the desired signal. In this dissertation, analysing the co-channel interference from primary transmission on the received signal at the secondary receiver is essential. Therefore, applying multiple antennas has been analysed in order to improve the system performance, where the average increase in signal power is proportional to the number of receive antennas [64].

Various linear combining strategies are used in order to combine the received data, such as maximal ratio combining (MRC), equal gain combining (EG) and selective combining (SC). The combining strategies can be applied to any type of diversity; it combines the independent fading versions of the signal. Mainly, the combining is applied in reception; however it is possible to be applied in transmission.

2.4.1 Maximal Ratio Combining (MRC)

In the case of maximum ratio combining, the received signals from all diversity branches are co-phased and weighted before summing. The configuration of MRC applied at the receiver with N receive antennas is shown in Figure 2.3. The weights are chosen to be proportional to the respective signals level for maximizing the average possible SNR at the receiver. The signals from strong diversity branches, which have

low level noise, are weighted more comparing to the signals from the weak branches with high level of noise.

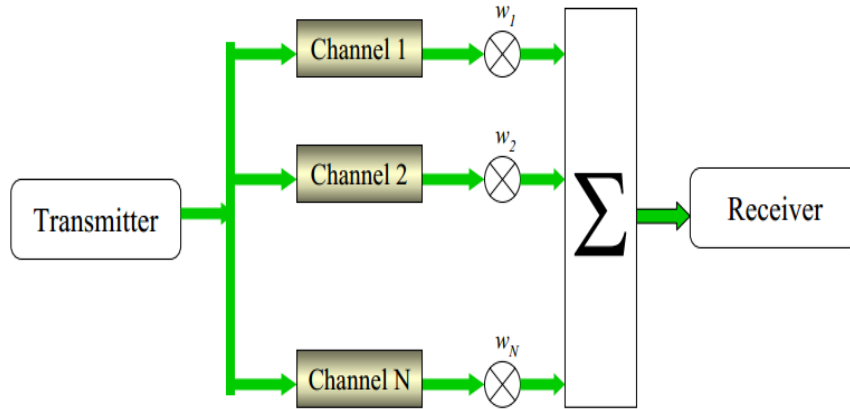


Figure 2.3 – MRC structure.

The average SNR (γ_N) of the combined signal is equal to the sum of the individual average SNRs as [65]

$$\gamma_N = \sum_{i=1}^N \bar{\gamma}_i = \sum_{i=1}^N \Gamma = N \Gamma, \quad (2.17)$$

where it is assumed that each channel has the same average SNR given as $\bar{\gamma}_i = \Gamma$. Hence, MRC can give an acceptable average SNR, even when none of the individual $\bar{\gamma}_i$ is acceptable. Figure 2.4 presents the channel quality at a receiver employed with 3 antennas after applying MRC.

Even if MRC is more complex than the other diversity combining techniques, but it has the most effective performance in achieving high SNR and minimizing the bit error rate comparing with the other techniques [66].

In cognitive radio system, in order to improving the performances of secondary user, various diversity combining techniques have been studied, like MRC and selection combining (SC) in [67]. Furthermore, ergodic capacity of system applying MRC in Nakagami fading has been derived in [68]. Performance improvement of underlay spectrum sharing under the co-channel interference effect applying MRC at the receiver with imperfect channel state information (CSI) has been studied in this work.

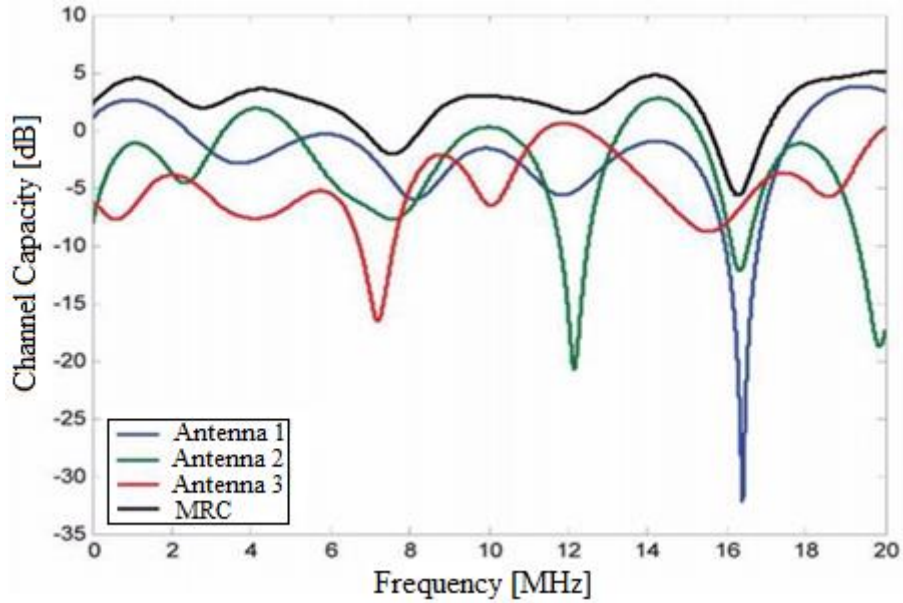


Figure 2.4 – Effect of MRC on the channel capacity.

2.4.2 Alamouti Orthogonal Space Time Block Codes (OSTBC)

Assuming a multi-input single-output (MISO) with M transmit antennas transmits a multiple versions of the signal to enable coherent combining at the receiver. The transmitter can transmit signals without any information about the channel, which is called open loop mode. Or in the other mode, closed loop mode, the receiver sends information about CSI to the transmitter to adjust its transmission. Transmit diversity uses one of the following methods: receiver-based transmit selection, transmit redundancy, and orthogonal space time block codes (OSTBC) [69], which Alamouti scheme is a special case of it where $M=2$ [70].

The pioneering work of Alamouti [67] has been a basis to create OSTBCs for more than two transmit antennas. The Alamouti code promises full diversity and full data rate in case of two transmit antennas. The key feature of this scheme is the orthogonality between the signal's vectors transmitted over the two transmit antennas. This scheme was generalized to an arbitrary number of transmit antennas by applying the theory of orthogonal design [71]. The generalized schemes are referred to as space-time block codes [69].

Orthogonal Space time block codes perform two-dimensional mapping in time and space over transmit antennas. In general form OSTBC can be seen as $(n_t \times M)$ transmission matrix, where M is the number of transmit antennas, and n_t is the number of time periods for transmission one block of coded symbols. To understand OSTBC, we will take the special case of it which is Alamouti scheme.

If we have a transmission sequence like $[x_1, x_2]$, in normal transmission, we will be sending x_1 in the first time period via all transmit antennas simultaneously, which are $M=2$, and x_2 in the second time period. However, using Alamouti, we will send during the first transmission period, the symbols x_1 and x_2 are transmitted simultaneously from antenna one and antenna two respectively. In the second transmission period, the symbol $-x_2^*$ is transmitted from antenna one and the symbol x_1^* from transmit antenna two according to the following code matrix.

$$X = \begin{bmatrix} x_1 & x_2 \\ -x_2^* & x_1^* \end{bmatrix}, \quad (2.18)$$

Where the first row represents the first transmission period and the second row represents the second transmission period. The two rows and columns of X are orthogonal to each other [72]. This property enables the receiver to detect x_1 and x_2 by a simple linear signal processing operation

$$XX^H = \begin{bmatrix} x_1 & x_2 \\ -x_2^* & x_1^* \end{bmatrix} \begin{bmatrix} x_1^* & -x_2 \\ x_2^* & x_1 \end{bmatrix} = \begin{bmatrix} |x_1|^2 + |x_2|^2 & 0 \\ 0 & |x_1|^2 + |x_2|^2 \end{bmatrix} = (|x_1|^2 + |x_2|^2) I_2, \quad (2.19)$$

where I_2 is a (2×2) identity matrix.

Figure 2.5 compares between the transmit diversity and receive diversity through MRC and Alamouti schemes through evaluating the bit error rate (BER) for Binary Phase Shift Keying (BPSK) modulation in Rayleigh fading distribution.

From simulation results, it can be seen that increasing the number of transmit antennas can provide significant performance gain. One of the most important advantages of OSTBCs is the fact that increasing the number of transmit antennas does not increase the decoding complexity substantially, due to the fact that only linear processing is required for decoding.

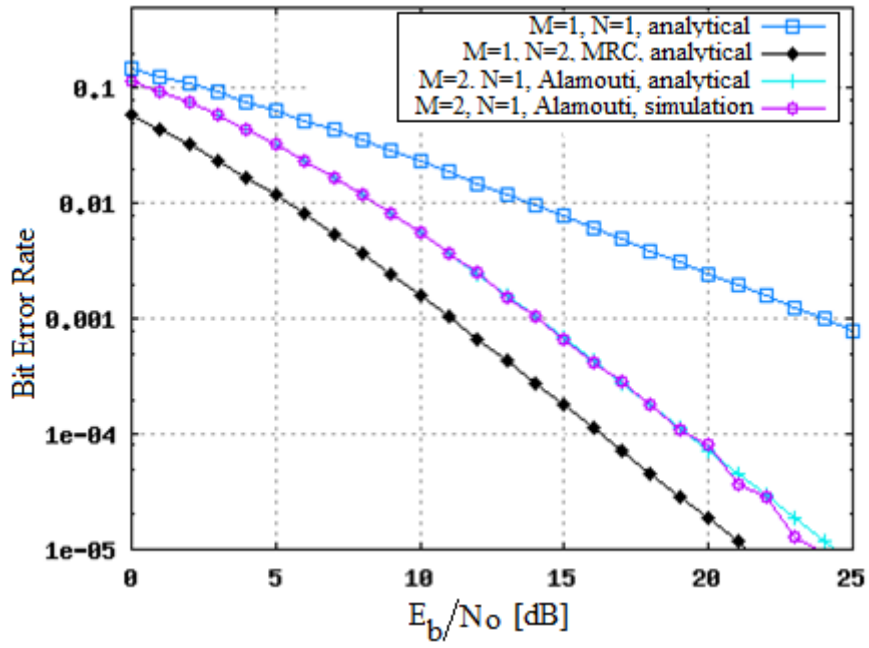


Figure 2.5 – Transmit diversity vs. receive diversity.

3. Statistical properties of spectrum sharing systems with co-channel interference

The basic idea in this chapter is analyzing the effect of the co-channel Nakagami distributed interference signal that primary user (PU) originates from to the secondary user's (SU) performances. The performance of the secondary user is studied by deriving the outage probability and the moments of the signal to interference and noise ratio at the output of secondary receiver. The derivations are done for the both cases of perfect and outdated Channel State Information (CSI) of the link between the secondary transmitter (SU-Tx) and the primary receiver (PU-Rx). Underlay spectrum sharing in cognitive radio is analyzed under both of the constraints: peak interference power constraint at the primary receiver and maximal transmission power constraint at the secondary transmitter.

In underlay concept, the secondary user can coexists with the primary user in the same band of spectrum as long as the interference caused by the secondary transmission is under a predefined threshold, in order to protect the primary user, which is also known as the interference temperature concept [33]. The received power at the primary receiver can be constrained by an average or peak interference power value (AIP or PIP, respectively). Optimal power allocation strategy for secondary user under received power constraints is analysed in [58] for different types of fading models (e.g. Rayleigh, Nakagami and log-normal fading). It is found that a constraint on the received-power is fundamentally equivalent to one on the transmitted-power. Furthermore, the work [58] analysed the secondary link performance under average and peak interference power

constraint for the single antenna primary and secondary terminals, where in the extended work [72] it is analysed for the case of asymmetric fading Rayleigh/Rician.

On the other hand, the author in [73] compared between the impact of the long-term (average) and the short-term (peak) received power constraint to the performances of secondary link. It is observed that the average interference power constraint based optimal power control performs better than the peak interference power constraint based one. Furthermore, the average interference power constraint results in larger capacities than peak one for both cognitive radio and primary system transmissions

The analysis to the case when the transmission power of the secondary user is also constrained is presented in [59], where optimal power allocation strategies have been analysed for various combination of transmit (average/peak) and received (average/peak) power constraints. The results showed a gain in the secondary capacity under the average over the peak transmit/receive power constraints.

Perfect knowledge of channel state information of the channel from SU-Tx to PU-Rx is supposed in all the previous works, furthermore, in [75] and [76] the studies were done relating on the additional channel state knowledge of the primary link. Both papers proposed a new power control strategy which serves as an alternative way to protect the primary user's transmission. Proposed strategies lead to easiness in the cognitive radio functions in addition to capacity gains for both the primary and secondary systems over the conventional policy.

Achieving the optimal system performance requires that the secondary transmitter acquires full channel state information knowledge of the link between its transmitter and primary receiver, which is used to calculate the maximum allowable transmission power in order to limit the interference caused by secondary transmitter to primary receiver. All the above studies assume perfect or full channel knowledge, which is very difficult to implement in practice even when there is cooperation between the secondary and primary users. A few recent papers address this concern by investigating the performance analysis with various forms of partial CSI available at secondary transmitter. With an assumption of perfect knowledge of CSI of the secondary link, authors in [77] studied the effect of the imperfect channel information of the link between SU-Tx and PU-Rx under average interference power constraint for Rayleigh flat-fading channels.

However the interference from the primary transmission to the secondary receiver has been ignored in all of the previous mentioned works. The impact of co-channel interference and fading to the performances of wireless communications systems is well studied for various propagation conditions and system architectures [78] – [80].

The influence of primary's transmission on the secondary link performance of underlay cognitive radio systems is analysed in [81] for the case of Rayleigh fading environment under peak received interference power constraint considering imperfect CSI knowledge case of the channel from SU-Tx to PU-Rx. Closed-form expression of secondary link capacity is derived taking into account a probability of exceeding the interference constraint at the primary receiver due to the incorrectly measured gain of the link from secondary transmitter to primary receiver.

Furthermore, the effect of outdated channel state information and corresponding power adaptation along with the optimum power allocation under the average received-power constraint is considered in [82] for the case of Rayleigh distributed fading. The power margin required to satisfy the interference outage probability at the primary user under the peak received-power constraint is provided. Outage probability of secondary link and minimizing it is studied in [83] with quantized CSI under average transmit power constraint at secondary transmitter and peak interference power constraint at the primary receiver. For analytical simplicity, the interference from the primary transmitter to secondary receiver is neglected; therefore, the derived outage probability in [83] can be taken as lower bounds on the actual outage under primary-induced interference.

However, the impact of primary signal's interference on the secondary performances for the case of Nakagami propagation is analysed in [84], but no closed-form expression for the outage probability of the signal-to-interference and noise ratio (SINR) is provided, where it is derived in [85].

Specifically in this chapter:

- Statistical analysis of signal to interference and noise ratio for the case of perfect CSI.
- Statistical analysis of signal to interference and noise ratio for the case of outdated CSI.

- Probability density function, outage probability and moments of SINR are derived in final expressions.
- Corollary cases are discussed depending on the value of the transmit power constraint compared to the peak interference power one.

3.1 Cognitive Radio System Model with Perfect CSI

A simple underlay spectrum sharing scenario is considered, where a secondary user and a licensed user (primary user) share the same narrow-band frequency with a bandwidth B for transmission. All terminals are assumed to be equipped with a single antenna as the system model is shown in Figure 3.1. A slow fading environment is assumed, where the channel changes at a rate much slower than the data rate.

All the channels have been assumed to be subjected to the same conditions. Thus, y_i denotes the fading envelopes, where $i=1, 2, 3$, in the channels between secondary transmitter and receiver SU-Rx, secondary transmitter and primary receiver PU-Rx, and between primary transmitter PU-Tx and secondary receiver, respectively.

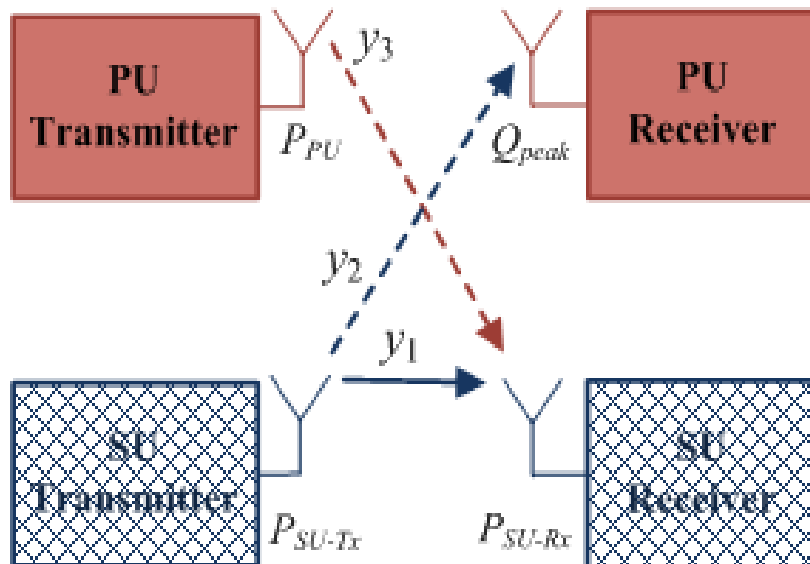


Figure 3.1 – Cognitive radio system model with co-channel interference.

In underlay spectrum sharing as it is mentioned previously, secondary user can transmit and coexist in the same band with primary user as long as the transmission of SU does not affect the quality of the transmission of PU. Secondary user transmission power is defined as P_{SU-Tx} . The interference that can be tolerated by primary user is known as the interference power constraint, Q_p . In every moment, secondary user must adapt its transmission power to fulfill the following rule

$$y_2 P_{SU-Tx} \leq Q_p. \quad (3.1)$$

At the output of secondary receiver, signal to interference and noise ratio (SINR), which is denoted as γ , is the ratio of the received signal power, P_{SU-Rx} at secondary receiver to the interference power (P_I) caused by the primary user transmission and the AWGN noise power at the receiver which has the common distribution $CN(0, \sigma^2)$ (circularly symmetric complex Gaussian variables with zero mean and variance σ^2).

The received power at the secondary user is equal to

$$P_{SU-Rx} = y_1 P_{SU-Tx}, \quad (3.2)$$

where P_{SU-Tx} fulfills the condition given in (3.1) to be equal to

$$P_{SU-Tx} = \frac{Q_p}{y_2}. \quad (3.3)$$

The transmission power of the primary user is equal to P_{PU} ; hence the transmission power from primary user multiplied by the channel power gain of the channel between primary transmitter and secondary receiver, y_3 , represents the interference power at the secondary receiver

$$P_I = P_{PU} y_3. \quad (3.4)$$

Depending on the previous expressions (3.2) and (3.3), SINR can be written as the following expression

$$\gamma = \frac{P_{SU-Rx}}{P_I + noise} = \frac{y_1 P_{SU-Tx}}{P_{PU} y_3 + \sigma^2}. \quad (3.5)$$

When the interference value is much bigger than the noise power ($P_{PU} \gg \sigma^2$), then we have an *interference-limited case* where SINR in (3.5) will be simplified into SIR as follows

$$SIR = \gamma = \frac{P_{SU-Rx}}{P_I + noise} \approx \frac{y_1 P_{SU-Tx}}{y_3 P_{PU}}. \quad (3.6)$$

On the other hand when the interference is much smaller than the noise ($P_{PU} \ll \sigma^2$), then the interference can be neglected to have a *noise-limited case*, and the expression (3.5) is simplified into SNR as

$$SNR = \gamma = \frac{P_{SU-Rx}}{P_I + noise} \approx \frac{y_1 P_{SU-Tx}}{\sigma^2}. \quad (3.7)$$

Substituting the value of secondary user transmission power (3.1) in the expression (3.5), SINR is written as

$$\gamma = \frac{y_1 (Q_p / y_2)}{P_{PU} y_3 + \sigma^2} = \frac{y_1}{y_2} \frac{Q_p}{P_{PU} (y_3 + \sigma^2 / P_{PU})}, \quad (3.8)$$

substituting $x = y_1 / (y_3 + \sigma^2 / P_{PU})$, SINR can be written in the form

$$\gamma = \frac{P_{SU-Tx}}{P_{PU}} x = \frac{Q_p}{P_{PU}} \frac{x}{y_2}. \quad (3.9)$$

In order to protect the primary user, another constraint has been applied in the studies, which is the maximum allowable transmission power of secondary transmitter, P_m . Therefore, the transmission power of secondary user is adapted according to the both constraints, the peak interference and transmission power constraints to be given in the following expression

$$P_{SU-Tx} = \min \left(P_m, \frac{Q_p}{y_2} \right), \quad (3.10)$$

in other words, it can be written as

$$P_{SU-Tx} = \begin{cases} P_m, & y_2 \leq \frac{Q_p}{P_m}, \\ \frac{Q_p}{y_2}, & y_2 > \frac{Q_p}{P_m}. \end{cases} \quad (3.11)$$

Substituting (3.11) in (3.8), SINR expression can be written as

$$\gamma = \frac{P_{SU-Tx}}{P_{PU}} x = \begin{cases} \frac{P_m}{P_{PU}} x, & y_2 \leq \frac{Q_p}{P_m}, \\ \frac{Q_p}{P_{PU}} \frac{x}{y_2}, & y_2 > \frac{Q_p}{P_m}. \end{cases} \quad (3.12)$$

For the case when the transmission power of SU-Tx is unlimited ($P_m \gg Q_p$), (3.10) will be adapted according to (3.3) and SINR in this case will be reduced to

$$\gamma = \frac{P_{SU-Tx}}{P_{PU}} x = \frac{Q_p}{P_{PU}} \frac{x}{y_2}. \quad (3.13)$$

Whereas in the region when $Q_p \gg P_m$, the system in this case presents the system with fixed (non-adaptable) transmission power where SINR reduces to

$$\gamma = \frac{P_{SU-Tx}}{P_{PU}} x = \frac{P_m}{P_{PU}} x. \quad (3.14)$$

3.1.1 Probability Density Function of SINR

It is assumed that the fading envelopes in each particular link are independent and identically distributed (i. i. d.) random variables (RVs) following the Nakagami distribution with a fading parameter m_i in the corresponding channel, where $i = 1, 2, 3$. The Probability Density Function (PDF) of the fading envelop is given as [58, eq. (14)]

$$f_{h_i}(h_i) = \frac{2h_i^{2m_i-1}}{(\lambda_i)^{m_i} \Gamma(m_i)} e^{-h_i^2/\lambda_i}, \quad h_i \geq 0. \quad (3.15)$$

where $\lambda_i = E\{h_i^2\}/m_i$ and $E\{\cdot\}$ is the expectation operator.

Whereby the previous definition of fading envelopes, the corresponding channel power gain is defined as $y_i = |h_i|^2$ and the corresponding PDF expression is given with [86, eq. (16)]

$$f_{y_i}(y_i) = \frac{y_i^{m_i-1}}{\lambda_i^{m_i} \Gamma(m_i)} e^{-y_i/\lambda_i}, \quad y_i > 0, \quad (3.16)$$

To derive the probability density function of SINR, the linear transformation of RVs [87] is applied on the two segments of (3.12) to get

$$f_\gamma(\gamma) = \frac{f_x(\gamma P_{PU} / P_m)}{P_m / P_{PU}} \int_0^{Q_p/P_m} f_{y_2}(y_2) dy_2 + \int_{Q_p/P_m}^{+\infty} \frac{f_x(\gamma P_{PU} y_2 / Q_p)}{Q_p / (P_{PU} y_2)} f_{y_2}(y_2) dy_2, \quad (3.17)$$

where $f_x(x)$ is the probability density function of the variable $x = y_1 / (y_3 + \sigma^2 / P_{PU})$ which we get it by applying the linear transformation as $x = y_1 / w$, then applying the transformation of two random variables [87, eq. (6-63)] using the substitution $z = y_1 / w$, $t = w$ to obtain the joint PDF of the variables x and w as follows

$$f_{x,w}(x, w) = |J| \times f_{y_1}(xw) f_w(w), \quad (3.18)$$

where Jacobean matrix is defines as [87, eq. (6-64)]

$$J = \begin{vmatrix} \partial(xw)/\partial x & \partial(xw)/\partial w \\ \partial w/\partial x & \partial w/\partial w \end{vmatrix} = |w|, \quad (3.19)$$

then applying the PDF of y_1 in the equation (3.18) to write the PDF of x as follows

$$\begin{aligned} f_x(x) &= \int_{\sigma^2}^{+\infty} w f_{y_1}(xw) f_w(w) dw = \int_0^{+\infty} (y_3 + \sigma^2 / P_{PU}) f_{y_1}(x(y_3 + \sigma^2 / P_{PU})) f_{y_3}(y_3) dy_3 \\ &= \frac{x^{m_1-1} e^{-x\sigma^2/(\lambda_1 P_{PU})}}{\lambda_1^{m_1} \Gamma(m_1) \lambda_3^{m_3} \Gamma(m_3)} \int_0^{+\infty} (y_3 + \sigma^2 / P_{PU})^{m_1} y_3^{m_3-1} e^{-y_3 \left[\frac{x}{\lambda_1} + \frac{1}{\lambda_3} \right]} dy_3, \end{aligned} \quad (3.20)$$

using the binomial function [88, eq. (1.111)] and the expression of incomplete gamma function in [88, eq. (8.350-2)], the PDF of x is obtained as

$$f_x(x) = \sum_{k=0}^{m_1} \binom{m_1}{k} \frac{\Gamma(k+m_3)}{\Gamma(m_1)\Gamma(m_3)} \left(\frac{\lambda_1}{\lambda_3} \right)^{m_3} \left(\frac{\sigma^2}{\lambda_1 P_{PU}} \right)^{m_1-k} \frac{x^{m_1-1} e^{-x\sigma^2/(\lambda_1 P_{PU})}}{(x + \lambda_1/\lambda_3)^{k+m_3}}. \quad (3.21)$$

It can be written in a shortcut form as follows

$$f_x(x) = \sum_{k=0}^{m_1} \alpha_k \frac{x^{m_1-1} e^{-x\sigma^2/(\lambda_1 P_{PU})}}{(x\lambda_3 + \lambda_1)^{k+m_3}}, \quad (3.22)$$

where

$$\alpha_k = \binom{m_1}{k} \frac{\Gamma(k+m_3)}{\Gamma(m_1)\Gamma(m_3)} \lambda_1^{m_3} \lambda_3^k \left(\frac{\sigma^2}{\lambda_1 P_{PU}} \right)^{m_1-k}. \quad (3.23)$$

Applying the PDF of x as it is written in (3.22) in the expression (3.17)

$$f_\gamma(\gamma) = \left(\frac{P_{PU}}{P_m} \right)^{m_1} \sum_{k=0}^{m_1} \alpha_k \frac{\gamma^{m_1-1} e^{-\frac{\gamma\sigma^2}{\lambda_1 P_m}}}{(\gamma\lambda_3 P_{PU} / P_m + \lambda_1)^{k+m_3}} \left[\frac{1}{\lambda_2^{m_2} \Gamma(m_2)} \int_0^{Q_p/P_m} y_2^{m_2-1} e^{-y_2/\lambda_2} dy_2 \right] \\ + \left(\frac{P_{PU}}{Q_p} \right)^{m_1} \frac{\gamma^{m_1-1}}{\lambda_2^{m_2} \Gamma(m_2)} \sum_{k=0}^{m_1} \alpha_k \left[\int_{Q_p/P_m}^{+\infty} y_2^{m_1+m_2-1} \frac{e^{-y_2 \left[\frac{\gamma\sigma^2}{\lambda_1 Q_p} + \frac{1}{\lambda_2} \right]}}{(\gamma y_2 \lambda_3 P_{PU} / Q_p + \lambda_1)^{k+m_3}} dy_2 \right]. \quad (3.24)$$

Using some substitutions and following the derivation steps given in Appendix 3 – A, the final PDF expression of SINR is given as follows

$$f_\gamma(\gamma) = \left(\frac{\lambda_1 P_m}{\lambda_3 P_{PU}} \right)^{m_3} \sum_{k=0}^{m_1} \binom{m_1}{k} \frac{\Gamma(k+m_3)}{\Gamma(m_1)\Gamma(m_3)} \left(\frac{\sigma^2}{\lambda_1 P_m} \right)^{m_1-k} \frac{\gamma^{m_1-1} e^{-\gamma\sigma^2/\lambda_1 P_m}}{(\gamma + \lambda_1 P_m / \lambda_3 P_{PU})^{k+m_3}} \left[1 - \frac{\Gamma(m_2, Q_p / P_m)}{\Gamma(m_2)} \right] \\ + \frac{e^{\frac{\sigma^2}{\lambda_3 P_{PU}} + \frac{\lambda_1 Q_p}{\gamma \lambda_2 \lambda_3 P_{PU}}}}{\gamma} \sum_{k=0}^{m_1} \binom{m_1}{k} \frac{\Gamma(k+m_3)}{\Gamma(m_1)\Gamma(m_2)\Gamma(m_3)} \left(\frac{\sigma^2}{\lambda_3 P_{PU}} \right)^{m_1-k} \sum_{l=0}^{m_1+m_2-1} \binom{m_1+m_2-1}{l} (-1)^{m_1+m_2-l-1} \\ \times \left(\frac{\lambda_1 Q_p}{\gamma \lambda_2 \lambda_3 P_{PU}} \right)^{m_2+m_3+k-l-1} \left(\frac{\gamma \lambda_2 \sigma^2}{\lambda_1 Q_p} + 1 \right)^{m_3+k-l-1} \Gamma \left(l - k - m_3 + 1, \frac{\gamma \sigma^2 \lambda_2 + \lambda_1 Q_p}{\lambda_1 \lambda_2 P_m} + \frac{\gamma \sigma^2 \lambda_2 + \lambda_1 Q_p}{\gamma \lambda_2 \lambda_3 P_{PU}} \right), \quad (3.25)$$

whereas $\Gamma(\dots)$ denotes the upper incomplete Gamma function [50, eq. (6.5.3)].

For the integer value of the first argument of incomplete Gamma function it can be expressed in a simpler form using the identities [88, eq. (3.351-2)] and [50, eqs. (6.5.15) and (6.5.19)]

$$\Gamma(\alpha, g) = \begin{cases} (\alpha - 1)! e^{-g} \sum_{j=0}^{\alpha-1} \frac{(g)^j}{j!} & \alpha > 0, \\ E_1(g) & \alpha = 0, \\ \frac{(-1)^{-\alpha}}{(-\alpha)!} \left[E_1(g) - e^{-g} \sum_{j=0}^{-\alpha-1} \frac{(-1)^j j!}{(g)^{j+1}} \right] & \alpha < 0. \end{cases} \quad (3.26)$$

3.1.2 Outage Probability of SINR

Outage probability is an important parameter in evaluating systems. As it is mentioned previously, outage probability is defined as the probability that the received SINR goes below a defined threshold ρ , given by the expression

$$P_{out} = \int_{-\infty}^{\rho} f_{\gamma}(\gamma) d\gamma = 1 - \int_{\rho}^{\infty} f_{\gamma}(\gamma) d\gamma, \quad (3.27)$$

where $f_{\gamma}(\gamma)$ is the PDF of SINR given in the closed-form in (3.25), therefore

$$\begin{aligned} P_{out}(\rho) = 1 - & \frac{P_{PU}}{P_m} \left[\int_0^{Q_p/P_m} f_{y_2}(y_2) dy_2 \right] \int_{\rho}^{\infty} f_x(\gamma P_{PU} / P_m) d\gamma \\ & - \frac{P_{PU}}{Q_p} \int_{Q_p/P_m}^{+\infty} y_2 f_{y_2}(y_2) \int_{\rho}^{\infty} f_x(\gamma y_2 P_{PU} / Q_p) d\gamma dy_2. \end{aligned} \quad (3.28)$$

Let us define

$$a(\rho) = \frac{P_{PU}}{P_m} \left[\int_0^{Q_p/P_m} f_{y_2}(y_2) dy_2 \right] \int_{\rho}^{\infty} f_x(\gamma P_{PU} / P_m) d\gamma, \quad (3.29)$$

and

$$b(\rho) = \frac{P_{PU}}{Q_p} \int_{Q_p/P_m}^{+\infty} y_2 f_{y_2}(y_2) \int_{\rho}^{\infty} f_x(\gamma y_2 P_{PU} / Q_p) d\gamma dy_2. \quad (3.30)$$

The derivation of outage probability of SINR is explained in the Appendix 3 – B in details, where by applying [88, eq. (2.323)] and some additional substitutions, we get

$$a(\rho) = \sum_{k=0}^{m_1} \binom{m_1}{k} \frac{\Gamma(k+m_3)}{\Gamma(m_1)\Gamma(m_3)} \left[1 - \frac{\Gamma(m_2, Q_p / \lambda_2 P_m)}{\Gamma(m_2)} \right] \sum_{l=0}^{m_1-1} \binom{m_1-1}{l} (-1)^{m_1-1-l} \times \left(\frac{\sigma^2}{\lambda_3 P_{PU}} \right)^{m_1+m_3-1-l} e^{\frac{\sigma^2}{\lambda_3 P_{PU}}} \Gamma \left(l - k - m_3 + 1, \frac{\rho \sigma^2}{\lambda_1 P_m} + \frac{\sigma^2}{\lambda_3 P_{PU}} \right), \quad (3.31)$$

and

$$b(\rho) = \frac{e^{\left(\frac{\lambda_1 Q_p}{\rho \lambda_3 P_{PU}} \right) \left(\frac{\rho \sigma^2}{\lambda_1 Q_p} + \frac{1}{\lambda_2} \right)}}{\Gamma(m_2)\Gamma(m_3)\lambda_2^{m_2}} \sum_{k=0}^{m_1-1} \sum_{l=0}^k \binom{k}{l} \frac{\Gamma(m_3+l)}{k!} \left(\frac{\sigma^2}{\lambda_3 P_{PU}} \right)^{k-l} \times \sum_{j=0}^{m_2+k-1} \binom{m_2+k-1}{j} (-1)^{m_2+k-1-j} \left(\frac{\lambda_1 \lambda_2 Q_p}{\lambda_1 Q_p + \lambda_2 \rho \sigma^2} \right)^{j-m_3-l+1} \times \left(\frac{\lambda_1 Q_p}{\rho \lambda_3 P_{PU}} \right)^{m_2+m_3+l-1-j} \Gamma \left(j - m_3 - l + 1, \left(\frac{Q_p}{P_m} + \frac{\lambda_1 Q_p}{\rho \lambda_3 P_{PU}} \right) \left(\frac{\rho \sigma^2}{\lambda_1 Q_p} + \frac{1}{\lambda_2} \right) \right). \quad (3.32)$$

Finally the last expression of outage probability is computed using the following

$$P_{out}(\rho) = 1 - a(\rho) - b(\rho). \quad (3.33)$$

In the region $P_m \ll Q_p$, The incomplete gamma function in eq. (3.32) is equal to zero and $b(\rho) = 0$. Then, the expression in the square brackets in eq. (3.31) has a unit value and the outage probability in this case can be simplified into

$$P_{out}(\rho) = 1 - e^{\frac{\sigma^2}{\lambda_3 P_{PU}}} \sum_{k=0}^{m_1} \binom{m_1}{k} \frac{\Gamma(k+m_3)}{\Gamma(m_1)\Gamma(m_3)} \sum_{l=0}^{m_1-1} \binom{m_1-1}{l} (-1)^{m_1-1-l} \times \left(\frac{\sigma^2}{\lambda_3 P_{PU}} \right)^{m_1+m_3-1-l} \Gamma \left(l - k - m_3 + 1, \frac{\rho \sigma^2}{\lambda_1 P_m} + \frac{\sigma^2}{\lambda_3 P_{PU}} \right). \quad (3.34)$$

It should be noticed that in this region the maximum transmit power constraint dominates, and the outage probability does not depend on the predefined threshold Q_p .

This case corresponds to the system with fixed (non-adaptable) power of secondary transmitter.

In the region $Q_p \ll P_m$, the expression in the square brackets in eq. (3.31) is equal to zero and $a(\rho) = 0$. Then the simplified outage probability expression can be written in the following form

$$\begin{aligned}
P_{out}(\rho) = & 1 - \frac{e^{-\left(\frac{\lambda_1 Q_p}{\rho \lambda_3 P_{PU}}\right)\left(\frac{\rho \sigma^2 + 1}{\lambda_1 Q_p + \lambda_2}\right)}}{\Gamma(m_2)\Gamma(m_3)\lambda_2^{m_2}} \sum_{k=0}^{m_1-1} \sum_{l=0}^k \binom{k}{l} \frac{\Gamma(m_3 + l)}{k!} \left(\frac{\sigma^2}{\lambda_3 P_{PU}}\right)^{k-l} \\
& \times \sum_{j=0}^{m_2+k-1} \binom{m_2+k-1}{j} (-1)^{m_2+k-1-j} \left(\frac{\lambda_1 \lambda_2 Q_p}{\lambda_1 Q_p + \lambda_2 \rho \sigma^2}\right)^{j-m_3-l+1} \\
& \times \left(\frac{\lambda_1 Q_p}{\rho \lambda_3 P_{PU}}\right)^{m_2+m_3+l-1-j} \Gamma\left(j-m_3-l+1, \left(\frac{Q_p}{P_m} + \frac{\lambda_1 Q_p}{\rho \lambda_3 P_{PU}}\right)\left(\frac{\rho \sigma^2}{\lambda_1 Q_p} + \frac{1}{\lambda_2}\right)\right).
\end{aligned} \tag{3.35}$$

The performance of outage probability as a function of the peak interference power constraint Q_p under different values of fading parameters is discussed in the Figures 3.2, 3.3 and 3.4. It is supposed that SU has perfect channel knowledge about the channel between SU-Tx and PU-Rx under other various conditions. In these three figures, it is supposed that the channels have a unit power, $\lambda_i=1/m_i$ ($i= 1, 2, 3$ denoting the corresponding channels). The two special cases when $P_m \ll Q_p$ and $Q_p \ll P_m$ are plotted in the figures to be as references for the different results. The analytical results are plotted using (3.31) - (3.33), and asymptotic behaviours using (3.34) and (3.35).

It is noticed that the outage probability decreases with the increase of interference power constraint Q_p , which is already noticed for the case of Rayleigh fading channel in [79].

The impact of the fading parameter (m_1) in the secondary link, and the SINR threshold (ρ) on the performance of outage probability is presented in Figure 3.3, applying a transmit power constraint $P_m=10$ and fading parameters $m_2= m_3=3$. The increase in m_1 value decreases the outage probability for a fixed Q_p as it is noticed in [89]. The signal goes in outage, when the received signal to noise and interference ratio drops under a defined threshold ρ . Therefore, outage probability of SINR is the

probability that the received SINR goes under this threshold. As expected, the outage probability decreases for higher SINR threshold, which is in agreement with the results from [78] and [79].

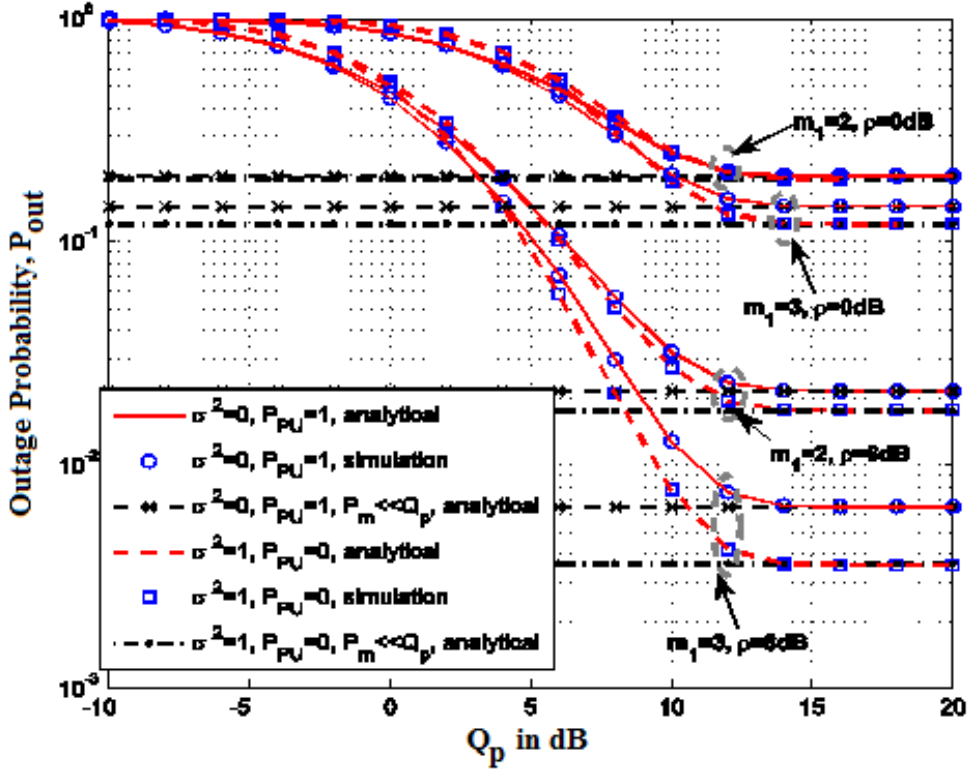


Figure 3.2 – Outage probability for noise and interference limited cases when $m_2=m_3=3$, $\lambda_i=1/m_i$ and $P_m=10$ for various values of SINR-threshold and m_1 .

These results are experienced under two limited scenarios, the noise-limited case ($P_{PU}=0$ with $\sigma^2=1$) and the co-channel interference-limited case ($\sigma^2 \rightarrow 0$ with $P_{PU}=1$). When the co-channel interference is negligible compared to the noise power (noise-limited case), the outage probability has lower values for high Q_p compared with the interference-limited case. While when the interference from PU dominates, the system has better performance for lower values of Q_p . The last effect is more noticeable for larger value of fading parameter m_1 . The difference between these two curves (Interference limited and noise limited curves) decreases for the lower value of SINR threshold and the same value of m_1 as it can be seen in the Figure 3.2.

In Figure 3.3, the effect of the fading parameter in the channel between primary transmitter and secondary receiver (m_3) for different values of the co-channel

interference power (P_{PU}) on the outage probability performance is studied. It is supposed that the transmission power is limited with the constraint $P_m=10$, SINR threshold $\rho=6$ dB, and the fading parameters are equal to $m_1 = m_2 = 2$. For a fixed value of Q_p , SINR increases as the interference signal goes smaller, therefore the outage probability decreases with the decrease of the co-channel interference value from PU. On the other hand, the effect of m_3 can be concluded in that: the raise of m_3 value increases the outage probability, where the increase of m_3 means that the effect of fading decreases and this allows the transmission of PU making a higher interference to the SU-Rx, which in its turn decreases the SINR value at the receiver.

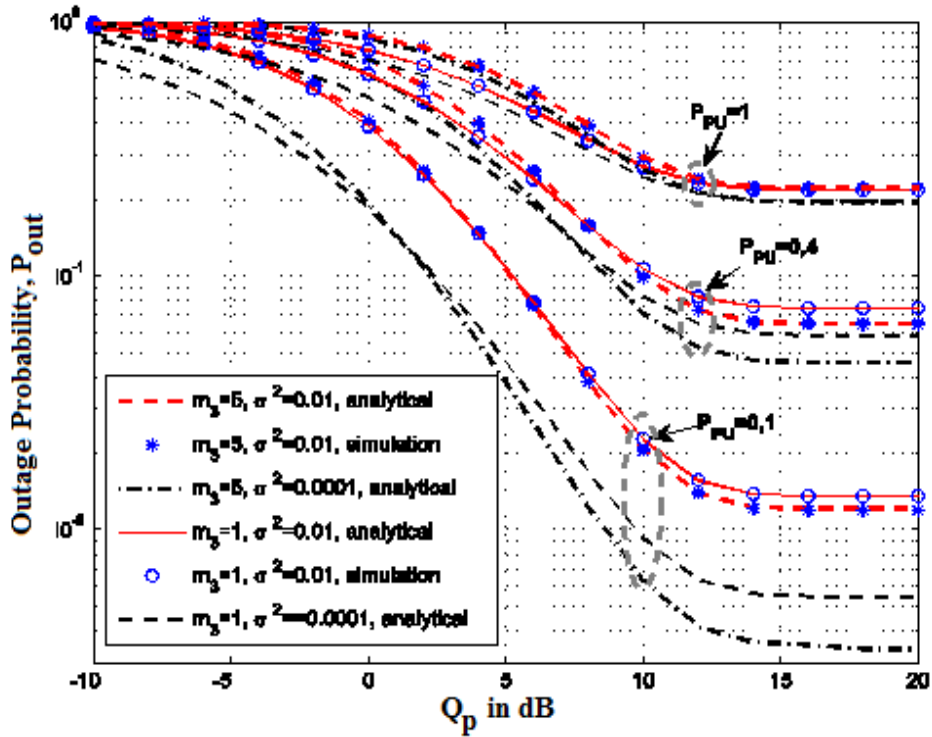


Figure 3.3 – Outage probability in the presence and absence of noise when $m_1=m_2=2$, $\lambda_i=1/m_i$, $P_m=10$, $\rho=6$ dB for different values of co-channel interference and m_3 .

It is good to mention that the presence of noise can be neglected if $\sigma^2 \ll m_3 \lambda_3 P_{PU}$ (e.g. $\sigma^2 = 0.01$, $P_{PU} = 1$, $m_3 \lambda_3 = 1$), but it cannot be neglected even if the noise power is one order of magnitude smaller than $m_3 \lambda_3 P_{PU}$ (e.g. $\sigma^2 = 0.01$, $P_{PU} = 0.4$, $m_3 \lambda_3 = 0.5$). Comparing the results in Figure 3.2 and Figure 3.3, it can be observed that the impact of m_3 is smaller than the impact of m_1 on the outage probability performance.

In the previous two figures has been analysed the effect of the fading parameters in the SU channel and the interference channel between PU-Tx and SU-Tx, (m_1 and m_3 , respectively) on the performance of outage probability. Whereas the effect of the fading parameter in the channel from secondary transmitter to primary receiver, m_2 , is presented in Figure 3.4 for different values of the transmit power constraint at the secondary transmitter. The analysis in this Figure is limited to the interference-limited case ($\sigma^2 \ll m_3 \lambda_3 P_{PU}$) when $m_1 = m_3 = 2$ and SINR threshold $\rho = 0$ dB. As the transmit power increases, SINR value increases which lowers the outages probability for a fixed value of Q_p . While, for a fixed transmission power, the outage probability decreases with the increase of interference power constraint till it reaches to a floor for the larger values of Q_p (where the value of Q_p is much bigger than P_m).

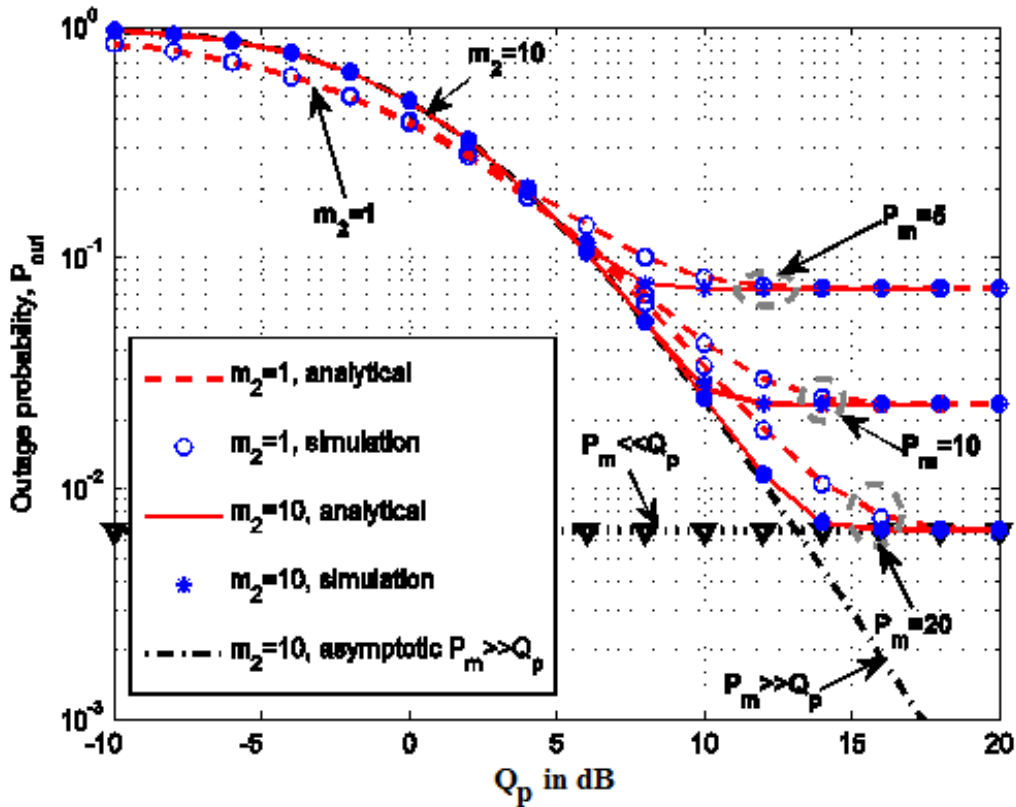


Figure 3.4 – Outage probability for different values of P_m and m_2 , when $m_1 = m_3 = 2$, $\lambda_i = 1/m_i$, $P_{PU} = 1$ and $\rho = 0$ dB.

For the effect of m_2 , it can be differentiated between two regions according to the value of the interference power constraint. The increase of m_2 increases the outage

probability for small values of Q_p , while it decreases outage probability for larger values of Q_p . One more thing is nice to be mentioned that in the region where $P_m \ll Q_p$, the outage floor has the same value for various value of m_2 and fixed P_m . This effect corresponds to the one that was noticed in [79], where the capacity of the noise-limited system was analysed.

3.1.3 Moments of SINR

The n -th moment of SINR is given as [87, eq. (7-1)]

$$E(\gamma^n) = \int_0^{+\infty} \gamma^n f_\gamma(\gamma) d\gamma, \quad (3.36)$$

where $f_\gamma(\gamma)$ is the PDF of SINR given in equation (3.25), therefore using (3.17)

$$E(\gamma^n) = \left[\frac{P_{PU}}{P_m} \int_0^\infty \gamma^n f_x(\gamma P_{PU} / P_m) d\gamma \right] \left[\int_0^{Q_p/P_m} f_{y_2}(y_2) dy_2 \right] - \frac{P_{PU}}{Q_p} \int_{Q_p/P_m}^{+\infty} y_2 f_{y_2}(y_2) \left[\int_0^\infty \gamma^n f_x(\gamma y_2 P_{PU} / Q_p) d\gamma \right] dy_2. \quad (3.37)$$

Applying the substitution $t = y_3 + \sigma^2/P_{PU}$ and then following the derivation explained in Appendix 3 – C, the closed-form expression for the moments of SINR can be obtained as

$$E(\gamma^n) = \frac{e^{\sigma^2/\lambda_3 P_{PU}}}{\Gamma(m_1)\Gamma(m_3)} \left(\frac{\lambda_1 P_m}{\lambda_3 P_{PU}} \right)^n \times \left\{ \sum_{k=0}^{m_1} \binom{m_1}{k} \Gamma(k+m_3) \sum_{l=0}^{m_1+n-1} \binom{m_1+n-1}{l} (-1)^{m_1+n-1-l} \left(\frac{\sigma^2}{\lambda_3 P_{PU}} \right)^{m_1+m_3-1-l} \Gamma\left(l-k-m_3+1, \frac{\sigma^2}{\lambda_3 P_{PU}}\right) \left[1 - \frac{\Gamma(m_2, Q_p / (\lambda_2 P_m))}{\Gamma(m_2)} \right] + \frac{\Gamma(m_1+n)}{\Gamma(m_2)} \left(\frac{Q_p}{\lambda_2 P_m} \right)^n \sum_{k=0}^{m_3-1} \binom{m_3-1}{k} \left(\frac{-\sigma^2}{\lambda_3 P_{PU}} \right)^{m_3-1-k} \Gamma\left(k-n+1, \frac{\sigma^2}{\lambda_3 P_{PU}}\right) \Gamma\left(m_2-n, \frac{Q_p}{\lambda_2 P_m}\right) \right\}. \quad (3.38)$$

3.2 Cognitive Radio System Model with Outdated CSI

Perfect Channel State Information (CSI) is usually assumed to simplify the study; where the information is provided to the secondary transmitter by the band manager or by a feedback signal from the primary receiver when the primary and secondary users cooperate with each other. However in practical systems, the situation is different.

In this section, due to the critical importance of the channel state information of the channel between secondary transmitter and primary receiver in protecting the primary user from the secondary transmission's interference, it has been assumed that no full knowledge of CSI is available at the secondary user. Practically, even if there is cooperation between the secondary and primary user, the feedback signal could be delayed by a τ time due to the fading in the channel. Moreover, the fading is not static and changes through the time, therefore the secondary user will adapt its power transmission according to the previous CSI value \hat{y}_2 which is called outdated CSI instead of the right value y_2 . The concept of outdated channel state information is explained in Figure 3.5.

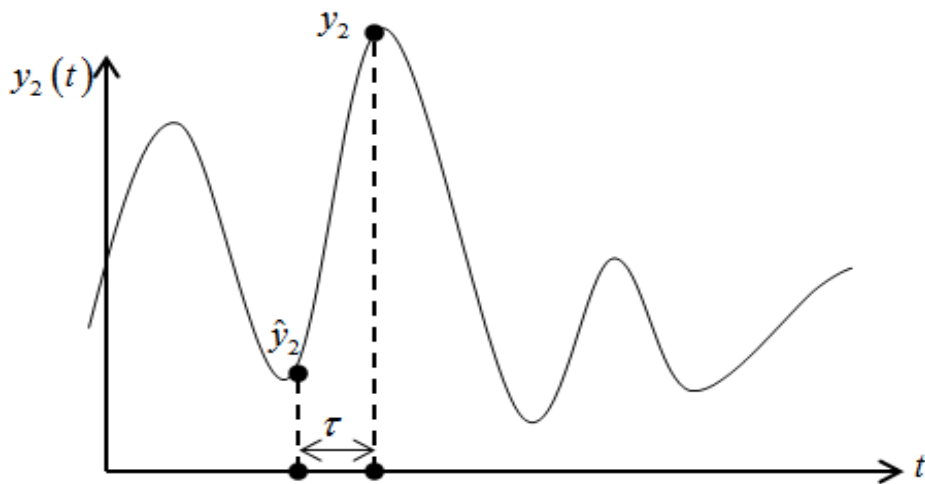


Figure 3.5 – Outdated CSI concept.

The measure of “similarity” between the actual value of channel power gain y_2 and the corresponding estimated value \hat{y}_2 is represented by the correlation coefficient R . In general, correlation coefficient depends on Doppler speed f_D and delay τ , it is

given by $R = J_0(2\pi f_D \tau)$, where $J_0(\cdot)$ is modified Bessel function of zeroth order and first kind. As the similarity between the actual value and estimated one of the channel power gain is higher, the correlation coefficient, R , goes to 1 and the delay τ goes to 0. On the other hand, as the CSI gets more outdated, the correlation coefficient value gets smaller toward 0 and the time delay in feedback signal gets bigger.

The random variables y_2 and \hat{y}_2 , actual and outdated value for the channel power gain of the channel between SU-Tx and PU-Rx, respectively, are not independent and their mutual dependence is described through a joint PDF given in [90] as

$$f_{y_2, \hat{y}_2}(u, v) = \frac{(uv)^{\frac{m_2-1}{2}} e^{-\frac{u+v}{(1-R^2)\lambda_2}}}{(1-R^2)\Gamma(m_2)R^{m_2-1}\lambda_2^{m_2+1}} I_{m_2-1}\left(\frac{2R\sqrt{uv}}{(1-R^2)\lambda_2}\right), \quad (3.39)$$

where $I_{m-1}(\cdot)$ is modified Bessel function of $(m-1)$ -th order and first kind, and R is the correlation coefficient.

Since fulfilling the strict rule given in the expression (3.1), which protects the primary receiver, is such difficult; the primary user allows the secondary transmitter to exceed the value of the peak interference power constraint with a maximal permitted probability of interference outage represented by P_o , expressed in the following expression

$$P_o = \Pr\{P_{SU-Tx}(R, \hat{y}_2)y_2 \geq Q_p\}. \quad (3.40)$$

Secondary user from its side, in order to protect the primary user through the outdated CSI case, uses a protection factor represented as k_o . Secondary transmitter, in order not to exceed the interference constraint level at primary user, minimizes its transmission power in each moment by the value of k_o . Therefore, secondary transmission power can be written as [79, eq. (27)]

$$P_{SU-Tx} = \min\left\{k_o \frac{Q_p}{\hat{y}_2}, P_m\right\}, \quad (3.41)$$

furthermore,

$$P_{SU-Tx} = \begin{cases} P_m, & \hat{y}_2 \leq k_o Q_p / P_m, \\ k_o Q_p / \hat{y}_2, & \hat{y}_2 > k_o Q_p / P_m. \end{cases} \quad (3.42)$$

Protection coefficient k_o depends on the correlation coefficient R and the permitted values of interference power constraint Q_p , transmission power constraint P_m and probability of interference outage P_o , where $k_o = k_o(R, Q_p, P_m, P_o)$. In each moment $k_o < 1$ when outdated CSI is available, while it is equal to $k_o = 1$ for the case of perfect CSI where secondary transmitter transmits with its actual adapted transmission power value without any reduction.

Substituting equation (3.41) in (3.40), the maximal permitted probability of interference outage can be written as follows

$$P_o = \Pr \left\{ \min \left\{ k_o \frac{Q_p}{\hat{y}_2} y_2, P_m y_2 \right\} \geq Q_p \right\} = \Pr \left\{ \hat{y}_2 \leq k_o y_2 \wedge y_2 \geq \frac{Q_p}{P_m} \right\}. \quad (3.43)$$

Furthermore, the probability of permitted interference outage can be written in the integral form as [79] by substituting the joint PDF of RVs y_2 and \hat{y}_2 in the previous equation to get

$$P_o = \int_{Q_p/P_m}^{+\infty} \int_0^{k_o u} f_{y_2, \hat{y}_2}(u, v) dv du. \quad (3.44)$$

In the special case when transmit power of SU-Tx is not limited ($P_m \rightarrow \infty$), the condition (3.1) reduces into [79, eq. (30)], where the interference constraint is dominant, and the transmission power of SU-Tx is adapted to $P_{SU-Tx} = k_o Q_p / \hat{y}_2$, then the interference outage probability is given as

$$P_o = \Pr \left\{ \frac{k_o Q_p}{\hat{y}_2} y_2 \geq Q_p \right\} = \Pr \left\{ \frac{y_2}{\hat{y}_2} \geq \frac{1}{k_o} \right\}, \quad (3.45)$$

where in this case, the protection coefficient k_o does not depend on the threshold Q_p , but only on the fading parameters and permitted probability of interference outage P_o .

Applying the power constraints and substituting the secondary transmission power given in (3.41) in the expression of SINR given in (3.5), signal to interference and noise ratio for the outdated CSI case is given as follows

$$\gamma = \begin{cases} \frac{k_o Q_p y_1 / \hat{y}_2}{P_{PU} (y_3 + \sigma^2 / P_{PU})} & \hat{y}_2 \geq \frac{k_o Q_p}{P_m}, \\ \frac{P_m y_1}{P_{PU} (y_3 + \sigma^2 / P_{PU})} & \hat{y}_2 < \frac{k_o Q_p}{P_m}. \end{cases} \quad (3.46)$$

Defining $x = y_1 / (y_3 + \sigma^2 / P_{PU})$, the previous equation can be rewritten in the form

$$\gamma = \begin{cases} \frac{k_o Q_p x}{P_{PU} \hat{y}_2} & \hat{y}_2 \geq \frac{k_o Q_p}{P_m}, \\ \frac{P_m x}{P_{PU}} & \hat{y}_2 < \frac{k_o Q_p}{P_m}. \end{cases} \quad (3.47)$$

3.2.1 Probability Density Function of SINR

To get the closed-form expression of probability density function of SINR for the case of outdated CSI, the linear transformation of RVs is applied on both segments of (3.47) to get

$$f_\gamma(\gamma) = \int_0^{k_o Q_p / P_m} \frac{f_x(\gamma P_{PU} / P_m)}{P_m / P_{PU}} f_{\hat{y}_2}(\hat{y}_2) d\hat{y}_2 + \int_{k_o Q_p / P_m}^{+\infty} \frac{f_x(\gamma P_{PU} y_2 / Q_p)}{Q_p / (P_{PU} y_2)} f_{\hat{y}_2}(\hat{y}_2) d\hat{y}_2. \quad (3.48)$$

Following the same sequence of operations and calculations described in Appendix 3 – A deriving for the perfect CSI case, the final expression is given in

$$\begin{aligned} f_\gamma(\gamma) &= \left(\frac{P_{PU}}{P_m} \right)^{m_1} \sum_{k=0}^{m_1} \alpha_k \frac{\gamma^{m_1-1} e^{-\gamma \sigma^2 / \lambda_1 P_m}}{(\gamma \lambda_3 P_{PU} / P_m + \lambda_1)^{k+m_3}} \left[1 - \frac{\Gamma(m_2, k_o Q_p / P_m)}{\Gamma(m_2)} \right] \\ &+ \frac{e^{\frac{\gamma \sigma^2 \lambda_2 + \lambda_1 k_o Q_p}{\gamma \lambda_2 \lambda_3 P_{PU}}}}{\gamma \lambda_3^{m_1} \Gamma(m_2)} \sum_{k=0}^{m_1} \frac{\alpha_k}{\lambda_1^{m_3+k}} \sum_{l=0}^{m_1+m_2-1} \binom{m_1+m_2-1}{l} (-1)^{m_1+m_2-l-1} \left(\frac{\lambda_1 k_o Q_p}{\gamma \lambda_2 \lambda_3 P_{PU}} \right)^{m_2+m_3+k-l-1} \\ &\times \left(\frac{\gamma \sigma^2 \lambda_2}{\lambda_1 k_o Q_p} + 1 \right)^{m_3+k-l-1} \Gamma \left(l - k - m_3 + 1, \frac{\gamma \sigma^2 \lambda_2 + \lambda_1 k_o Q_p}{\lambda_1 P_m \lambda_2} + \frac{\gamma \sigma^2 \lambda_2 + \lambda_1 k_o Q_p}{\gamma \lambda_2 \lambda_3 P_{PU}} \right), \end{aligned} \quad (3.49)$$

where α_k is given in (3.23).

For the special case when the transmission power of secondary user is not limited ($P_m \rightarrow \infty$), i.e. $P_m \gg Q_p$, the interference constraint power dominates and the transmission power is written as $P_{SU-Tx} = k_o Q_p / \hat{y}_2$, therefore the expression (3.48) is written as

$$\begin{aligned} f_\gamma(\gamma) &= \int_0^{+\infty} f_{\gamma|\hat{y}_2}(\gamma | (\hat{y}_2 > k_o Q_p / P_m)) f_{\hat{y}_2}(\hat{y}_2) d\hat{y}_2, \\ &= \int_0^{+\infty} \frac{f_x(\gamma / (k_o Q_p / P_{PU} \hat{y}_2))}{k_o Q_p / P_{PU} \hat{y}_2} f_{\hat{y}_2}(\hat{y}_2) d\hat{y}_2, \end{aligned} \quad (3.50)$$

where $f_x(x)$ is given in (3.22), and after substituting it with the probability density function of the channel power gain \hat{y}_2 , we get

$$f_\gamma(\gamma) = \left(\frac{P_{PU}}{k_o Q_p} \right)^{m_1} \frac{\gamma^{m_1-1}}{\lambda_2^{m_2} \Gamma(m_2)} \sum_{k=0}^{m_1} \alpha_k \left(\frac{k_o Q_p}{\gamma \lambda_3 P_{PU}} \right)^{k+m_3} \int_0^{+\infty} \frac{\hat{y}_2^{m_1+m_2-1} e^{-\hat{y}_2 \left(\frac{\gamma \sigma^2}{\lambda_1 k_o Q_p} + \frac{1}{\lambda_2} \right)}}{(\hat{y}_2 + \lambda_1 / \gamma \lambda_3 P_{PU})^{k+m_3}} d\hat{y}_2. \quad (3.51)$$

Applying the substitution $\hat{y}_2 + \lambda_1 / \gamma \lambda_3 P_{PU} = t$ and the binomial expansion [88, eq. (1.111)], the integral will be simplified to the identity of incomplete gamma function [50, eq. (6.5.3)]. Then the probability density function of SINR can be simplified into

$$\begin{aligned} f_\gamma(\gamma) &= \frac{e^{\frac{\gamma \sigma^2 \lambda_2 + \lambda_1 k_o Q_p}{\gamma \lambda_2 \lambda_3 P_{PU}}}}{\gamma \lambda_3^{m_1} \Gamma(m_2)} \sum_{k=0}^{m_1} \frac{\alpha_k}{\lambda_1^{m_3+k}} \sum_{l=0}^{m_1+m_2-1} \binom{m_1+m_2-1}{l} \left(\frac{\lambda_1 k_o Q_p}{\gamma \lambda_2 \lambda_3 P_{PU}} \right)^{m_2+m_3+k-l-1} \\ &\quad \times (-1)^{m_1+m_2-l-1} \left(\frac{\gamma \sigma^2 \lambda_2}{\lambda_1 k_o Q_p} + 1 \right)^{m_3+k-l-1} \Gamma \left(l - k - m_3 + 1, \frac{\sigma^2}{\lambda_3 P_{PU}} + \frac{\lambda_1 k_o Q_p}{\gamma \lambda_2 \lambda_3 P_{PU}} \right). \end{aligned} \quad (3.52)$$

For the opposite special case when transmission power constraint of secondary user dominates ($P_m \ll Q_p$), the transmission power will be equal to $P_{SU-Tx} = P_m$, which is valid for the system with a fixed transmission power value. Then (3.48) will be simplified into

$$\begin{aligned} f_\gamma(\gamma) &= \int_0^{+\infty} f_{\gamma|\hat{y}_2}(\gamma | (\hat{y}_2 < k_o Q_p / P_m)) f_{\hat{y}_2}(\hat{y}_2) d\hat{y}_2, \\ &= \frac{f_x(\gamma / (P_m / P_{PU}))}{P_m / P_{PU}} \int_0^{+\infty} f_{\hat{y}_2}(\hat{y}_2) d\hat{y}_2, \end{aligned} \quad (3.53)$$

which can be written after substituting the PDF of x (3.22) as

$$f_\gamma(\gamma) = \left(\frac{P_{PU}}{P_m} \right)^{m_1} \sum_{k=0}^{m_1} \alpha_k \frac{\gamma^{m_1-1} e^{-\frac{\gamma\sigma^2}{\lambda_1 P_m}}}{(\gamma\lambda_3 P_{PU} / P_m + \lambda_1)^{k+m_3}} \left[\frac{1}{\lambda_2^{m_2} \Gamma(m_2)} \int_0^{+\infty} \hat{y}_2^{m_2-1} e^{-\hat{y}_2/\lambda_2} d\hat{y}_2 \right]. \quad (3.54)$$

Then the probability density function is given in the form

$$f_\gamma(\gamma) = \left(\frac{P_{PU}}{P_m} \right)^{m_1} \sum_{k=0}^{m_1} \alpha_k \frac{\gamma^{m_1-1} e^{-\gamma\sigma^2/\lambda_1 P_m}}{(\gamma\lambda_3 P_{PU} / P_m + \lambda_1)^{k+m_3}} \left[1 - \frac{\Gamma(m_2, k_o Q_p / P_m)}{\Gamma(m_2)} \right]. \quad (3.55)$$

3.2.2 Outage Probability of SINR

The closed-form expression of outage probability is derived using (3.27), where $f_\gamma(\gamma)$ is the probability density function of SINR given in (3.49) when the available channel knowledge is outdated, hence

$$P_{out}(\rho) = 1 - \frac{P_{PU}}{P_m} \int_{\rho}^{\infty} f_x(\gamma P_{PU} / P_m) d\gamma \left[\int_0^{k_o Q_p / P_m} f_{\hat{y}_2}(\hat{y}_2) d\hat{y}_2 \right] - \frac{P_{PU}}{k_o Q_p} \int_{k_o Q_p / P_m}^{+\infty} \hat{y}_2 f_{\hat{y}_2}(\hat{y}_2) \int_{\rho}^{\infty} f_x(\gamma \hat{y}_2 P_{PU} / k_o Q_p) d\gamma d\hat{y}_2. \quad (3.56)$$

Following the same process described in Appendix 3-B, the final closed-form expression of outage probability for the outdated CSI case is given in the form

$$P_{out}(\rho) = 1 - a(\rho) - b(\rho), \quad (3.57)$$

where

$$a(\rho) = \frac{e^{\sigma^2/\lambda_3 P_{PU}}}{\Gamma(m_1)\Gamma(m_3)} \left[1 - \frac{\Gamma(m_2, k_o Q_p / (\lambda_2 P_m))}{\Gamma(m_2)} \right] \sum_{k=0}^{m_1} \binom{m_1}{k} \Gamma(k+m_3) \times \sum_{l=0}^{m_1-1} \binom{m_1-1}{l} (-1)^{m_1-1-l} \left(\frac{\sigma^2}{\lambda_3 P_{PU}} \right)^{m_1+m_3-1-l} \Gamma \left(l-k-m_3+1, \frac{\rho\sigma^2}{\lambda_1 P_m} + \frac{\sigma^2}{\lambda_3 P_{PU}} \right). \quad (3.58)$$

and

$$\begin{aligned}
b(\rho) &= \frac{e^{\frac{\sigma^2}{\lambda_3 P_{PU}} + \frac{\lambda_1 k_o Q_p}{\rho \lambda_2 \lambda_3 P_{PU}}}}{\Gamma(m_2)\Gamma(m_3)\lambda_2^{m_2}} \sum_{k=0}^{m_1-1} \sum_{l=0}^k \binom{k}{l} \frac{\Gamma(m_3+l)}{k!} \left(\frac{\sigma^2}{\lambda_3 P_{PU}}\right)^{k-l} \sum_{j=0}^{m_2+k-1} \binom{m_2+k-1}{j} (-1)^{m_2+k-1-j} \\
&\times \left(\frac{\lambda_1 \lambda_2 k_o Q_p}{\lambda_1 k_o Q_p + \lambda_2 \rho \sigma^2}\right)^{j-m_3-l+1} \left(\frac{\lambda_1 k_o Q_p}{\rho \lambda_3 P_{PU}}\right)^{m_2+m_3+l-1-j} \Gamma\left(j-m_3-l+1, \left(\frac{Q_p}{P_m} + \frac{\lambda_1 Q_p}{\rho \lambda_3 P_{PU}}\right) \left(\frac{\rho \sigma^2}{\lambda_1 Q_p} + \frac{k_o}{\lambda_2}\right)\right).
\end{aligned} \tag{3.59}$$

In the region $P_m \ll Q_p$, the outage probability expression in (3.56) is simplified into

$$P_{out}(\rho) = 1 - \frac{P_{PU}}{P_m} \int_{\frac{\rho}{P_m}}^{\infty} f_x(\gamma P_{PU} / P_m) d\gamma \left[\int_0^{\infty} f_{\hat{y}_2}(\hat{y}_2) d\hat{y}_2 \right], \tag{3.60}$$

to be written in the closed-form as

$$\begin{aligned}
P_{out}(\rho) &= 1 - \sum_{k=0}^{m_1} \binom{m_1}{k} \frac{e^{\sigma^2/\lambda_3 P_{PU}} \Gamma(k+m_3)}{\Gamma(m_1)\Gamma(m_3)} \sum_{l=0}^{m_1-1} \binom{m_1-1}{l} (-1)^{m_1-1-l} \\
&\times \left(\frac{\sigma^2}{\lambda_3 P_{PU}}\right)^{m_1+m_3-1-l} \Gamma\left(l-k-m_3+1, \frac{\rho \sigma^2}{\lambda_1 P_m} + \frac{\sigma^2}{\lambda_3 P_{PU}}\right).
\end{aligned} \tag{3.61}$$

While in the region $Q_p \ll P_m$, the simplified outage probability is expressed only by the modified $b(\rho)$ as follows

$$\begin{aligned}
P_{out}(\rho) &= 1 - \frac{e^{\left(\frac{\sigma^2}{\lambda_3 P_{PU}} + \frac{\lambda_1 k_o Q_p}{\rho \lambda_2 \lambda_3 P_{PU}}\right)}}{\Gamma(m_2)\Gamma(m_3)\lambda_2^{m_2}} \sum_{k=0}^{m_1-1} \frac{\Gamma(m_3+l)}{k!} \sum_{l=0}^k \binom{k}{l} \left(\frac{\sigma^2}{\lambda_3 P_{PU}}\right)^{k-l} \\
&\times \sum_{j=0}^{m_2+k-1} \binom{m_2+k-1}{j} (-1)^{m_2+k-1-j} \left(\frac{\lambda_1 k_o Q_p}{\rho \lambda_3 P_{PU}}\right)^{m_2+m_3+l-1-j} \\
&\times \left(\frac{\lambda_1 \lambda_2 k_o Q_p}{\lambda_1 k_o Q_p + \rho \lambda_2 \sigma^2}\right)^{j-m_3-l+1} \Gamma\left(j-m_3-l+1, \frac{\lambda_1 Q_p}{\rho \lambda_3 P_{PU}} \left(\frac{\rho \sigma^2}{\lambda_1 Q_p} + \frac{k_o}{\lambda_2}\right)\right).
\end{aligned} \tag{3.62}$$

The impact of the outdated CSI of the link from secondary transmitter to primary receiver on the system performances is analysed in the following paragraph.

Figure 3.6 represents the dependence of the protection coefficient k_o on both the fading parameter m_2 and the channel correlation coefficient R . The protection coefficient is calculated numerically from equation (3.45) for fixed values of probability of interference outage $P_o = 0.01$, transmission power constraint $P_m = 10$ dB and different values of interference power constraint Q_p . As it is mentioned earlier that when R has higher values, the outdated CSI value is more similar to the accurate one and in this case k_o goes to 1. On the other hand, for a given correlation factor, the higher values of m_2 , the closer value of k_o to 1.

Since the primary receiver has its constraint power for protection Q_p , it is noticed that the protection coefficient k_o increases as the primary user can tolerate higher value of interference, Q_p gets bigger, then the secondary user can transmit higher power.

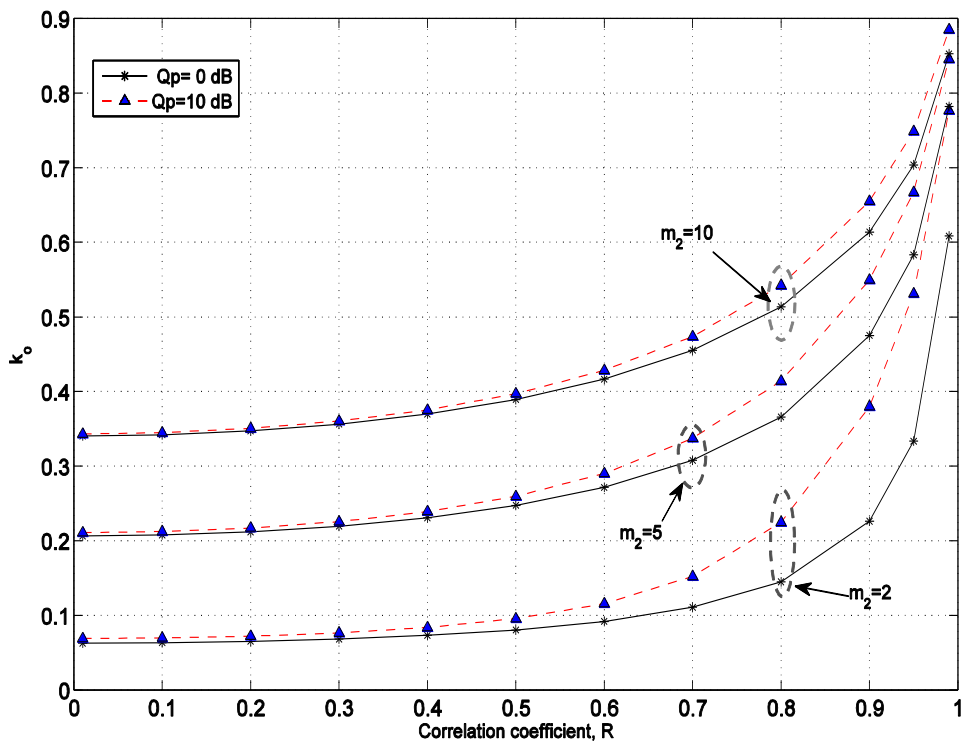


Figure 3.6 – Dependence of protection coefficient for various values of m_2 and constraint Q_p when $\lambda_2 = 1/m_2$, $P_m = 10$ dB and $P_o = 0.01$.

How the outdated channel state information affect the performance of outage probability? The answer is given in Figure 3.7 for different values of the probability of interference outage (P_o) and correlation coefficient (R). The results are plotted when

3.2.3 Moments of SINR at the SU-Rx

The n -th moment of SINR is given in the equation (3.36), where $f_\gamma(\gamma)$ is the PDF of SINR given in equation (3.49) for the outdated CSI case. Using some expressions as it is done for the case of perfect CSI explained in Appendix 3 – D; the final closed-form expression for the moments is

$$\begin{aligned}
 E(\gamma^n) &= \frac{e^{\sigma^2/\lambda_3 P_{PU}}}{\Gamma(m_1)\Gamma(m_3)} \left(\frac{\lambda_1 P_m}{\lambda_3 P_{PU}} \right)^n \times \left\{ \sum_{k=0}^{m_1} \binom{m_1}{k} \Gamma(k+m_3) \sum_{l=0}^{m_1+n-1} \binom{m_1+n-1}{l} (-1)^{m_1+n-1-l} \right. \\
 &\quad \left. \left(\frac{\sigma^2}{\lambda_3 P_{PU}} \right)^{m_1+m_3-1-l} \Gamma \left(l-k-m_3+1, \frac{\sigma^2}{\lambda_3 P_{PU}} \right) \left[1 - \frac{\Gamma(m_2, k_0 Q_p / (\lambda_2 P_m))}{\Gamma(m_2)} \right] \right. \\
 &\quad \left. + \frac{\Gamma(m_1+n)}{\Gamma(m_2)} \left(\frac{k_0 Q_p}{\lambda_2 P_m} \right)^n \sum_{k=0}^{m_3-1} \binom{m_3-1}{k} \left(\frac{-\sigma^2}{\lambda_3 P_{PU}} \right)^{m_3-1-k} \Gamma \left(k-n+1, \frac{\sigma^2}{\lambda_3 P_{PU}} \right) \Gamma \left(m_2-n, \frac{k_0 Q_p}{\lambda_2 P_m} \right) \right\}. \tag{3.63}
 \end{aligned}$$

In the region $P_m \ll Q_p$, equation (3.63) reduces into the expression for the case of fixed (non-adaptable) transmit power at SU-Tx as

$$\begin{aligned}
 E(\gamma^n) &= \frac{e^{\sigma^2/\lambda_3 P_{PU}}}{\Gamma(m_1)\Gamma(m_3)} \left(\frac{\lambda_1 P_m}{\lambda_3 P_{PU}} \right)^n \sum_{k=0}^{m_1} \binom{m_1}{k} \Gamma(k+m_3) \sum_{l=0}^{m_1+n-1} \binom{m_1+n-1}{l} \\
 &\quad \times (-1)^{m_1+n-1-l} \left(\frac{\sigma^2}{\lambda_3 P_{PU}} \right)^{m_1+m_3-1-l} \Gamma \left(l-k-m_3+1, \frac{\sigma^2}{\lambda_3 P_{PU}} \right). \tag{3.64}
 \end{aligned}$$

While in the region $P_m \gg Q_p$, the expression of moments is valid for unlimited transmission power of the SU-Tx

$$\begin{aligned}
 E(\gamma^n) &= \frac{\Gamma(m_1+n)\Gamma(m_2-n)}{\Gamma(m_1)\Gamma(m_2)\Gamma(m_3)} e^{\frac{\sigma^2}{\lambda_3 P_{PU}}} \left(\frac{\lambda_1 k_0 Q_p}{\lambda_2 \lambda_3 P_{PU}} \right)^n \\
 &\quad \times \sum_{k=0}^{m_3-1} \binom{m_3-1}{k} \left(\frac{-\sigma^2}{\lambda_3 P_{PU}} \right)^{m_3-1-k} \Gamma \left(k-n+1, \frac{\sigma^2}{\lambda_3 P_{PU}} \right). \tag{3.65}
 \end{aligned}$$

First Moment (Mean Value)

The most effective use from the moments is to calculate the first moment when ($n=1$) which gives the mean value of SINR

$$\begin{aligned}
 E(\gamma) &= \frac{e^{\sigma^2/\lambda_3 P_{PU}}}{\Gamma(m_1)\Gamma(m_3)} \left(\frac{\lambda_1 P_m}{\lambda_3 P_{PU}} \right) \times \left\{ \sum_{k=0}^{m_1} \binom{m_1}{k} \Gamma(k+m_3) \sum_{l=0}^{m_1} \binom{m_1}{l} (-1)^{m_1-l} \right. \\
 &\quad \left. \left(\frac{\sigma^2}{\lambda_3 P_{PU}} \right)^{m_1+m_3-1-l} \Gamma\left(l-k-m_3+1, \frac{\sigma^2}{\lambda_3 P_{PU}}\right) \left[1 - \frac{\Gamma(m_2, k_0 Q_p / (\lambda_2 P_m))}{\Gamma(m_2)} \right] \right. \\
 &\quad \left. + \frac{\Gamma(m_1+1)}{\Gamma(m_2)} \left(\frac{k_0 Q_p}{\lambda_2 P_m} \right) \sum_{k=0}^{m_3-1} \binom{m_3-1}{k} \left(\frac{-\sigma^2}{\lambda_3 P_{PU}} \right)^{m_3-1-k} \Gamma\left(k, \frac{\sigma^2}{\lambda_3 P_{PU}}\right) \Gamma\left(m_2-1, \frac{k_0 Q_p}{\lambda_2 P_m}\right) \right\}. \tag{3.66}
 \end{aligned}$$

It is interesting that for Rayleigh fading and when $\lambda_1=1/m_1$, the mean value does not depend on the parameter m_1 as we obtain

$$\begin{aligned}
 E(\gamma) &= \frac{e^{\sigma^2/(\lambda_3 P_{PU})}}{\Gamma(m_3)} \sum_{k=0}^{m_3-1} \binom{m_3-1}{k} \left(\frac{-\sigma^2}{\lambda_3 P_{PU}} \right)^{m_3-1-k} \Gamma\left(k, \frac{\sigma^2}{\lambda_3 P_{PU}}\right) \\
 &\quad \times \left\{ (P_m / \lambda_3 P_{PU}) \left[1 - \frac{\Gamma(m_2, k_0 Q_p / (\lambda_2 P_m))}{\Gamma(m_2)} \right] - \frac{(k_0 Q_p / \lambda_3 P_{PU})}{\lambda_2 \Gamma(m_2)} \Gamma\left(m_2-1, \frac{k_0 Q_p}{\lambda_2 P_m}\right) \right\}. \tag{3.67}
 \end{aligned}$$

Using the equation (3.66), the mean value of received signal to interference and noise ratio is presented as a function of the interference power constraint Q_p in Figure 3.8. It is assumed that perfect CSI is available to the secondary user ($k_o=1$) and $m_1=m_2=m_3=2$. The analysis is studied for different values of transmission power constraint P_m and interference-to-noise ratio (INR) values, where $\text{INR} = m_3 \lambda_3 P_{PU} / \sigma^2$ considering the case when the total average interference co-channel P_{PU} , and noise power at the receiver have fixed value $P_{PU} + \sigma^2 = 1$. Numerical results are obtained using (3.63), (3.64) and (3.65) when $n=1$.

As expected, the mean value of SINR increases with the raise of interference power constraint Q_p . On the other hand, for a fixed Q_p average SINR increases for larger values of transmit power constraint P_m . Furthermore, for a given value of P_m , with the increase of INR, the average value of SINR increases.

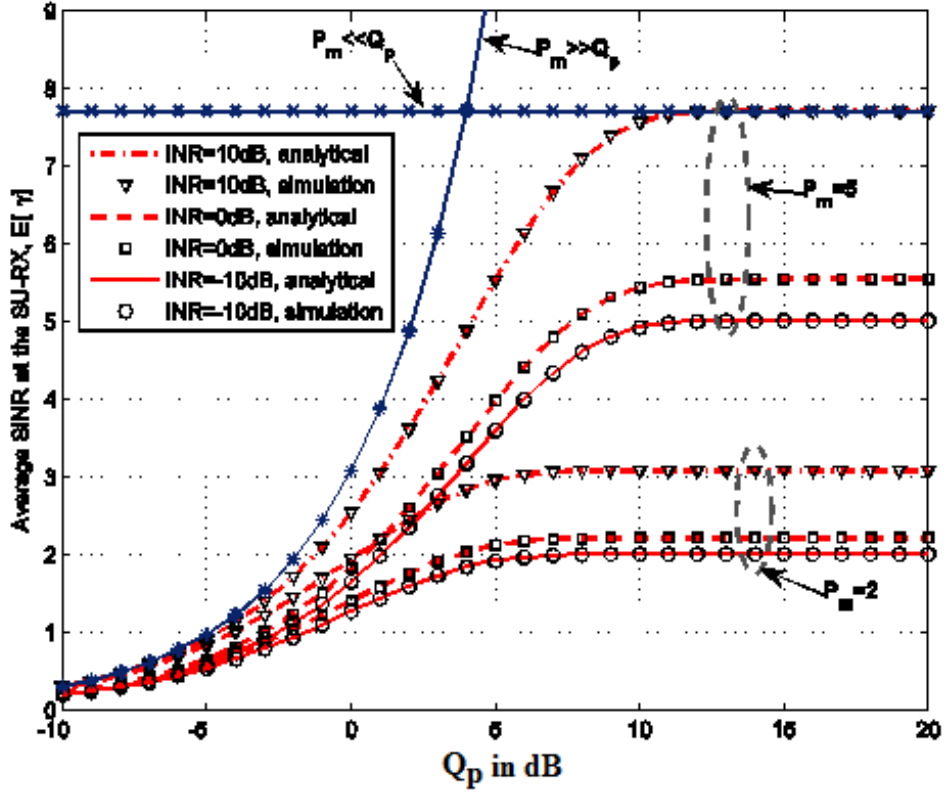


Figure 3.8 – Mean value of SINR for various values of P_m and INR when $m_i=2$, $\lambda_i=1/m_i$, $k_o=1$, and $P_{PU}+\sigma^2=1$.

This indicates that the quality of secondary link should be improved in the case when INR=10dB (interference \gg noise, interference-limited case) compared to the case where INR=-10dB (interference \ll noise, noise-limited case). However, this conclusion seems to be in contradiction with the effect noticed in Figure 3.2, where the presence of interference is more critical than the noise as it results in a higher outage probability.

This effect can be explained by calculating the amount of fading (AF), which is usually, computed using the moments of SINR given in

$$AF = \frac{\sigma_\gamma^2}{E(\gamma)^2} = \frac{\left(\sqrt{E(\gamma^2) - (E(\gamma))^2}\right)^2}{E(\gamma)^2} = \frac{E(\gamma^2)}{E(\gamma)^2} - 1. \quad (3.68)$$

The amount of fading is defined as the ratio of the received signal variance to its mean value square.

The importance of AF is to understand how it is in some cases larger outage probability gives a better quality in the system as it is explained in Figure 3.9.

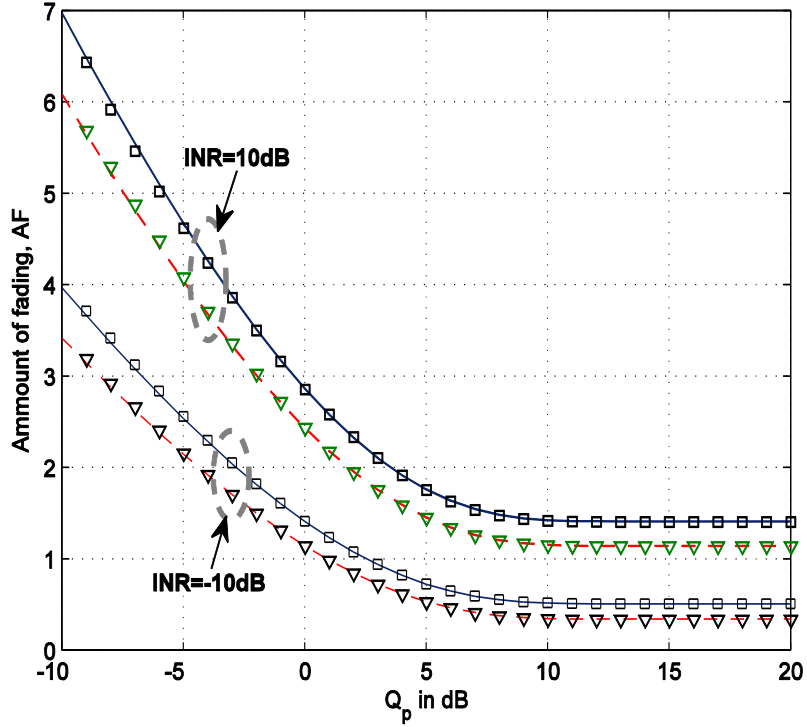


Figure 3.9 – Amount of fading for SINR, $m_i=2$, $\lambda_i=1/m_i$, $P_m=5$, $P_{PU}+\sigma^2=1$.

The results clearly show that the amount of fading decreases as Q_p increases. For the case of interference-limited system (INR=10dB), it can be noticed that $AF > 1$ in the whole range of Q_p . Therefore, even in the cases when SINR mean value is much larger than threshold ($E(\gamma) \gg \rho$), the random process $\gamma(t)$ is more frequently below the threshold due to the large value of σ_γ^2 (the fluctuations of the signal). However, when system is dominantly limited by noise (INR=-10dB), the AF decreases faster and for the large values of Q_p , we have $AF < 1$. In the noise-limited systems this results in a lower outage probability for large Q_p , although the average value of SINR is smaller than it is in the PU interference-limited case. This effect is more noticeable for large values of the fading parameter m_1 , which corresponds to the numerical results presented in Figure 3.2.

Appendix 3 – A

To derive of the closed form expression of PDF for SINR, that is given in equation (3.25) for perfect CSI case, beginning from the equation (3.24)

$$f_{\gamma}(\gamma) = \left(\frac{P_{PU}}{P_m} \right)^{m_1} \sum_{k=0}^{m_1} \alpha_k \frac{\gamma^{m_1-1} e^{-\frac{\gamma\sigma^2}{\lambda_1 P_m}}}{(\gamma\lambda_3 P_{PU} / P_m + \lambda_1)^{k+m_3}} \left[\frac{1}{\lambda_2^{m_2} \Gamma(m_2)} \int_0^{Q_p/P_m} y_2^{m_2-1} e^{-y_2/\lambda_2} dy_2 \right] \\ + \left(\frac{P_{PU}}{Q_p} \right)^{m_1} \frac{\gamma^{m_1-1}}{\lambda_2^{m_2} \Gamma(m_2)} \sum_{k=0}^{m_1} \alpha_k \left[\int_{Q_p/P_m}^{+\infty} y_2^{m_1+m_2-1} \frac{e^{-y_2 \left[\frac{\gamma\sigma^2}{\lambda_1 Q_p} + \frac{1}{\lambda_2} \right]}}{(\gamma y_2 \lambda_3 P_{PU} / Q_p + \lambda_1)^{k+m_3}} dy_2 \right], \quad (3A.1)$$

using [88, eq. (8.350-2)], it can be seen easily that

$$\frac{1}{\lambda_2^{m_2} \Gamma(m_2)} \int_0^{Q_p/P_m} y_2^{m_2-1} e^{-y_2/\lambda_2} dy_2 = 1 - \frac{\Gamma(m_2, Q_p/P_m)}{\Gamma(m_2)}. \quad (3A.2)$$

The other integral can be also easily expressed as a summation of incomplete Gamma functions [88, eq. (8.350-2)] after substituting $y_2 + \lambda_1 Q_p / \gamma \lambda_3 P_{PU} = t$ and applying the binomial expansions [88, eq. (1.111)] to get

$$I = \frac{e^{\frac{\sigma^2}{\lambda_3 P_{PU}} + \frac{\lambda_1 Q_p}{\gamma \lambda_2 \lambda_3 P_{PU}}}}{\gamma} \sum_{k=0}^{m_1} \binom{m_1}{k} \frac{\Gamma(k+m_3)}{\Gamma(m_1)\Gamma(m_2)\Gamma(m_3)} \left(\frac{\sigma^2}{\lambda_3 P_{PU}} \right)^{m_1-k} \sum_{l=0}^{m_1+m_2-1} \binom{m_1+m_2-1}{l} (-1)^{m_1+m_2-l-1} \\ \times \left(\frac{\lambda_1 Q_p}{\gamma \lambda_2 \lambda_3 P_{PU}} \right)^{m_2+m_3+k-l-1} \left(\frac{\gamma \lambda_2 \sigma^2}{\lambda_1 Q_p} + 1 \right)^{m_3+k-l-1} \Gamma \left(l-k-m_3+1, \frac{\gamma \sigma^2 \lambda_2 + \lambda_1 Q_p}{\lambda_1 \lambda_2 P_m} + \frac{\gamma \sigma^2 \lambda_2 + \lambda_1 Q_p}{\gamma \lambda_2 \lambda_3 P_{PU}} \right). \quad (3A.3)$$

Substituting (3A.2) and (3A.3) in the equation (3A.1), the final closed-form for probability density function of SINR is obtained.

Appendix 3 – B

Starting from the outage probability expression given in (3.28), the first integral defined in (3.29) can be solved first by substituting the PDF of x given in (3.22) and the PDF of y_2 given in (3.16) to get

$$a(\rho) = \left(\frac{P_{PU}}{P_m} \right)^{m_1} \sum_{k=0}^{m_1} \alpha_k \int_{\rho}^{\infty} \frac{\gamma^{m_1-1} e^{-\gamma\sigma^2/(\lambda_1 P_m)}}{(\gamma\lambda_3 P_{PU}/P_m + \lambda_1)^{k+m_3}} d\gamma \left[\int_0^{Q_p/P_m} \frac{y_2^{m_2-1} e^{-y_2/\lambda_2}}{\lambda_2^{m_2} \Gamma(m_2)} dy_2 \right], \quad (3B.1)$$

Substituting (3A.2) and applying the substitution $t = \gamma + \lambda_1 P_m / (P_{PU} \lambda_3)$ and the binomial expansion, the final expression of (3B.1) is given in (3.31).

For the second integral defined in (3.30), after using the PDF of x and y_2 given in (3.22) and (3.16), respectively, incomplete gamma function expression and binomial expansion [88, eqs. (8.350-2) and (1.111)] are applied to get

$$b(\rho) = \frac{1}{\Gamma(m_2)\Gamma(m_3)\lambda_2^{m_2}\lambda_3^{m_3}} \sum_{k=0}^{m_1-1} \frac{(\rho P_{PU}/\lambda_1 Q_p)^k}{k!} \sum_{l=0}^k \binom{k}{l} \left(\frac{\sigma^2}{P_{PU}} \right)^{k-l} \quad (3B.2)$$

$$\times \Gamma(m_3 + l) \left(\frac{\lambda_1 Q_p}{\rho P_{PU}} \right)^{m_3+l} \int_{Q_p/P_m}^{+\infty} \frac{y_2^{m_2+k-1} e^{-y_2 \left(\frac{\rho\sigma^2}{\lambda_1 k_m Q_p} + \frac{1}{\lambda_2} \right)}}{(y_2 + \lambda_1 Q_p / \rho \lambda_3 P_{PU})^{m_3+l}} dy_2,$$

using the substitution $t = y_2 + \lambda_1 Q_p / \rho \lambda_3 P_{PU}$, the equation (3B.2) can be written as

$$b(\rho) = \frac{1}{\Gamma(m_2)\Gamma(m_3)\lambda_2^{m_2}\lambda_3^{m_3}} \sum_{k=0}^{m_1-1} \frac{1}{k!} \sum_{l=0}^k \binom{k}{l} \Gamma(m_3 + l) \left(\frac{\sigma^2}{P_{PU}} \right)^{k-l} \left(\frac{\lambda_1 k_m Q_p}{\gamma P_{PU}} \right)^{m_3+l-k} \quad (3B.3)$$

$$\times \sum_{j=0}^{m_2+k-1} \binom{m_2+k-1}{j} \left(-\frac{\lambda_1 k_m Q_p}{\gamma \lambda_3 P_{PU}} \right)^{m_2+k-1-j} e^{\frac{\lambda_1 k_m Q_p}{\gamma \lambda_3 P_{PU}} \left(\frac{\gamma\sigma^2}{\lambda_1 k_m Q_p} + \frac{k_m}{\lambda_2} \right)} \int_{k_m Q_p / P_m + A}^{+\infty} t^{j-m_3-l} e^{-t \left(\frac{\rho\sigma^2}{\lambda_1 k_m Q_p} + \frac{1}{\lambda_2} \right)} dt.$$

Finally, applying the identity [88, eq. (8.350-2)], the last form of (3B.3) integral is given in (3.32).

Appendix 3 – C

Starting from the expression given in (3.37), the first part is given as

$$E_1(\gamma^n) = \int_0^\infty \gamma^n \frac{f_x(\gamma / (P_m / P_{PU}))}{P_m / P_{PU}} \left[\int_0^{Q_p / P_m} f_{y_2}(y_2) dy_2 \right] d\gamma, \quad (3C.1)$$

which can be solved substituting $t = \gamma + \lambda_1 P_m / (\lambda_3 P_{PU})$, using the binomial expansion and the expression for uncompleted gamma function to get

$$E_1(\gamma^n) = \frac{e^{\sigma^2 / \lambda_3 P_{PU}} \left(\frac{\lambda_1 P_m}{\lambda_3 P_{PU}} \right)^n}{\Gamma(m_1) \Gamma(m_3)} \times \left\{ \sum_{k=0}^{m_1} \binom{m_1}{k} \Gamma(k + m_3) \sum_{l=0}^{m_1+n-1} \binom{m_1+n-1}{l} (-1)^{m_1+n-1-l} \right. \\ \left. \left(\frac{\sigma^2}{\lambda_3 P_{PU}} \right)^{m_1+m_3-1-l} \Gamma \left(l - k - m_3 + 1, \frac{\sigma^2}{\lambda_3 P_{PU}} \right) \left[1 - \frac{\Gamma(m_2, Q_p / (\lambda_2 P_m))}{\Gamma(m_2)} \right] \right\}. \quad (3C.2)$$

The second part is given as

$$E_2(\gamma^n) = \int_0^\infty \int_{Q_p / P_m}^{+\infty} \gamma^n f_{y_2}(y_2) \frac{f_x(\gamma / (Q_p / (P_{PU} y_2)))}{Q_p / (P_{PU} y_2)} dy_2 d\gamma, \quad (3C.3)$$

following the same process like the outage probability derivation from (3B.2) to (3B.3) to get the final expression for the second part as follows

$$E_2(\gamma^n) = \frac{\lambda_1^n (Q_p / P_{PU})^n \Gamma(m_1 + n)}{\Gamma(m_1) \Gamma(m_2) \Gamma(m_3) \lambda_2^n \lambda_3^{m_3}} e^{\sigma^2 / \lambda_3 P_{PU}} \sum_{k=0}^{m_3-1} \binom{m_3-1}{k} \\ \times \left(\frac{-\sigma^2}{P_{PU}} \right)^{m_3-1-k} \lambda_3^{k-n+1} \Gamma \left(k - n + 1, \frac{\sigma^2}{\lambda_3 P_{PU}} \right) \Gamma \left(m_2 - n, \frac{Q_p}{\lambda_2 P_m} \right). \quad (3C.4)$$

Substituting (3C.2) and (3C.4) in (3.37), the closed-form expression for the moments of SINR is given in (3.38).

4. Spectrum sharing systems with co-channel interference and MRC diversity technique

It is well known that Maximal Ratio Combining (MRC) is the optimal combining diversity technique that maximizes the output signal-to-noise ratio (SNR) [91]. In this chapter, the analysis of a spectrum sharing system employing MRC at the secondary receiver in Nakagami fading environment is presented. The co-channel interference from the primary transmitter to secondary receiver is considered under the constraints of peak interference power at primary receiver and maximal transmit power at secondary transmitter. Three cases of Channel State Information (CSI) of the channel from SU-Tx to PU-Rx perfect: perfect, outdated and mean value based power allocation (statistical) have been analyzed. The results in this chapter are part from the published results in the international journal Frequenz [58].

The enhancement of the secondary link capacity by employing MRC at the secondary receiver under average transmit power constraint is proposed in [92], while it is studied under average interference power constraint in [67]. The closed-form expression of ergodic capacity for the secondary link is derived, where the authors have analyzed the case when the secondary link is under Rayleigh fading and the primary link is under Nakagami fading distribution, while the exact capacity expressions for Nakagami propagation are provided in [86]. Furthermore, the case when both the SU's transmit power and the peak interference power at PU receiver are limited is analyzed in [93], and in [94] with Orthogonal Space Time Block Codes (OSTBC) but only the approximate capacity expressions are provided for Rayleigh fading, while the closed-form expressions are given in [95]. For Nakagami fading environment, ergodic capacity

expression is derived in [96] but it is limited to the case when the instantaneous power gain from secondary transmitter to primary receiver is perfectly known.

The impact of imperfect channel state information of the link between secondary transmitter and primary receiver on cognitive radio system performance with MRC is studied in [97] for Rayleigh fading environment under average transmit power constrain only. It is shown that even when the estimation error variance in the CSI is large, increasing the degrees of MRC combining diversity could achieve more capacity than in estimation error free case. In mobile radio systems, antenna diversity is used to combat fading and reduce the impact of co-channel interference. Analysis given in [98] illustrates the improvement of the system performance in the presence of co-channel interference signal due to application of the MRC technique.

Outage probability in mobile radio system that uses MRC is derived in a closed form in the presence of multiple interferers [99]. Moreover, the performances of MRC are studied for Nakagami fading environment considering multiple equal power co-channel interferers and the closed-form expression for outage probability of SINR was derived in [100], while in [101] the expression was derived for the case of arbitrary power co-channel interference. Furthermore, the closed-form expression for outage probability in a mobile system is derived and the results indicate that MRC diversity effectively increases the fading parameter of the signal of interest (SOI) by a factor equal to the number of diversity branches.

Specifically in this chapter:

- Analysis of signal to interference and noise ratio when MRC is applied at secondary user.
- Closed-form expressions of probability density function, outage probability, in addition to the study of outage capacity with MRC diversity technique.
- Three cases of available channel state information have been assumed in the study: perfect, outdated and statistical CSI.
- Analysis of the noise-free case (SIR) with OSTBC.
- Numerical results are presented for various propagation conditions and the correctness of analytical results is verified by using an independent simulation method.

4.1 Cognitive Radio System with MRC Diversity for Perfect CSI

This section is extended from the section 3.1 in chapter 3, where the considered system model is the same but with a maximum ratio combining (MRC) diversity technique applied at the secondary receiver. System model block is given in Figure 4.1, where the secondary receiver uses an arbitrary number of antennas n_R , while the primary user is equipped with a single antenna at its transmitter and receiver. We assume a perfect CSI knowledge of the power gain in all channels.

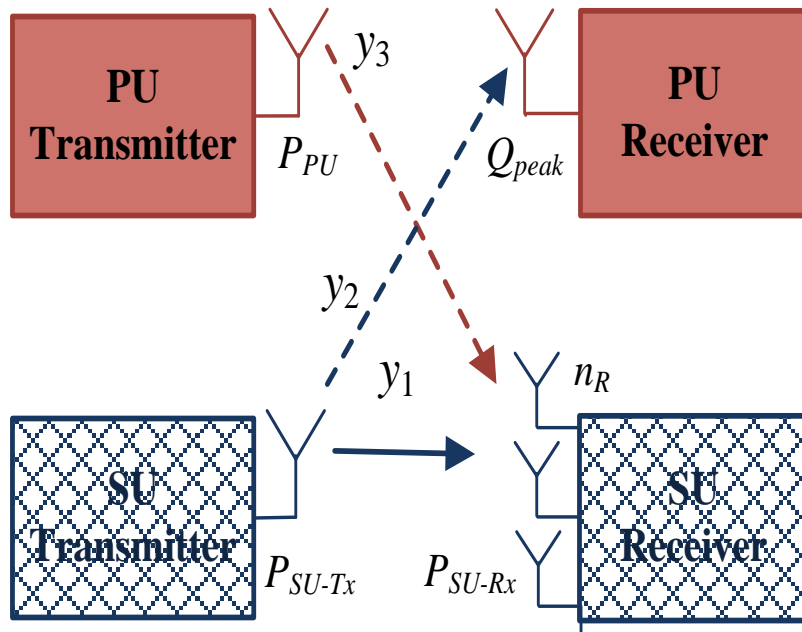


Figure 4.1 – Spectrum sharing system model with co-channel interference and receiving MRC diversity technique.

The fading envelopes in all channels have been assumed to be independent Nakagami random variables (RVs). Let m_i denotes the fading parameter and $\lambda_i = E[y_i]/m_i$ is the normalized value of the channel power gain y_i , where $i=1, 2, 3$, respectively, corresponds to the channels from SU-Tx to SU-Rx, SU-Tx to PU-Rx, and from PU-Tx to SU-Rx. Furthermore, it is supposed that the fading parameter in all the branches at secondary receiver is equal to $m_{1_j} = m_1$, where $j=1, \dots, n_R$.

The transmission power allocation of secondary transmitter is given in (3.11), and signal- to interference and noise ratio SINR is given in (3.8) as

$$\gamma = \frac{y_1 (\mathcal{Q}_p / y_2)}{P_{PU} y_3 + \sigma^2} = \frac{y_1}{y_2} \frac{\mathcal{Q}_p}{P_{PU} (y_3 + \sigma^2 / P_{PU})}. \quad (4.1)$$

4.1.1 Statistical Characterizations of SINR with MRC

As MRC diversity is employed at the secondary receiver with n_R antennas, the probability density function (PDF) of the equivalent power gain at the secondary link

$$y_1 = \sum_{j=1}^{n_R} |h_j|^2, \quad (j=1, \dots, n_R), \text{ where } h_j \text{ is the fading envelop in each branch at the secondary}$$

receiver, is given as [100, eq. (2)]

$$f_{y_1}(y_1) = \frac{y_1^{m_1 n_R - 1}}{\lambda_1^{m_1 n_R} \Gamma(m_1 n_R)} e^{-y_1 / \lambda_1}. \quad (4.2)$$

The probability density function of the power gain in the channel from secondary transmitter to primary receiver is given in (3.16). Although the MRC is applied, the power gain of the interference from primary transmitter to secondary receiver does not depend on the number of receive antennas, n_R , and the PDF of its channel power gain can be written as the expression in (3.16) [100, eq. (3)]. Following the same process in deriving the probability density function for SINR from (3.17)-(3.24) by substituting every m_1 with $m_1 n_R$, the PDF of SINR with MRC technique at the receiver can be written as

$$\begin{aligned} f_\gamma(\gamma) &= \left(\frac{\lambda_1 P_m}{\lambda_3 P_{PU}} \right)^{m_3} \sum_{k=0}^{m_1 n_R} \binom{m_1 n_R}{k} \frac{\Gamma(k + m_3)}{\Gamma(m_1 n_R) \Gamma(m_3)} \left(\frac{\sigma^2}{\lambda_1 P_m} \right)^{m_1 n_R - k} \frac{\gamma^{m_1 n_R - 1} e^{-\gamma \sigma^2 / \lambda_1 P_m}}{(\gamma + \lambda_1 P_m / \lambda_3 P_{PU})^{k + m_3}} \\ &\left[1 - \frac{\Gamma(m_2, \mathcal{Q}_p / P_m)}{\Gamma(m_2)} \right] + \frac{e^{\frac{\sigma^2}{\lambda_3 P_{PU}} + \frac{\lambda_1 \mathcal{Q}_p}{\gamma \lambda_2 \lambda_3 P_{PU}}}}{\gamma} \sum_{k=0}^{m_1} \binom{m_1 n_R}{k} \frac{\Gamma(k + m_3)}{\Gamma(m_1 n_R) \Gamma(m_2) \Gamma(m_3)} \left(\frac{\sigma^2}{\lambda_3 P_{PU}} \right)^{m_1 n_R - k} \\ &\sum_{l=0}^{m_1 n_R + m_2 - 1} \binom{m_1 n_R + m_2 - 1}{l} (-1)^{m_1 n_R + m_2 - l - 1} \left(\frac{\lambda_1 \mathcal{Q}_p}{\gamma \lambda_2 \lambda_3 P_{PU}} \right)^{m_2 + m_3 + k - l - 1} \\ &\left(\frac{\gamma \lambda_2 \sigma^2}{\lambda_1 \mathcal{Q}_p} + 1 \right)^{m_3 + k - l - 1} \Gamma \left(l - k - m_3 + 1, \frac{\gamma \sigma^2 \lambda_2 + \lambda_1 \mathcal{Q}_p}{\lambda_1 \lambda_2 P_m} + \frac{\gamma \sigma^2 \lambda_2 + \lambda_1 \mathcal{Q}_p}{\gamma \lambda_2 \lambda_3 P_{PU}} \right), \end{aligned} \quad (4.3)$$

where α_k is given as

$$\alpha_k = \binom{m_1 n_R}{k} \frac{\Gamma(k + m_3)}{\Gamma(m_1 n_R) \Gamma(m_3)} \lambda_1^{m_3} \lambda_3^k \left(\frac{\sigma^2}{\lambda_1 P_{PU}} \right)^{m_1 n_R - k}. \quad (4.4)$$

The closed-form expression for outage probability of SINR with MRC diversity can be similarly derived following the same procedure given in (3.27)-(3.30) by substituting each m_1 with $m_1 n_R$ to get the final expression of outage probability as $P_{out}(\rho) = 1 - a(\rho) - b(\rho)$, where

$$a(\rho) = \sum_{k=0}^{m_1 n_R} \binom{m_1 n_R}{k} \frac{\Gamma(k + m_3)}{\Gamma(m_1 n_R) \Gamma(m_3)} \left[1 - \frac{\Gamma(m_2, \mathcal{Q}_p / \lambda_2 P_m)}{\Gamma(m_2)} \right] \sum_{l=0}^{m_1 n_R - k} \binom{m_1 n_R - 1}{l} (-1)^{m_1 n_R - 1 - l} \left(\frac{\sigma^2}{\lambda_3 P_{PU}} \right)^{m_1 n_R + m_3 - 1 - l} e^{\frac{\sigma^2}{\lambda_3 P_{PU}}} \Gamma \left(l - k - m_3 + 1, \frac{\rho \sigma^2}{\lambda_1 P_m} + \frac{\sigma^2}{\lambda_3 P_{PU}} \right), \quad (4.5)$$

and

$$b(\rho) = \frac{e^{\left(\frac{\lambda_1 \mathcal{Q}_p}{\rho \lambda_3 P_{PU}} \right) \left(\frac{\rho \sigma^2}{\lambda_1 \mathcal{Q}_p} + \frac{1}{\lambda_2} \right)}}{\Gamma(m_2) \Gamma(m_3) \lambda_2^{m_2}} \sum_{k=0}^{m_1 n_R - 1} \sum_{l=0}^k \binom{k}{l} \frac{\Gamma(m_3 + l)}{k!} \left(\frac{\sigma^2}{\lambda_3 P_{PU}} \right)^{k-l} \sum_{j=0}^{m_2 + k - 1} \binom{m_2 + k - 1}{j} (-1)^{m_2 + k - 1 - j} \left(\frac{\lambda_1 \lambda_2 \mathcal{Q}_p}{\lambda_1 \mathcal{Q}_p + \lambda_2 \rho \sigma^2} \right)^{j - m_3 - l + 1} \times \left(\frac{\lambda_1 \mathcal{Q}_p}{\rho \lambda_3 P_{PU}} \right)^{m_2 + m_3 + l - 1 - j} \Gamma \left(j - m_3 - l + 1, \left(\frac{\mathcal{Q}_p}{P_m} + \frac{\lambda_1 \mathcal{Q}_p}{\rho \lambda_3 P_{PU}} \right) \left(\frac{\rho \sigma^2}{\lambda_1 \mathcal{Q}_p} + \frac{1}{\lambda_2} \right) \right). \quad (4.6)$$

Moreover, the moments of SINR is given in [87, eq. (7.1)], where $f_\gamma(\gamma)$ is the probability density function of SINR given in (4.3), which can be derived in a closed-form using the same procedure explained in Appendix 3 – C.

The closed-form for the moments of SINR when only statistical CSI is available at SU transmitter is given as follows

$$\begin{aligned}
E(\gamma^n) &= \frac{e^{\sigma^2/\lambda_3 P_{PU}}}{\Gamma(m_1 n_R) \Gamma(m_3)} \left(\frac{\lambda_1 P_m}{\lambda_3 P_{PU}} \right)^n \times \left\{ \sum_{k=0}^{m_1 n_R} \binom{m_1 n_R}{k} \Gamma(k + m_3) \sum_{l=0}^{m_1 n_R + n - 1} \binom{m_1 n_R + n - 1}{l} \right. \\
&\quad \left. (-1)^{m_1 n_R + n - 1 - l} \left(\frac{\sigma^2}{\lambda_3 P_{PU}} \right)^{m_1 n_R + m_3 - 1 - l} \Gamma\left(l - k - m_3 + 1, \frac{\sigma^2}{\lambda_3 P_{PU}}\right) \right. \\
&\quad \left[1 - \frac{\Gamma(m_2, Q_p / (\lambda_2 P_m))}{\Gamma(m_2)} \right] + \frac{\Gamma(m_1 n_R + n)}{\Gamma(m_2)} \left(\frac{Q_p}{\lambda_2 P_m} \right)^n \sum_{k=0}^{m_3 - 1} \binom{m_3 - 1}{k} \\
&\quad \left. \left(\frac{-\sigma^2}{\lambda_3 P_{PU}} \right)^{m_3 - 1 - k} \Gamma\left(k - n + 1, \frac{\sigma^2}{\lambda_3 P_{PU}}\right) \Gamma\left(m_2 - n, \frac{Q_p}{\lambda_2 P_m}\right) \right\}.
\end{aligned} \tag{4.7}$$

4.1.2 Statistical Characterizations of SIR with OSTBC

The considered system in this sub-section is when Orthogonal Space Time Block Codes (OSTBC) are applied at the secondary user with n_T antennas at the transmitter and n_R antennas at the receiver, while primary terminal is equipped with a single antenna as it is shown in Figure 4.2.

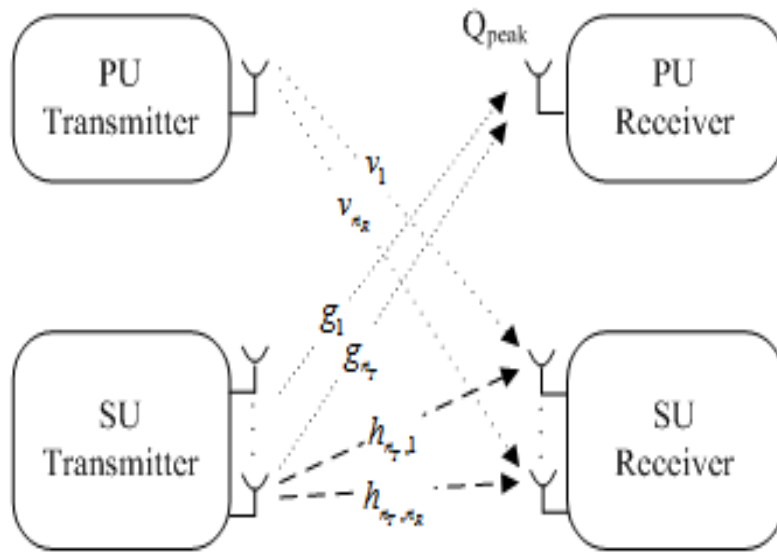


Figure 4.2 – Spectrum sharing system model with co-channel interference with OSTBC.

The fading envelopes between transmit and receive antennas of the secondary user are denoted by h_{ij} ($1 < i < n_T$, $1 < j < n_R$). Furthermore, the fading envelopes between SU transmit and PU receive antennas are denoted by g_i ($1 < i < n_T$), while between the primary transmit and each of the n_R SU receive antennas are denoted by v_j ($1 < j < n_R$). Fading envelopes are following the Nakagami distribution with fading parameters m_1 , m_2 , and m_3 , respectively and the corresponding PDFs are defined as [96]

$$f_{h_{i,j}}(h) = \frac{2h^{2m_1-1} e^{-h^2/\lambda_1}}{\lambda_1^{m_1} \Gamma(m_1)}, \quad h \geq 0, \quad 1 \leq i \leq n_T, \quad 1 \leq j \leq n_R, \quad (4.8)$$

$$f_{g_i}(g) = \frac{2g^{2m_2-1} e^{-g^2/\lambda_2}}{\lambda_2^{m_2} \Gamma(m_2)}, \quad g \geq 0, \quad 1 \leq i \leq n_T, \quad (4.9)$$

$$f_{v_j}(v) = \frac{2v^{2m_3-1} e^{-v^2/\lambda_3}}{\lambda_3^{m_3} \Gamma(m_3)}, \quad v \geq 0, \quad 1 \leq j \leq n_R, \quad (4.10)$$

where $\lambda_1 = E\{|h_{i,j}|^2\}/m_1$, $\lambda_2 = E\{|g_i|^2\}/m_2$ and $\lambda_3 = E\{|v_j|^2\}/m_3$.

The secondary user transmits with the maximal allowable power per transmit antenna as it is given in (3.10) where y_2 is defined as $y_2 = \sum_{i=1}^{n_T} |g_i|^2$. The co-channel signal power transmitted from primary user is given in (3.4), where $y_3 = \sum_{j=1}^{n_R} |g_j|^2$.

Interference-limited scenario is analyzed, where noise power is negligible compared to the interference at the secondary receiver ($\sigma^2 \ll P_i$). Therefore, signal to interference ratio given will be written as

$$\gamma = \frac{y_1 (Q_p / y_2)}{R \times P_{PU} y_3} = \frac{y_1}{y_2 y_3} \frac{Q_p}{R \times P_{PU}}, \quad (4.11)$$

where R is OSTBC rate, and $y_1 = \sum_{i=1}^{n_T} \sum_{j=1}^{n_R} |h_{ij}|^2$.

The previous channel power gains follow χ^2 distribution with $2s=2m_1n_Tn_R$, $2p=2m_2n_T$, and $2w=2m_3n_R$ degrees of freedom, respectively, to get the probability density function of them as follows

$$f_{y_1}(y_1) = \frac{y_1^{s-1} e^{-y_1/\lambda_1}}{\lambda_1^s \Gamma(s)}, y_1 \geq 0, \quad (4.12)$$

$$f_{y_2}(y_2) = \frac{y_2^{p-1} e^{-y_2/\lambda_2}}{\lambda_2^p \Gamma(p)}, y_2 \geq 0, \quad (4.13)$$

$$f_{y_3}(y_3) = \frac{y_3^{w-1} e^{-y_3/\lambda_3}}{\lambda_3^w \Gamma(w)}, y_3 \geq 0. \quad (4.14)$$

The probability density function of SIR can be derived first by deriving the PDF of the ratio of y_1/y_2 using the transformation of random variables [87, eq. (6-63)] and the identity [88, eq. (2.323)]

$$f_{y_1/y_2}(z) = \frac{(\lambda_1)^p (\lambda_2)^s (s+p-1)!}{\Gamma(s) \Gamma(p)} \frac{z^{(s-1)}}{(z\lambda_2 + \lambda_1)^{s+p}}. \quad (4.15)$$

Then by using the substitution $x=z/y_3$ and $t=y_3$, the joint PDF of x and t is given as

$$f_{x,t}(x,t) = \frac{(\lambda_1)^p (\lambda_2)^s (s+p-1)!}{(\lambda_3)^w \Gamma(s) \Gamma(p) \Gamma(w)} \frac{(xt)^{s-1} t^{w-1} e^{-t/\lambda_3}}{(xt\lambda_2 + \lambda_1)^{s+p}} t. \quad (4.16)$$

After computing the PDF of x , the probability density function of SIR can be computed applying linear transformation of random variables to get

$$f_\gamma(\gamma) = \left(\frac{R \times P_{PU}}{Q_p} \right)^s \frac{(\lambda_1)^p (\lambda_2)^s (s+p-1)! \gamma^{s-1}}{(\lambda_3)^w \Gamma(s) \Gamma(p) \Gamma(w)} \int_0^{+\infty} \frac{t^{s+w-1} e^{-t/\lambda_3}}{\left(\frac{\gamma t \lambda_2 R P_{PU}}{Q_p} + \lambda_1 \right)^{s+p}} dt. \quad (4.17)$$

Using the substitution $y = \gamma t \lambda_2 R P_{PU} / Q_p + \lambda_1$ and applying [88, eq. (8.350-2)], the closed-form expression for PDF of SIR is given as

$$f_\gamma(\gamma) = \left(\frac{Q_p}{R \times P_{PU}} \right)^w \frac{(\lambda_1)^p (s+p-1)!}{(\lambda_3)^w (\lambda_2)^w \Gamma(s) \Gamma(p) \Gamma(w)} \frac{e^{\frac{c\lambda_1}{\gamma\lambda_2\lambda_3}}}{\gamma^{w+1}} \sum_{k=0}^{s+w-1} \binom{s+w-1}{k} \times (-\lambda_1)^{s+w-1-k} \left(\frac{\gamma\lambda_2\lambda_3 R P_{PU}}{Q_p} \right)^{k-s-p+1} \Gamma \left(k-s-p+1, \frac{\lambda_1 Q_p}{\gamma\lambda_2\lambda_3 R P_{PU}} \right), \quad (4.18)$$

where the incomplete gamma function can be expressed in different expressions depending on the value of the first argument, as it is given in (3.26).

The probability density function of SIR is presented in Figure 4.3 when the channels do not have a unit power gain, $\lambda_1=1/6$, $\lambda_2=1/4$, $\lambda_3=1/2$, and in Figure 4.4 for the case of unit power gain. The ratio of Q_p/P_{PU} is assumed to equal to 1 for different values of fading parameters in the channels. Alamouti code, as a special case of OSTBC when $(n_T=n_R=2, R=1)$ is compared with the case when MRC $(n_T=1, n_R=2)$ is employed at SU-Rx. It can be noticed that the dependence of probability density function of SIR on fading parameters values is less noticeable when the channels have a unit power gain. Moreover, the analytical results are in agreement with the simulation ones.

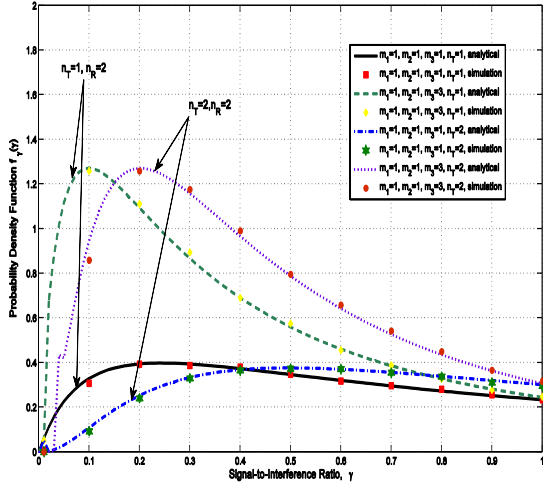


Figure 4.3 – PDF of SIR for Alamouti code scheme and MRC diversity at SU-Rx, $\lambda_1=1/6$, $\lambda_2=1/4$, $\lambda_3=1/2$.

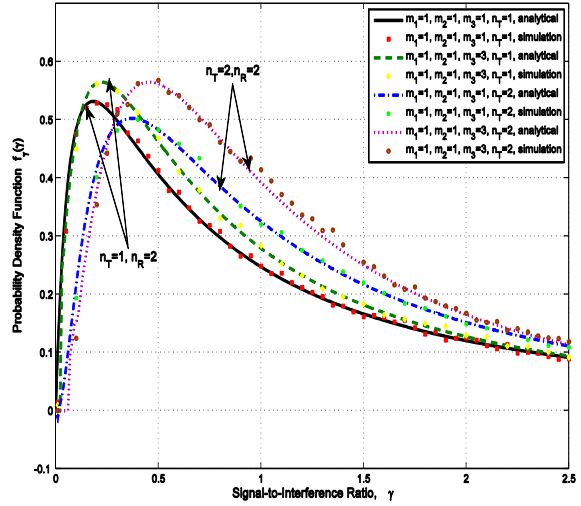


Figure 4.4 – PDF of SIR for Alamouti code scheme and MRC diversity at SU-Rx, $\lambda_i=1/m_i$.

The moments of SIR are derived applying the moment function given in [87, eq. (7.1)]. By substituting the form of probability density function of SIR (4.18) in (3.36) to get

$$E(\gamma^n) = \left(\frac{RP_{PU}}{Q_p} \right)^s \frac{\lambda_1^p \lambda_2^s (s+p-1)!}{\lambda_3^w \Gamma(s) \Gamma(p) \Gamma(w)} \int_0^{+\infty} t^{s+w-1} e^{-\frac{t}{\lambda_3}} \int_0^{+\infty} \frac{\gamma^{s+n-1}}{\left(\frac{\gamma t \lambda_2 RP_{PU}}{Q_p} + \lambda_1 \right)^{s+p}} d\gamma dt. \quad (4.19)$$

Using the substitution $y = \gamma t \lambda_2 R P_{PU} / Q_p + \lambda_1$, and then applying binomial expansion [88, eqs (8.350-2) and (1.111)], the closed-form expression for the moments of SIR is obtained as

$$E(\gamma^n) = \left(\frac{Q_p}{R P_{PU}} \right) \left(\frac{\lambda_1}{\lambda_2 \lambda_3} \right)^n \frac{(s+p-1)!}{\Gamma(s)\Gamma(p)\Gamma(w)} \Gamma(w-n) \sum_{k=0}^{s+n-1} \binom{s+n-1}{k} \frac{(-1)^{s+n-k}}{k-s-p+1}, p > 1. \quad (4.20)$$

The average SIR is presented when $n=1$ in Figure 4.5 for the both cases of Alamouti scheme and MRC. The case when $\lambda_i=1/m_i$ is considered for different values of fading parameters in primary and secondary links. It is noticed that for the given set of parameters, applying more transmit antennas does not give any benefit in the signal strength, furthermore average SIR has greater values for the case of just one transmit antenna.

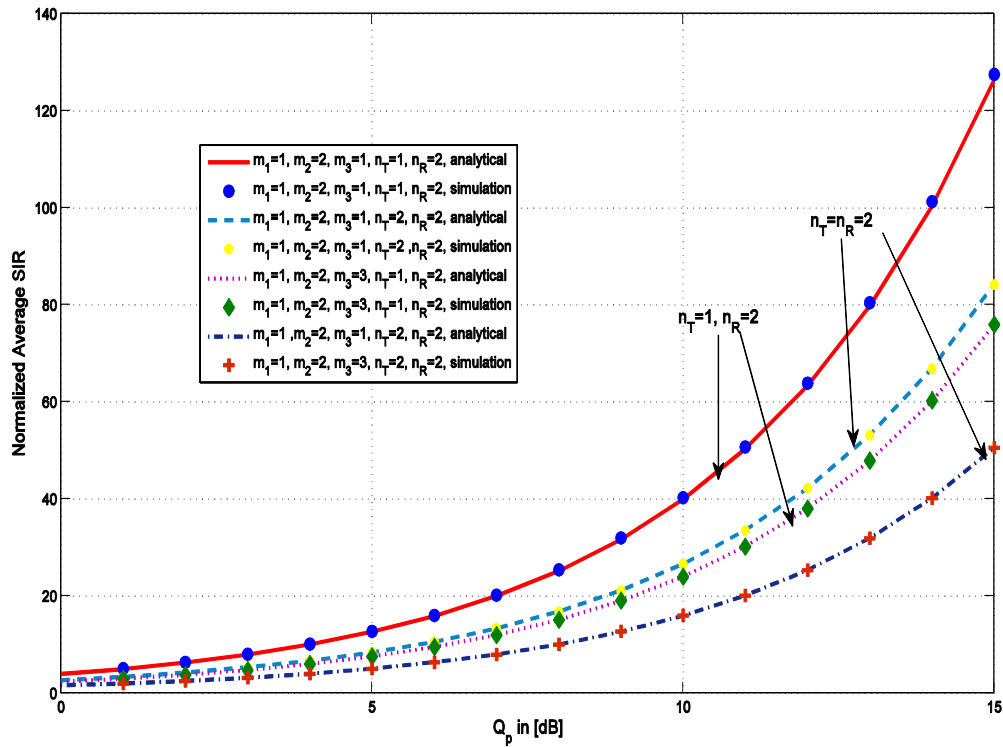


Figure 4.5 – Comparison between Alamouti and MRC.

4.2 Cognitive Radio System with MRC Diversity for Outdated CSI

The considered system in this section is the same one given in Figure 4.1. It is supposed that the secondary user has outdated channel state information of the channel power gain, y_2 , the channel from the secondary transmitter to the primary receiver and full knowledge of the other channels. The maximal transmission power of SU-Tx is given in (3.42), the probability of permitted interference outage is given in (3.43), where the protection coefficient can be calculated from (3.45). Furthermore, the signal to interference and noise ratio is given in (3.46), where the probability density function of the channel power gains is given in (4.2) for y_1 and (3.16) for y_2 and y_3 .

4.2.1 Statistical Characterizations of SINR with MRC and Outdated CSI

In order to derive the probability density function of SINR with MRC for the case of outdated CSI, it can be started from the expression given in (3.48) to get

$$f_{\gamma}(\gamma) = \left(\frac{P_{PU}}{P_m} \right)^{m_1 n_R} \sum_{k=0}^{m_1 n_R} \alpha_k \frac{\gamma^{m_1 n_R - 1} e^{-\frac{\gamma \sigma^2}{\lambda_1 P_m}}}{(\gamma \lambda_3 P_{PU} / P_m + \lambda_1)^{k+m_3}} \left[\frac{1}{\lambda_2^{m_2} \Gamma(m_2)} \int_0^{k_o Q_p / P_m} \hat{y}_2^{m_2-1} e^{-\hat{y}_2 / \lambda_2} d\hat{y}_2 \right] \\ + \left(\frac{P_{PU}}{k_o Q_p} \right)^{m_1 n_R} \frac{\gamma^{m_1 n_R - 1}}{\lambda_2^{m_2} \Gamma(m_2)} \sum_{k=0}^{m_1 n_R} \alpha_k \left[\int_{k_o Q_p / P_m}^{+\infty} \hat{y}_2^{m_1 n_R + m_2 - 1} \frac{e^{-\hat{y}_2 \left[\frac{\gamma \sigma^2}{\lambda_1 k_o Q_p} + \frac{1}{\lambda_2} \right]}}{(\gamma \hat{y}_2 \lambda_3 P_{PU} / k_o Q_p + \lambda_1)^{k+m_3}} d\hat{y}_2 \right], \quad (4.21)$$

where α_k is given in (4.4). Applying the identities in Appendix 3-A, we can get the closed-form expression for probability density function of SINR when MRC is applied for the case of outdated CSI as (3.49) after substituting $m_1 = m_1 n_R$

$$\begin{aligned}
f_\gamma(\gamma) &= \left(\frac{P_{PU}}{P_m} \right)^{m_1 n_R} \sum_{k=0}^{m_1 n_R} \alpha_k \frac{\gamma^{m_1 n_R - 1} e^{-\gamma \sigma^2 / \lambda_1 P_m}}{(\gamma \lambda_3 P_{PU} / P_m + \lambda_1)^{k+m_3}} \left[1 - \frac{\Gamma(m_2, k_o Q_p / P_m)}{\Gamma(m_2)} \right] \\
&+ \frac{e^{\frac{\gamma \sigma^2 \lambda_2 + \lambda_1 k_o Q_p}{\gamma \lambda_2 \lambda_3 P_{PU}}}}{\gamma \lambda_3^{m_1 n_R} \Gamma(m_2)} \sum_{k=0}^{m_1 n_R} \frac{\alpha_k}{\lambda_1^{m_3+k}} \sum_{l=0}^{m_1 n_R + m_2 - 1} \binom{m_1 n_R + m_2 - 1}{l} (-1)^{m_1 n_R + m_2 - l - 1} \\
&\times \left(\frac{\lambda_1 k_o Q_p}{\gamma \lambda_2 \lambda_3 P_{PU}} \right)^{m_2 + m_3 + k - l - 1} \left(\frac{\gamma \sigma^2 \lambda_2}{\lambda_1 k_o Q_p} + 1 \right)^{m_3 + k - l - 1} \\
&\times \Gamma \left(l - k - m_3 + 1, \frac{\gamma \sigma^2 \lambda_2 + \lambda_1 k_o Q_p}{\lambda_1 P_m \lambda_2} + \frac{\gamma \sigma^2 \lambda_2 + \lambda_1 k_o Q_p}{\gamma \lambda_2 \lambda_3 P_{PU}} \right).
\end{aligned} \tag{4.22}$$

The outage probability can be derived by substituting the expression for PDF of SINR (4.22) in the outage probability expression given in (3.27)

$$\begin{aligned}
P_{out}(\rho) &= \left(\frac{P_{PU}}{P_m} \right)^{m_1 n_R} \sum_{k=0}^{m_1 n_R} \alpha_k \int_{\rho}^{\infty} \frac{\gamma^{m_1 n_R - 1} e^{-\frac{\gamma \sigma^2}{\lambda_1 P_m}}}{(\gamma \lambda_3 P_{PU} / P_m + \lambda_1)^{k+m_3}} d\gamma \left[\frac{1}{\lambda_2^{m_2} \Gamma(m_2)} \int_0^{k_o Q_p / P_m} \hat{y}_2^{m_2 - 1} e^{-\hat{y}_2 / \lambda_2} d\hat{y}_2 \right] \\
&+ \left(\frac{P_{PU}}{k_o Q_p} \right)^{m_1 n_R} \sum_{k=0}^{m_1 n_R} \alpha_k \left[\int_{\rho}^{\infty} \frac{\gamma^{m_1 n_R - 1}}{\lambda_2^{m_2} \Gamma(m_2)} \int_{k_o Q_p / P_m}^{+\infty} \hat{y}_2^{m_1 n_R + m_2 - 1} \frac{e^{-\hat{y}_2 \left[\frac{\gamma \sigma^2}{\lambda_1 k_o Q_p} + \frac{1}{\lambda_2} \right]}}{(\gamma \hat{y}_2 \lambda_3 P_{PU} / k_o Q_p + \lambda_1)^{k+m_3}} d\hat{y}_2 d\gamma \right],
\end{aligned} \tag{4.23}$$

to get the final expression as it is in (3.58) and (3.59) after substituting $m_1 = m_1 n_R$ as follows

$$\begin{aligned}
a(\rho) &= \frac{e^{\sigma^2 / \lambda_3 P_{PU}}}{\Gamma(m_1 n_R) \Gamma(m_3)} \left[1 - \frac{\Gamma(m_2, k_o Q_p / (\lambda_2 P_m))}{\Gamma(m_2)} \right] \sum_{k=0}^{m_1 n_R} \binom{m_1 n_R}{k} \Gamma(k + m_3) \\
&\times \sum_{l=0}^{m_1 n_R - 1} \binom{m_1 n_R - 1}{l} (-1)^{m_1 n_R - 1 - l} \left(\frac{\sigma^2}{\lambda_3 P_{PU}} \right)^{m_1 n_R + m_3 - 1 - l} \Gamma \left(l - k - m_3 + 1, \frac{\rho \sigma^2}{\lambda_1 P_m} + \frac{\sigma^2}{\lambda_3 P_{PU}} \right),
\end{aligned} \tag{4.24}$$

and

$$\begin{aligned}
b(\rho) &= \frac{e^{-\frac{\sigma^2}{\lambda_3 P_{PU}} + \frac{\lambda_1 k_o Q_p}{\rho \lambda_2 \lambda_3 P_{PU}}}}{\Gamma(m_2) \Gamma(m_3) \lambda_2^{m_2}} \sum_{k=0}^{m_1 n_R - 1} \sum_{l=0}^k \binom{k}{l} \frac{\Gamma(m_3 + l)}{k!} \left(\frac{\sigma^2}{\lambda_3 P_{PU}} \right)^{k-l} \\
&\quad \times \sum_{j=0}^{m_2+k-1} \binom{m_2+k-1}{j} (-1)^{m_2+k-1-j} \left(\frac{\lambda_1 \lambda_2 k_o Q_p}{\lambda_1 k_o Q_p + \lambda_2 \rho \sigma^2} \right)^{j-m_3-l+1} \\
&\quad \times \left(\frac{\lambda_1 k_o Q_p}{\rho \lambda_3 P_{PU}} \right)^{m_2+m_3+l-1-j} \Gamma \left(j - m_3 - l + 1, \left(\frac{Q_p}{P_m} + \frac{\lambda_1 Q_p}{\rho \lambda_3 P_{PU}} \right) \left(\frac{\rho \sigma^2}{\lambda_1 Q_p} + \frac{k_o}{\lambda_2} \right) \right).
\end{aligned} \tag{4.25}$$

For the special case when the transmission power of the secondary transmitter is unlimited ($P_m \rightarrow \infty$), the probability density function of SINR can be simplified into

$$\begin{aligned}
f_\gamma(\gamma) &= \frac{e^{-\frac{\gamma \sigma^2 \lambda_2 + \lambda_1 n_R k_o Q_p}{\gamma \lambda_2 \lambda_3 P_{PU}}}}{\gamma \lambda_3^{m_1 n_R} \Gamma(m_2)} \sum_{k=0}^{m_1 n_R} \frac{\alpha_k}{\lambda_1^{m_3+k}} \sum_{l=0}^{m_1 n_R + m_2 - 1} \binom{m_1 n_R + m_2 - 1}{l} \left(\frac{\lambda_1 k_o Q_p}{\gamma \lambda_2 \lambda_3 P_{PU}} \right)^{m_2+m_3+k-l-1} \\
&\quad \times (-1)^{m_1 n_R + m_2 - l - 1} \left(\frac{\gamma \sigma^2 \lambda_2}{\lambda_1 k_o Q_p} + 1 \right)^{m_3+k-l-1} \Gamma \left(l - k - m_3 + 1, \frac{\sigma^2}{\lambda_3 P_{PU}} + \frac{\lambda_1 k_o Q_p}{\gamma \lambda_2 \lambda_3 P_{PU}} \right),
\end{aligned} \tag{4.26}$$

then the outage probability is simplified into the expression

$$\begin{aligned}
P_{out}(\rho) &= 1 - \frac{e^{-\left(\frac{\sigma^2}{\lambda_3 P_{PU}} + \frac{\lambda_1 k_o Q_p}{\rho \lambda_2 \lambda_3 P_{PU}} \right)}}{\Gamma(m_2) \Gamma(m_3) \lambda_2^{m_2}} \sum_{k=0}^{m_1 n_R - 1} \frac{\Gamma(m_3 + l)}{k!} \sum_{l=0}^k \binom{k}{l} \left(\frac{\sigma^2}{\lambda_3 P_{PU}} \right)^{k-l} \\
&\quad \times \sum_{j=0}^{m_2+k-1} \binom{m_2+k-1}{j} (-1)^{m_2+k-1-j} \left(\frac{\lambda_1 k_o Q_p}{\rho \lambda_3 P_{PU}} \right)^{m_2+m_3+l-1-j} \\
&\quad \times \left(\frac{\lambda_1 \lambda_2 k_o Q_p}{\lambda_1 k_o Q_p + \rho \lambda_2 \sigma^2} \right)^{j-m_3-l+1} \Gamma \left(j - m_3 - l + 1, \frac{\lambda_1 Q_p}{\rho \lambda_3 P_{PU}} \left(\frac{\rho \sigma^2}{\lambda_1 Q_p} + \frac{k_o}{\lambda_2} \right) \right).
\end{aligned} \tag{4.27}$$

While for the other special case, when the transmission power of secondary transmitter is a fixed value and ($P_m \ll Q_p$), the PDF of SINR can be simplified to

$$f_\gamma(\gamma) = \left(\frac{P_{PU}}{P_m} \right)^{m_1 n_R} \sum_{k=0}^{m_1 n_R} \alpha_k \frac{\gamma^{m_1 n_R - 1} e^{-\gamma \sigma^2 / \lambda_1 P_m}}{(\gamma \lambda_3 P_{PU} / P_m + \lambda_1)^{k+m_3}} \left[1 - \frac{\Gamma(m_2, k_o Q_p / P_m)}{\Gamma(m_2)} \right], \quad (4.28)$$

as a result the outage probability for this case is written as

$$P_{out}(\rho) = 1 - \sum_{k=0}^{m_1 n_R} \binom{m_1 n_R}{k} \frac{e^{\sigma^2 / \lambda_3 P_{PU}} \Gamma(k+m_3)}{\Gamma(m_1 n_R) \Gamma(m_3)} \sum_{l=0}^{m_1 n_R - 1} \binom{m_1 n_R - 1}{l} (-1)^{m_1 n_R - 1 - l} \times \left(\frac{\sigma^2}{\lambda_3 P_{PU}} \right)^{m_1 n_R + m_3 - 1 - l} \Gamma \left(l - k - m_3 + 1, \frac{\rho \sigma^2}{\lambda_1 P_m} + \frac{\sigma^2}{\lambda_3 P_{PU}} \right). \quad (4.29)$$

The outage probability is presented in Figure 4.6 as a function of the peak interference power constraint Q_p , from analytical and asymptotic results to Monte Carlo simulation, for transmission power constraint $P_m=20$, SINR threshold $\rho=0$ dB, fading parameters $m_i=2$ ($i=1, 2, 3$) and different values of the PU's transmit power P_{PU} . Two cases are analysed, the case without noise and the case when noise power is $\sigma^2 = 1$, for the scenario when outdated CSI with $k_o=0.9$ is available at SU-Tx. As expected, the outage probability decreases when MRC with more antennas is applied at the secondary receiver, and the increase of the transmit power of PU-Tx increases the outage probability for any number of antennas. It can also be noticed that when the noise power increases, for any number of receive antenna, outage probability increases. However, the outage probability decreases with the increase of Q_p , and for the high values, when $Q_p > 14$ dB, the outage probability reaches a plateau where P_m constraint dominates. The curves are plotted using (4.24), (4.25), (4.27) and (4.29), the obtained results are verified by simulations.

The Figure 4.7 presents the outage probability as a function of the protection coefficient k_o for the case of outdated CSI, different number of receive antennas, n_R , at secondary receiver when the transmission power constraint is equal to $P_m=10$, the transmission power of the primary transmitter $P_{PU}=4$, SINR threshold $\rho=0$ dB. Furthermore, the fading parameters in all channels are equal to $m_i=5$ (where $i=1, 2, 3$), $\sigma^2 = 1$ and two different values of the interference power constraint $Q_p=2$ dB or 4 dB.

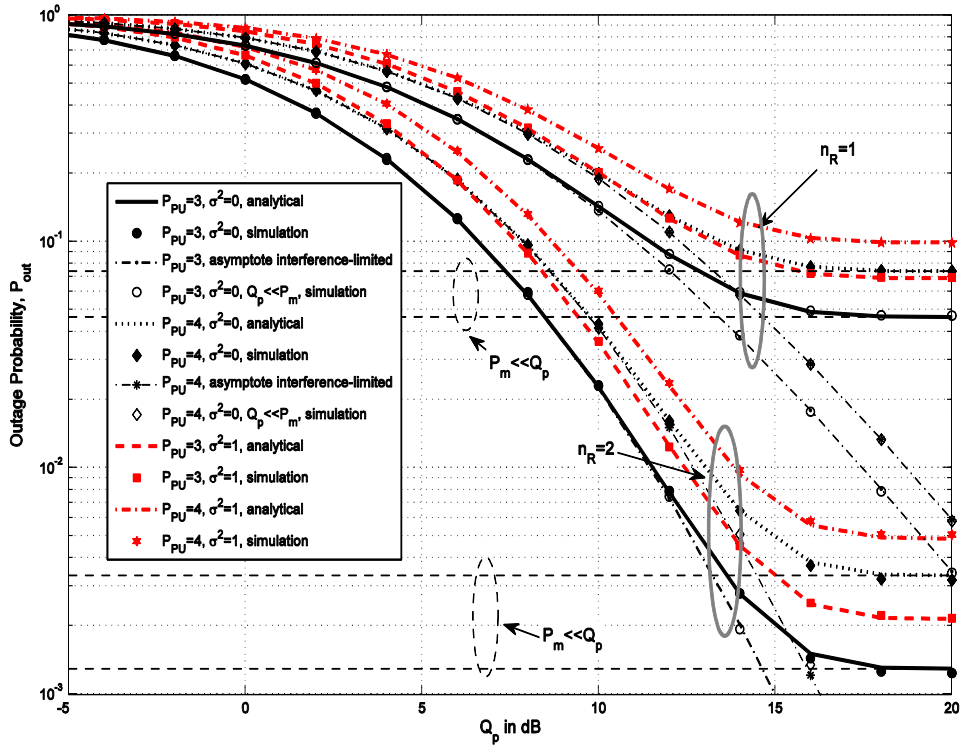


Figure 4.6 – Outage probability for the case of outdated CSI, MRC diversity with $n_R=1$ or $n_R=2$ antennas, $P_m=20$, $\rho=0\text{dB}$, and various values of P_{PU} , with and without noise.

As k_o goes toward 1, outdated CSI is approaching the case of perfect CSI; hence, outage probability decreases as the value of k_o increases for any number of receive antennas. As it is known, outage probability decreases as the maximal allowed interference power Q_p increases, and this effect is more significant for larger number of antennas (the slope of the curve is higher). For a fixed value of k_o , the raise in the number of receive antennas decreases the outage probability. Applying MRC with more receive antennas at SU-Rx can be a reasonable solution in order to obtain a better performance in the presence of outdated CSI. As it is well known, MRC is the optimal combining diversity technique for the case of perfect CSI, and in our results, it can be noticed that the more receive antennas are applied, the less outage probability is obtained. Hence, it has been confirmed that MRC can enhance the performance of the system even in the presence of outdated CSI.

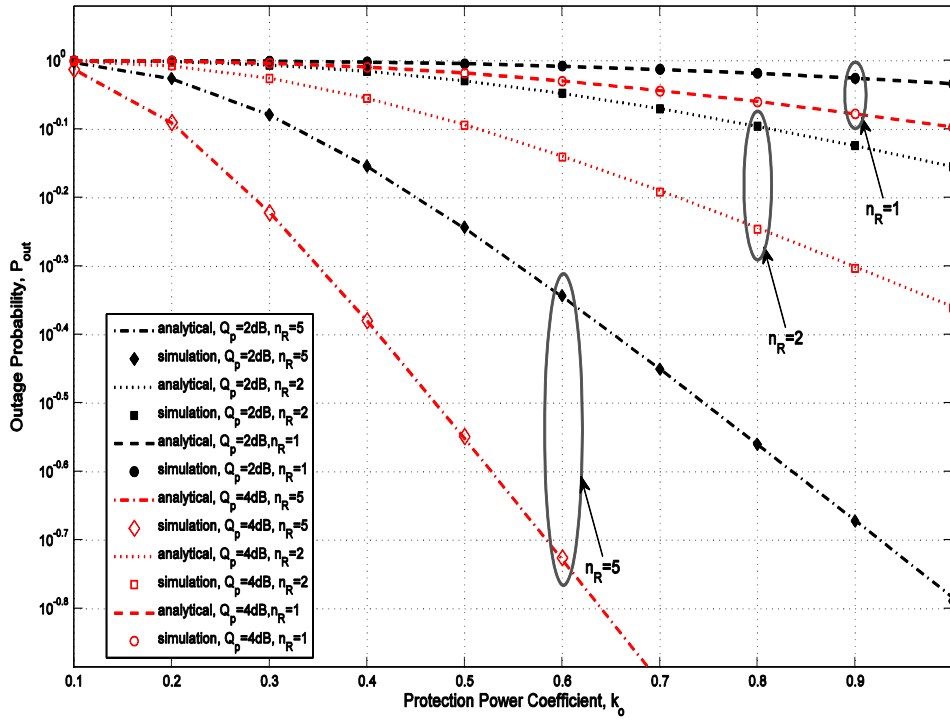


Figure 4.7 – Outage probability vs. protection coefficient, outdated CSI, $P_m = 10$, $\rho = 0\text{dB}$, $P_{PU} = 4$, $Q_p = 2\text{dB}$ or 4dB , $\sigma^2 = 1$ and $m_i = 5$ ($i = 1, 2, 3$) for different number of receive antennas n_R .

4.3 Cognitive Radio System with MRC Diversity for Statistical CSI

The imperfect channel state information of the channel from secondary transmitter to primary receiver has been analysed for the case of outdated CSI, where it supposes that there is cooperation between primary and secondary user, but in some and maybe most realistic cases, primary user does not communicate with the secondary user. In this case, the only available information about the channel state is some statistical characterization of the channel like the average power gain and the fading parameter in that channel, which is known as statistical CSI.

The mean value of the power gain in the link from secondary transmitter to primary receiver is given as $E[y_2] = m_2 \lambda_2$. Using this average value, the transmit power

of SU-Tx can be adjusted to be the maximal available power that secondary user can transmit under the peak received power constraint (3.1) regardless the constrain of its own transmit power as following

$$P_{SU-Tx,max} = k_s \frac{Q_p}{E[y_2]} = k_s \frac{Q_p}{m_2 \lambda_2}, \quad (4.30)$$

where k_s is the protection parameter that tries to protect the primary receiver in the case of imperfect CSI, where the primary user allows the secondary user to exceed the value of peak interference constraint with a maximal permitted probability of interference outage P_o^{th} , and fulfil the following condition

$$\Pr\{y_2 P_{SU-Tx} \leq Q_p\} \geq 1 - P_o^{th}. \quad (4.31)$$

The protection factor k_s can be calculated numerically by substituting the mean value of channel power gain and the transmission value of secondary transmitter given in (4.30) to get

$$\Gamma(m_2, m_2 / k_s) / \Gamma(m_2) = P_o^{th}, \quad (4.32)$$

where it can be seen that the protection parameter depends on m_2 and P_o^{th} . In the special case of Rayleigh fading ($m_2=1$), the protection parameter $k_s < 1$ and can be represented in a closed-form

$$k_s = \frac{1}{\log(1 / P_o^{th})}. \quad (4.33)$$

The maximal transmission power of secondary transmitter is constrained by the transmit power constraint P_m , therefore the power allocation at SU-Tx is given in the following

$$P_{SU-Tx,max} = \min\left(\frac{k_s Q_p}{m_2 \lambda_2}, P_m\right), \quad (4.34)$$

furthermore,

$$P_{SU-Tx} = \begin{cases} P_m, & y_2 \leq k_s Q_p / P_m, \\ k_s Q_p / m_2 \lambda_2, & y_2 > k_s Q_p / P_m, \end{cases} \quad (4.35)$$

that for $m_2=1$, $k_s=1$ corresponds to the approach from [102].

Signal to interference and noise ratio for the case of statistical channel state information is given as in (3.5), where P_{SU-Tx} is given in (4.36).

4.3.1 Statistical Characterizations of SINR with MRC with Statistical CSI

In order to get the probability density function of signal to interference and noise ratio $\gamma = y_1 P_{SU-Tx} / (P_{PU} y_3 + \sigma^2)$ by applying the linear transformation of random variables to get

$$f_\gamma(\gamma) = \frac{f_x(\gamma / (P_{SU-Tx} / P_{PU}))}{(P_{SU-Tx} / P_{PU})}, \quad (4.36)$$

where $f_x(x)$ is the probability density function of the RV $x = y_1 / (y_3 + \sigma^2 / P_{PU})$, following the steps for deriving it in (3.17)-(3.20), the PDF for x can be written as

$$f_x(x) = \sum_{k=0}^{m_1 n_R} \alpha_k \frac{x^{m_1 n_R - 1} e^{-x \sigma^2 / (\lambda_1 P_{PU})}}{(x \lambda_3 + \lambda_1)^{k+m_3}}, \quad \alpha_k = \binom{m_1 n_R}{k} \frac{\Gamma(k+m_3)}{\Gamma(m_1 n_R) \Gamma(m_3)} \lambda_1^{m_3} \lambda_3^k \left(\frac{\sigma^2}{\lambda_1 P_{PU}} \right)^{m_1 n_R - k}. \quad (4.37)$$

Substituting (4.37) in the expression (4.36), the final form for PDF of SINR for the case of statistical CSI is given as follows

$$f_\gamma(\gamma) = \left(\frac{\lambda_1 P_{SU-Tx}}{\lambda_3 P_{PU}} \right)^{m_3} \sum_{k=0}^{m_1 n_R} \binom{m_1 n_R}{k} \frac{\Gamma(k+m_3)}{\Gamma(m_1 n_R) \Gamma(m_3)} \left(\frac{\sigma^2}{\lambda_1 P_{SU-Tx}} \right)^{m_1 n_R - k} \frac{\gamma^{m_1 n_R - 1} e^{-\gamma \sigma^2 / (\lambda_1 P_{SU-Tx})}}{(\gamma + \lambda_1 P_{SU-Tx} / \lambda_3 P_{PU})^{k+m_3}}. \quad (4.38)$$

If it is supposed that $c = \lambda_1 \min(k_s Q_p / m_2 \lambda_2, P_m) / \lambda_3 P_{PU}$, the last expression can be written as

$$f_\gamma(\gamma) = \sum_{k=0}^{m_1 n_R} \binom{m_1 n_R}{k} \frac{\Gamma(k+m_3)}{\Gamma(m_1 n_R) \Gamma(m_3)} \left(\frac{\sigma^2}{\lambda_3 P_{PU}} \right)^{m_1 n_R - k} \frac{c^{m_3 - m_1 n_R + k} \gamma^{m_1 n_R - 1} e^{-\gamma \sigma^2 / (c \lambda_3 P_{PU})}}{(\gamma + c)^{k+m_3}}. \quad (4.39)$$

For this case, the outage probability can be derived using (3.27) after substituting the PDF of SINR (4.40) to get

$$P_{out} = 1 - \sum_{k=0}^{m_1 n_R} \binom{m_1 n_R}{k} \frac{c^{m_3 - m_1 n_R + k} \Gamma(k + m_3)}{\Gamma(m_1 n_R) \Gamma(m_3)} \left(\frac{\sigma^2}{\lambda_3 P_{PU}} \right)^{m_1 n_R - k} \int_{\rho}^{\infty} \frac{\gamma^{m_1 n_R - 1} e^{-\gamma \sigma^2 / (c \lambda_3 P_{PU})}}{(\gamma + c)^{k + m_3}} d\gamma. \quad (4.40)$$

Substituting $\gamma + c = t$, applying the binomial expansion [88, eq. (1.111)] then the incomplete gamma function in [88, eq. (8.350-2)], the final closed-form expression of outage probability for SINR for the case of statistical CSI is given as follows

$$P_{out} = 1 - \sum_{k=0}^{m_1 n_R} \binom{m_1 n_R}{k} \frac{c^{m_3 - m_1 n_R + k} \Gamma(k + m_3) e^{\sigma^2 / (\lambda_3 P_{PU})} \left(\frac{\sigma^2}{\lambda_3 P_{PU}} \right)^{m_1 n_R - k}}{\Gamma(m_1 n_R) \Gamma(m_3)} \sum_{l=0}^{m_1 n_R - 1} \binom{m_1 n_R - 1}{l} \times (-1)^{m_1 n_R - 1 - l} \left(\frac{\sigma^2}{\lambda_3 P_{PU}} \right)^{m_1 n_R + m_3 - l - 1} \Gamma \left(l - k - m_3 + 1, \frac{\sigma^2}{c \lambda_3 P_{PU}} (\rho + c) \right). \quad (4.41)$$

When only statistical CSI of channel power gain for the link from SU-Tx to PU-Rx is available, outage probability vs. peak interference power constraint Q_p is plotted in Figure 4.8 for the case when the noise is not present ($\sigma^2 = 0$). It is assumed that the average power gain has a unit value, i.e. $m_i \lambda_i = 1$ ($i=1, 2, 3$), transmit power of the PU interference is $P_{PU}=4$ and MRC diversity with $n_R=2$ is applied. Results are presented for different interference outage probability values P_o^{th} and two cases of parameter sets, the first one with fading parameter $m_2=3$ and transmit power constraint $P_m=5$, and the second one with $m_2=5$ and $P_m=20$. It can be noticed that the smaller interference outage probability value leads to a higher outage probability of SIR for a fixed value of Q_p . Moreover, the knowledge about statistical CSI results in the practically same P_o^{th} values as for the perfect CSI if the tolerated interference outage probability is large enough. On the other hand, if the fading parameter in the link from SU-Tx to PU-Rx is large enough, the outage probability can be accurately lower bounded by (3.61) and (3.62) when m_l is replaced by $m_l n_R$ and can be upper bounded by (3.62).

This effect can be explained with the fact that the variations from the mean power gain are smaller for larger m_2 . In such a case, in the scenario of available statistical CSI, the protection parameter k_s has large values even for small required P_o^{th} , and this effect is illustrated in the Figure 4.9. For large values of parameter k_s , the reduction of the transmitted power is not significant and the outage probability has small values, similar to the case when perfect CSI is available.

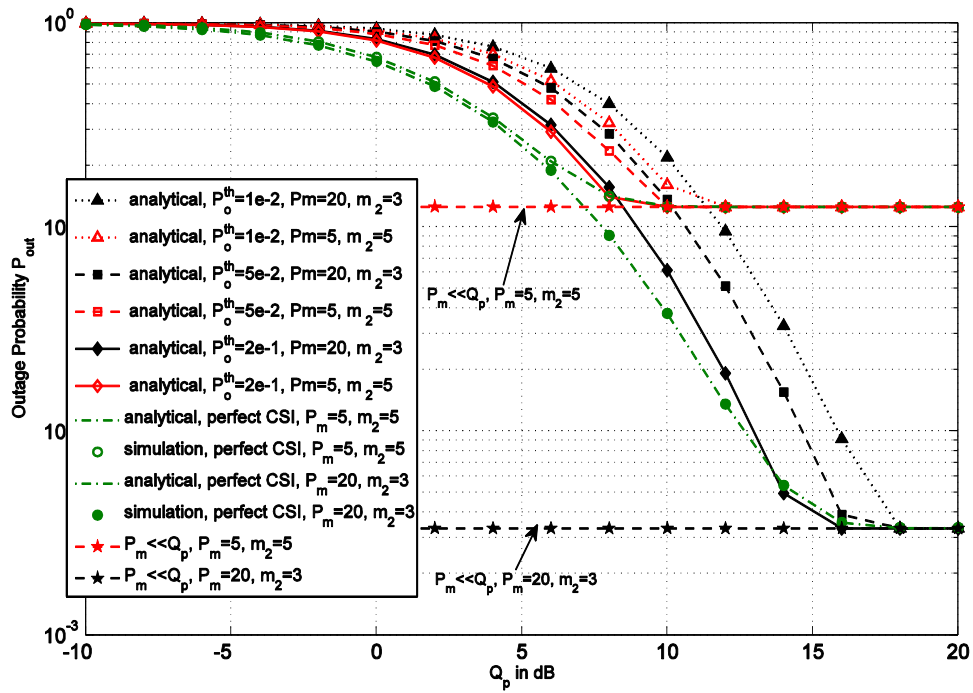


Figure 4.8 – Outage probability for the case of statistical CSI, MRC diversity with $n_R=2$, $m_1=m_3=2$, $P_{PU}=4$ and different values of permitted interference probability.

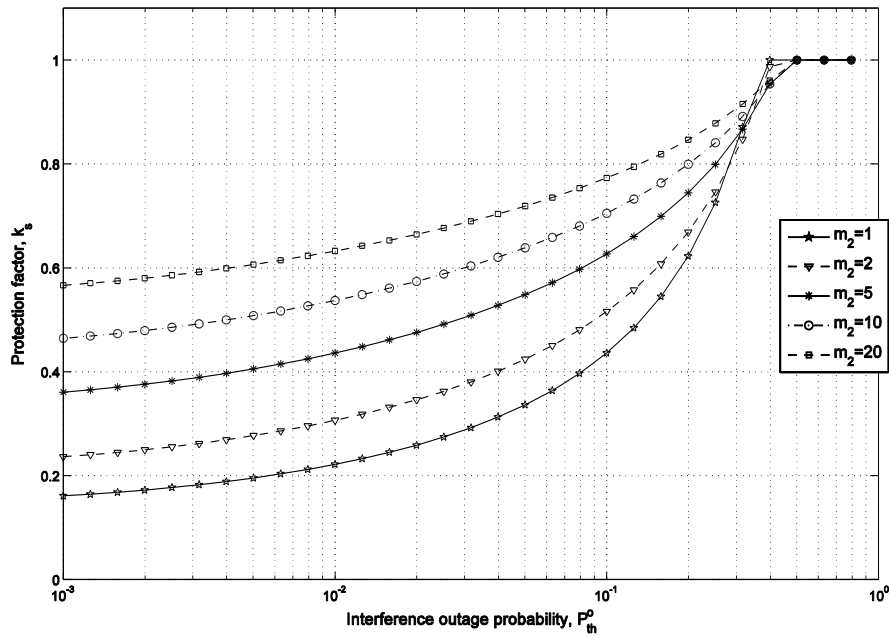


Figure 4.9 – Protection factor for various values of m_2 and interference outage probability at the link from SU-Tx to PU-Rx.

In Figure 4.10, the impact of average INR (interference-to-noise ratio) on the outage probability is studied, where $INR = m_3 \lambda_3 P_{PU} / \sigma^2$, and the case when the total average interference and noise power is fixed, ($P_{PU} + \sigma^2 = 1$), has been considered. It was assumed that statistical CSI is available at SU-Tx with permitted outage interference $P_o^{th} = 1e^{-2}$, and MRC diversity is applied for transmit power constraint $P_m=5$, and two different values for fading parameter in SU link $m_1=2$ or $m_1=3$.

As expected, MRC enhances the performance of the system, and the results show how the increase in the number of receive antennas decreases the outage probability. We can notice that when the fading parameter in SU link increases, the outage probability decreases for any number of receive antennas. The outage probability decreases as the value of m_1 increases, this impact of m_1 is more obvious when MRC ($n_R=2$) is applied. For large values of Q_p , it can be observed that the interference is more critical for SU link performance compared to the PU interference for both cases of MRC diversity and no diversity case.

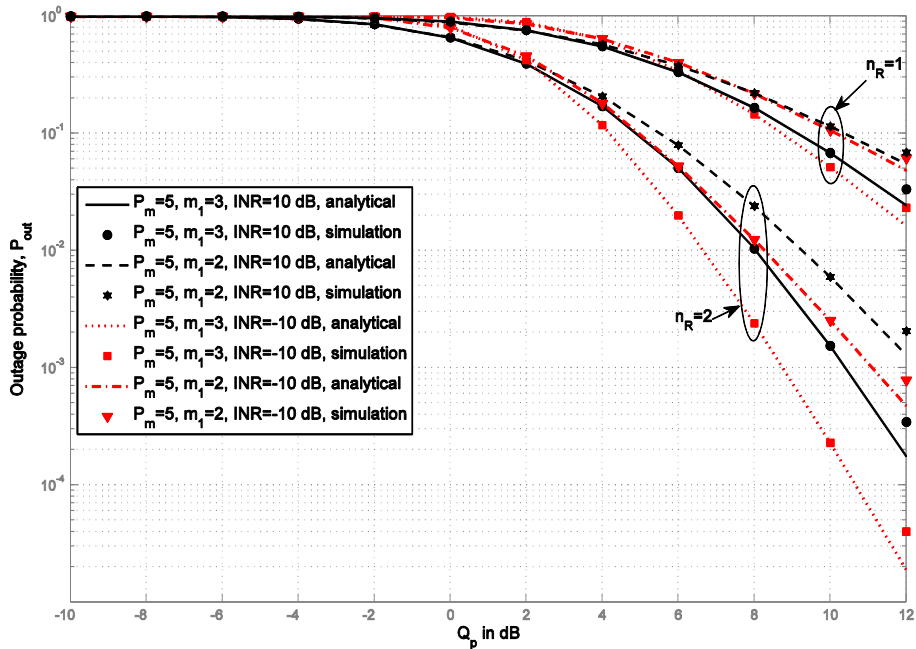


Figure 4.10 – Outage Probability for the case of statistical CSI, $P_o^{th} = 10^{-2}$, MRC diversity with $n_R=1$ or $n_R=2$ antennas, $P_m=5$, $m_3 = m_2=3$ and $m_1=2$ or $m_1=3$.

Figure 4.11 presents the outage capacity as a function of peak interference power constraint Q_p , for the no noise case, when the fading parameters in the channels are given as $m_1=m_3=2$, $m_2=5$ ($m_i\lambda_i=1$, $i=1, 2, 3$), transmission power constraint $P_m=20$ and transmit power of primary user is $P_{PU}=5$ when MRC diversity is applied with $n_R=2$, and when only statistical CSI of channel power gain for the link from SU-Tx to PU-Rx is available at secondary transmitter. Outage capacity is a useful metric, appropriate for delay constrained limitations and it determines the maximum data rate that can be maintained in fading states that are not subject to very deep fading that occurs with a given outage probability.

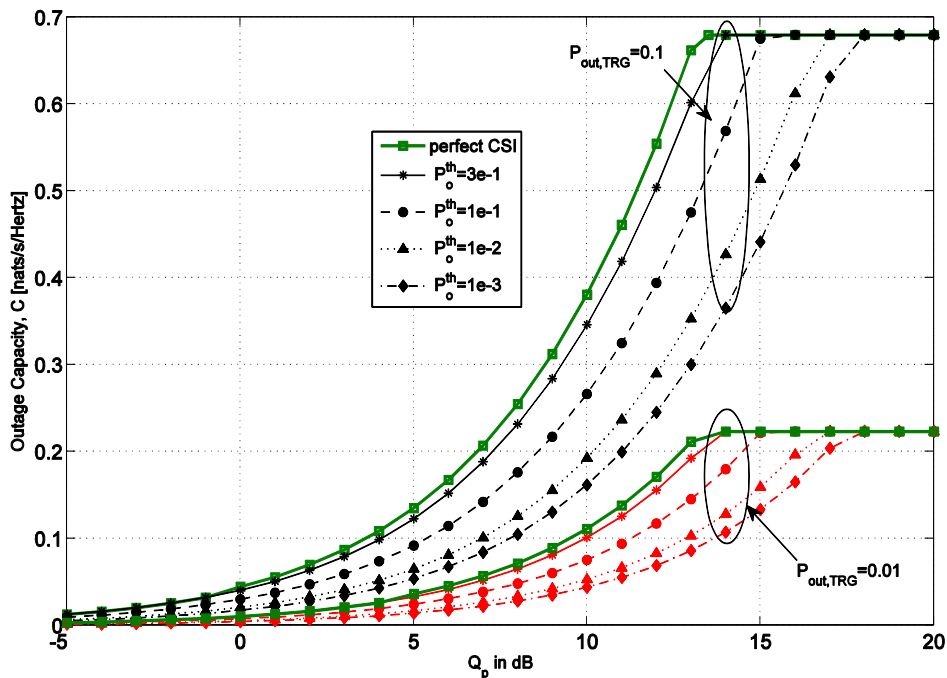


Figure 4.11 – Outage capacity vs. peak interference power Q_p for the case of the perfect CSI, MRC diversity with $n_R=2$ antennas, $P_m=20$, $P_{PU}=5$, $m_1= m_3=2$, $m_2=5$, and different values of the interference probability.

Therefore, for the given target outage probability we numerically determined ρ such that the probability that SINR is below a threshold ρ is equal to $P_{out,TRG}$, and then the normalized value of outage capacity is obtained as $C_{out} = B \log_2(1 + \rho)$. It can be noticed that the outage capacity increases with the increase of Q_p , and when $Q_p > 14$ dB, the outage capacity gets saturated due to P_m . The parameter $P_{out,TRG}$ indicates the

probability that the system can be in outage, and we can realize that the outage capacity increases with the increase of this probability. For a given $P_{out,TRG}$, a decreased value of the tolerated interference outage probability P_o^{th} results in a decreased outage capacity. Moreover, as the interference outage probability P_o^{th} decreases, the outage capacity gets saturated at higher Q_p values.

5. Ergodic Capacity of cognitive radio system with co-channel interference and MRC diversity for imperfect CSI

Analysing the channel capacity is one of the most important performance metrics in wireless communication systems. Many works had and still study the capacity of cognitive radio systems. Capacity of AWGN channels is derived in [52] under average interference power constraint, where it was shown that the transmitted and received power constraints give the same results in rising the capacity value in the absence of fading. While the results in [103] show that the channel capacity is lower under fading with the transmitted power constrained instead of the received one. Furthermore, for the same limits on the received power level, channel capacity in sever fading exceeds that of the non-fading AWGN channel [44]. The authors in [59] show that the capacity of secondary link is higher under the average constraint compared with the peak interference power constraint and the fading in the channel between SU-Tx and PU-Rx is beneficial for enhancing the SU capacity and outage capacity, besides that and according to [54] the average constraint provides better PU performance. Moreover, [58] shows that the capacity of channels under sever fading is higher than that of the AWGN channel for all values of average signal-to-noise ratio, so the secondary user can may take advantage of this fact by opportunistically transmitting with high power when its signal received by PU is deeply faded. Ergodic capacity of secondary link has been studied for different fading environments and in [104] they show that it is sensitive to

the fading type in the secondary link as well as in the link from secondary transmitter to primary receiver.

It is well known that the diversity techniques improve the capacity of the wireless communication channels, especially the Maximum Ratio Combining diversity (MRC) which is the optimal combining diversity technique that maximizes the output signal-to-noise ratio (SNR) [91]. Capacity of point-to-point communication system for Rayleigh fading environment and various diversity techniques is given in [92] and the ergodic capacity for MRC system and Nakagami fading channels is given in [68]. The enhancement of the SU capacity by employing MRC is proposed in [67] for Rayleigh propagation under the average power constraint, while the corresponding capacity expressions are derived in [86] for Nakagami fading environment. Furthermore, useful analysis of spectrum sharing system with OSTBC is provided in [94] but the exact analytical results are derived in [96].

All of the previous works have assumed that the secondary user has full channel state information knowledge of the link between SU-Tx and PU-Rx. However, in practice, obtaining full CSI is difficult and often only partial CSI can be acquired. This situation has been studied in [105] and [106] where optimal power allocation and mean channel capacity is investigated for a secondary system under limited channel knowledge of the SU-Tx to PU-Rx link and in [107] but only under the average interference power constraint. While the impact of imperfect CSI on the SU link capacity is analysed under peak interference and transmit power constraints for the case of partial CSI knowledge due to an error in the channel estimation, feedback delay and limited feedback in [81]. The case of multiple antenna deployment also has been studied in literature, where the capacity of the secondary link with MRC at the secondary receiver is studied in [97] with imperfect CSI. Their results show that the deployment of a multi antenna array with MRC allows the secondary system to achieve a higher capacity as well as the opportunity to tolerate larger estimation errors.

Although the previous analysis is important, but the corresponding capacity expressions are derived for the case when the interference from the primary user is neglected. The impact of PU's transmission on the performances of SU link is analysed in [81] for the case of Rayleigh fading and imperfect channel state information (CSI). Moreover, the performances of MRC were studied for Nakagami fading environment

considering multiple equal power co-channel interferers and the closed-form expression for outage probability of SINR was derived in [100], while in [101] the expression was derived for the case of arbitrary power co-channel interference.

Closed-form expressions for ergodic capacity of the secondary link in cognitive radio system when the interference generated from primary user and the noise are present at the input of the secondary receiver that employs MRC diversity when only statistical CSI is available to the secondary user has not been derived earlier. In this chapter, closed-form expressions of ergodic capacity when the available channel state information is imperfect (outdated and statistical), under the both constraints; the peak interference power constraint and the maximal transmit power constraint have been derived. The results given in this chapter are part from the published work in [108].

5.1 Ergodic Capacity of Cognitive Radio System with MRC Diversity for outdated CSI

Ergodic capacity is a significant performance measure, defined in [88, eq. (4)] (normalized to the bandwidth unit) as

$$C = \int_0^{+\infty} \log(1 + \gamma) f_\gamma(\gamma) d\gamma, \quad (5.1)$$

where $f_\gamma(\gamma)$ is the probability density function of SINR given in (4.22) for the case of outdated CSI when MRC is applied. Substituting the PDF of SINR in its integral form

$$C = \int_0^{+\infty} \log(1 + \gamma) \int_0^{k_o Q_p / P_m} \frac{f_x(\gamma P_{PU} / P_m)}{P_m / P_{PU}} f_{\hat{y}_2}(\hat{y}_2) d\hat{y}_2 d\gamma \\ + \int_0^{+\infty} \log(1 + \gamma) \int_{k_o Q_p / P_m}^{+\infty} \frac{f_x(\gamma P_{PU} y_2 / Q_p)}{Q_p / (P_{PU} y_2)} f_{\hat{y}_2}(\hat{y}_2) d\hat{y}_2 d\gamma. \quad (5.2)$$

The ergodic capacity of the secondary link can be written in form $C = C_1 + C_2$, where

$$C_1 = \frac{P_{PU}}{P_m} \left[1 - \frac{\Gamma(m_2, k_o Q_p / (\lambda_2 P_m))}{\Gamma(m_2)} \right] \int_0^\infty \log(1 + \gamma) f_x \left(\frac{\gamma P_{PU}}{P_m} \right) d\gamma, \quad (5.3)$$

$$C_2 = \frac{P_{PU}}{k_o Q_p} \int_{k_o Q_p / P_m}^{+\infty} \hat{y}_2 f_{\hat{y}_2}(\hat{y}_2) \left[\int_0^\infty \log(1 + \gamma) f_x \left(\frac{\gamma \hat{y}_2 P_{PU}}{k_o Q_p} \right) d\gamma \right] d\hat{y}_2. \quad (5.4)$$

Substituting $f_x(x)$ given in (3.21), where $m_1 = m_1 n_R$, and representing $\log(1 + \gamma)$ by the special function Meijer-G function [109, eq. (01.04.26.0003.01)], the expression (5.3) is written as follows

$$C_1 = \left(\frac{P_{PU}}{\lambda_1 P_m} \right)^{m_1 n_R} \left[1 - \frac{\Gamma(m_2, k_o Q_p / (\lambda_2 P_m))}{\Gamma(m_2)} \right] \int_0^\infty G_{2,2}^{1,2} \left(\begin{matrix} 1, 1 \\ 1, 0 \end{matrix} \middle| \gamma \right) \times \frac{\gamma^{m_1 n_R - 1} e^{-\gamma \frac{\sigma^2}{\lambda_1 P_m}}}{\lambda_3^{m_3} \Gamma(m_1 n_R) \Gamma(m_3)} \int_0^{+\infty} (y_3 + \sigma^2 / P_{PU})^{m_1 n_R} y_3^{m_3 - 1} e^{-y_3 \left[\frac{\gamma P_{PU}}{\lambda_1 P_m} + \frac{1}{\lambda_3} \right]} dy_3 d\gamma. \quad (5.5)$$

Following the steps given in Appendix 5 – A by applying the convolutional integral for Meijer-G function [109, eq. (07.34.21.0088.01)] plus some additional manipulations, the final form for the first part of capacity is given as follows

$$C_1 = \frac{e^{\sigma^2 / \lambda_3 P_{PU}}}{\Gamma(m_1 n_R) \Gamma(m_3)} \left[1 - \frac{\Gamma(m_2, k_o Q_p / (\lambda_2 P_m))}{\Gamma(m_2)} \right] \sum_{l=0}^{m_3 - 1} \binom{m_3 - 1}{l} \times (-1)^{m_3 - 1 - l} \left[\left(\frac{\sigma^2}{\lambda_3 P_{PU}} \right)^{m_3 - 1 - l} G_{3,3}^{2,3} \left(\begin{matrix} 1 - m_1 n_R, 1, 1 \\ 1 + l, 1, 0 \end{matrix} \middle| \frac{\lambda_1 P_m}{\lambda_3 P_{PU}} \right) - \sum_{k=0}^{+\infty} \frac{(-1)^k}{k!} \left(\frac{\sigma^2}{\lambda_3 P_{PU}} \right)^{m_3 - k} G_{3,4}^{3,2} \left(\begin{matrix} -l - k, 0, 1 \\ m_1 n_R, 0, 0, -l - k - 1 \end{matrix} \middle| \frac{\sigma^2}{\lambda_1 P_m} \right) \right]. \quad (5.6)$$

The second part of capacity is given after substituting the PDF of x as follows

$$C_2 = \frac{\left(P_{PU} / \lambda_1 k_o Q_p \right)^{m_1 n_R}}{\Gamma(m_1 n_R) \lambda_3^{m_3} \Gamma(m_3) \lambda_2^{m_2} \Gamma(m_2)} \int_{k_o Q_p / P_m}^{+\infty} \hat{y}_2^{m_1 n_R + m_2 - 1} e^{-\hat{y}_2 / \lambda_2} \times \int_0^{+\infty} (y_3 + \sigma^2 / P_{PU})^{m_1 n_R} y_3^{m_3 - 1} e^{-y_3 / \lambda_3} \left[\int_0^\infty \gamma^{m_1 n_R - 1} \log(1 + \gamma) e^{-\gamma \frac{\hat{y}_2 (y_3 P_{PU} + \sigma^2)}{\lambda_1 k_o Q_p}} d\gamma \right] dy_3 d\hat{y}_2. \quad (5.7)$$

Substituting the logarithm with the special function Meijer-G [109, eq. (01.04.26.0003.01)], then applying the convolutional integral for Meijer-G functions given in [109, eq. (07.34.21.0088.01)] and following the explanation in Appendix 5-B, the final form of the second part of capacity is obtained as

$$\begin{aligned}
C_2 = & \frac{e^{\sigma^2/\lambda_3 P_{PU}}}{\Gamma(m_1 n_R) \Gamma(m_2) \Gamma(m_3)} \sum_{l=0}^{m_3-1} \binom{m_3-1}{l} \left(-\frac{\sigma^2}{\lambda_3 P_{PU}} \right)^{m_3-1-l} \\
& \times \left\{ \left[G_{4,3}^{2,4} \left(\begin{matrix} 1-m_2, -l, 0, 1 \\ m_1 n_R, 0, 0 \end{matrix} \middle| \frac{\lambda_2 \lambda_3 P_{PU}}{\lambda_1 k_o Q_p} \right) - \sum_{k=0}^{+\infty} \frac{(-1)^k}{k!} \left(\frac{k_o Q_p}{\lambda_2 P_m} \right)^{m_2+k} \right. \right. \\
& G_{4,4}^{2,4} \left(\begin{matrix} 1-m_2-k, -l, 0, 1 \\ m_1 n_R, 0, 0, -m_2-k \end{matrix} \middle| \frac{\lambda_3 P_{PU}}{\lambda_1 P_m} \right) \left. \left. - \sum_{k_2=0}^{+\infty} \frac{(-1)^{k_2}}{k_2!} \left(\frac{\sigma^2}{\lambda_2 P_{PU}} \right)^{l+k_2+1} \right. \right. \\
& \left. \left. \left[G_{4,4}^{3,3} \left(\begin{matrix} 1-m_2, -l-k_2, 0, 1 \\ m_1 n_R, 0, 0, -l-k_2-1 \end{matrix} \middle| \frac{\lambda_2 \sigma^2}{\lambda_1 k_o Q_p} \right) - \sum_{k_3=0}^{+\infty} \frac{(-1)^{k_3}}{k_3!} \left(\frac{k_o Q_p}{\lambda_2 P_m} \right)^{m_2+k_3} \right. \right. \right. \\
& \left. \left. \left. G_{4,5}^{3,3} \left(\begin{matrix} 1-m_2-k_3, -l-k_2, 0, 1 \\ m_1 n_R, 0, 0, -l-k_2-1, -m_2-k_3 \end{matrix} \middle| \frac{\sigma^2}{\lambda_1 P_m} \right) \right] \right] \right\}. \tag{5.8}
\end{aligned}$$

It can be noticed that in the case when $P_m \ll Q_p$, equation (5.7) further simplifies as the expression in the squared brackets is equal to one, $C_2=0$ and capacity reduces into

$$\begin{aligned}
C = & \frac{e^{\sigma^2/\lambda_3 P_{PU}}}{\Gamma(m_1 n_R) \Gamma(m_3)} \sum_{l=0}^{m_3-1} \binom{m_3-1}{l} (-1)^{m_3-1-l} \left[\left(\frac{\sigma^2}{\lambda_3 P_{PU}} \right)^{m_3-1-l} G_{3,3}^{2,3} \left(\begin{matrix} 1-m_1 n_R, 1, 1 \\ 1+l, 1, 0 \end{matrix} \middle| \frac{\lambda_1 P_m}{\lambda_3 P_{PU}} \right) \right. \\
& \left. - \sum_{k=0}^{+\infty} \frac{(-1)^k}{k!} \left(\frac{\sigma^2}{\lambda_3 P_{PU}} \right)^{m_3-k} G_{3,4}^{3,2} \left(\begin{matrix} -l-k, 0, 1 \\ m_1 n_R, 0, 0, -l-k-1 \end{matrix} \middle| \frac{\sigma^2}{\lambda_1 P_m} \right) \right], \tag{5.9}
\end{aligned}$$

while for $Q_p \ll P_m$, $C_1=0$ and the capacity is expressed in the compact form as

$$\begin{aligned}
C = & \frac{e^{\sigma^2/\lambda_3 P_{PU}}}{\Gamma(m_1 n_R) \Gamma(m_2) \Gamma(m_3)} \sum_{l=0}^{m_3-1} \binom{m_3-1}{l} \left(-\frac{\sigma^2}{\lambda_3 P_{PU}} \right)^{m_3-1-l} \left[G_{4,3}^{2,4} \left(\begin{matrix} 1-m_2, -l, 0, 1 \\ m_1 n_R, 0, 0 \end{matrix} \middle| \frac{\lambda_2 \lambda_3 P_{PU}}{\lambda_1 k_o Q_p} \right) \right. \\
& \left. - \sum_{k_2=0}^{+\infty} \frac{(-1)^{k_2}}{k_2!} \left(\frac{\sigma^2}{\lambda_2 P_{PU}} \right)^{l+k_2+1} G_{4,4}^{3,3} \left(\begin{matrix} 1-m_2, -l-k_2, 0, 1 \\ m_1 n_R, 0, 0, -l-k_2-1 \end{matrix} \middle| \frac{\lambda_2 \sigma^2}{\lambda_1 k_o Q_p} \right) \right], \tag{5.10}
\end{aligned}$$

It is obvious that the parameters m_2 and λ_2 do not have any impact on the capacity value when $P_m \ll Q_p$, as they do not appear in (5.9), but the increase of these factors decreases the capacity when $Q_p \ll P_m$, as it can be seen from (5.10).

The whole analysis is considered the general case of Nakagami fading environment, suitable for wide range of applications (that includes the case of Rayleigh propagation as the special case when fading parameter is equal $m=1$). It can be seen that the analysed scenario is complex enough; therefore, the ergodic capacity can be expressed in a significantly simpler form when $Q_p \ll P_m$ in the following important asymptotic cases:

- a) **Noise-limited case:** The noise power at the secondary receiver is dominant compared to interference power, ($\sigma^2 \gg y_3 P_{PU}$) so the SINR can be approximated as SNR

$$\gamma = \frac{\frac{k_o Q_p}{\hat{y}_2} y_1}{P_{PU} y_3 + \sigma^2} \approx \frac{k_o Q_p}{\sigma^2} \frac{y_1}{\hat{y}_2}. \quad (5.11)$$

In order to derive the ergodic capacity, the definition (5.1) is used where $f_\gamma(\gamma)$ is the probability density function of SNR. Applying the transformations for RVs $x = y_1 / \hat{y}_2$, the probability density function of x is given as

$$f_x(x) = \frac{1}{\Gamma(m_1 n_R) \Gamma(m_2)} \frac{x^{m_1 n_R - 1}}{\lambda_1^{m_1 n_R} \lambda_2^{m_2}} \frac{\Gamma(m_1 n_R + m_2)}{\left(\frac{x}{\lambda_1} + \frac{1}{\lambda_2}\right)^{m_1 n_R + m_2}}. \quad (5.12)$$

Further, the previous PDF can be expressed by Meijer-G function by using the transformation [109, eq. (01.02.26.0007.01)]

$$f_x(x) = \frac{(\lambda_2 / \lambda_1)^{m_1 n_R}}{\Gamma(m_1 n_R) \Gamma(m_2)} \frac{x^{m_1 n_R - 1}}{\Gamma(m_2)} G_{1,1}^{1,1} \left[\begin{matrix} \lambda_2 x \\ \lambda_1 \end{matrix} \middle| \begin{matrix} -m_1 n_R - m_2 + 1 \\ 0 \end{matrix} \right]. \quad (5.13)$$

The PDF of γ is obtained by applying $f_\gamma^{NL}(\gamma) = 1/K f_x(\gamma/K)$ to get the closed-form for probability density function of SNR for noise-limited system as

$$f_\gamma^{NL}(\gamma) = \left(\frac{\lambda_2 \sigma^2}{\lambda_1 k_o Q_p} \right)^{m_1 n_R} \frac{(\gamma)^{m_1 n_R - 1}}{\Gamma(m_1 n_R) \Gamma(m_2)} G_{1,1}^{1,1} \left[\begin{matrix} \lambda_2 \sigma^2 \gamma \\ \lambda_1 k_o Q_p \end{matrix} \middle| \begin{matrix} -m_1 n_R - m_2 + 1 \\ 0 \end{matrix} \right]. \quad (5.14)$$

Using definition in (5.1) and the transformations given in [109, eqs. (01.02.26.0007.01), (01.04.26.0003.01) and (07.34.21.0011.01)], the closed-form of ergodic capacity for the noise-limited system is obtained

$$C^{NL} = \left(\frac{\lambda_2 \sigma^2}{\lambda_1 k_o Q_p} \right)^{m_1 n_R} \frac{1}{\Gamma(m_1 n_R)} \frac{1}{\Gamma(m_2)} G_{3,2}^{3,2} \left(\frac{\lambda_2 \sigma^2}{\lambda_1 k_o Q_p} \middle| \begin{matrix} -m_1 n_R - m_2 + 1, & -m_1 n_R, & 1 - m_1 n_R \\ 0, & -m_1 n_R, & -m_1 n_R \end{matrix} \right). \quad (5.15)$$

a) **Interference-limited case:** The transmission of the secondary user is dominantly disturbed by the interference originating from the primary transmitter, ($y_3 P_{PU} \gg \sigma^2$). In this limiting case signal to interference ratio (SIR) can be expressed as

$$\gamma = \frac{\frac{k_o Q_p}{\hat{y}_2} y_1}{P_{PU} y_3 + \sigma^2} \approx \frac{\frac{k_o Q_p}{\hat{y}_2} y_1}{P_{PU} y_3} = \frac{k_o Q_p}{P_{PU}} (y_1 / \hat{y}_2 / y_3). \quad (5.16)$$

By applying the transformation of RVs $z = x/y_3$, where $x = y_1/\hat{y}_2$ and its PDF is given in (5.13), the probability density function of z can be obtained in the form

$$f_z(z) = \frac{(\lambda_2/\lambda_1)^{m_1 n_R} \Gamma(m_1 n_R + m_2)}{\lambda_3^{m_3} \Gamma(m_1 n_R) \Gamma(m_2) \Gamma(m_3)} z^{m_1 n_R - 1} \int_0^\infty \frac{x^{m_1 n_R + m_3 - 1} e^{-\frac{x}{\lambda_3}} dx}{\left(z \frac{x \lambda_2}{\lambda_1} + 1 \right)^{m_1 n_R + m_2}} \quad (5.17)$$

Using the transformation [109, eq. (01.02.26.0007.01)] and representing the exponential function with power series, the closed-form of PDF for SIR can be obtained as the following expression

$$f_\gamma^{IL}(\gamma) = \left(\frac{\lambda_1 k_o Q_p}{\lambda_2 \lambda_3 P_{PU}} \right)^{m_3} \frac{\gamma^{-m_3 - 1}}{\Gamma(m_1 n_R) \Gamma(m_2) \Gamma(m_3)} G_{2,1}^{1,2} \left(\frac{\lambda_2 \lambda_3 P_{PU}}{\lambda_1 k_o Q_p} \gamma \middle| \begin{matrix} 1, & 1 - m_2 + m_3 \\ m_1 n_R + m_3 \end{matrix} \right). \quad (5.18)$$

And the interference-limited system ergodic capacity is obtained in the following closed-form

$$C^{IL} = \left(\frac{\lambda_1 k_o Q_p}{\lambda_2 \lambda_3 P_{PU}} \right)^{m_3} \frac{1}{\Gamma(m_1 n_R) \Gamma(m_2) \Gamma(m_3)} G_{4,3}^{3,3} \left(\frac{\lambda_2 \lambda_3 P_{PU}}{\lambda_1 k_o Q_p} \middle| \begin{matrix} 1, & 1 - m_2 + m_3, & m_3, & m_3 + 1 \\ m_1 n_R + m_3, & m_3, & m_3 \end{matrix} \right). \quad (5.19)$$

The ergodic capacity is presented as a function of the interference power constraint Q_p , in Figure 5.1 for the case when outdated CSI ($k_o=0.9$) is available to

secondary transmitter when the fading parameter in the channel from SU-Tx to PU-Rx $m_2=2$, and the transmission power of the primary $P_{PU}=1$ for the maximal permitted transmission power $P_m=5$. The scenario where the transmission of SU is dominantly imposed by interference and $\sigma^2 = 0$ is analysed (interference-limited case). Although analytical results are more general, for each link it is assumed that the average power gain has a unit value, that means $m_i\lambda_i=1$. For the case when neither one of the constraints dominates, ergodic capacity is calculated as a summation of (5.6) and series (5.8), under assumption that any term smaller than 0.1% of the summation of previous terms can be neglected. Obtained simulation results indicate excellent accuracy of the derived expressions.

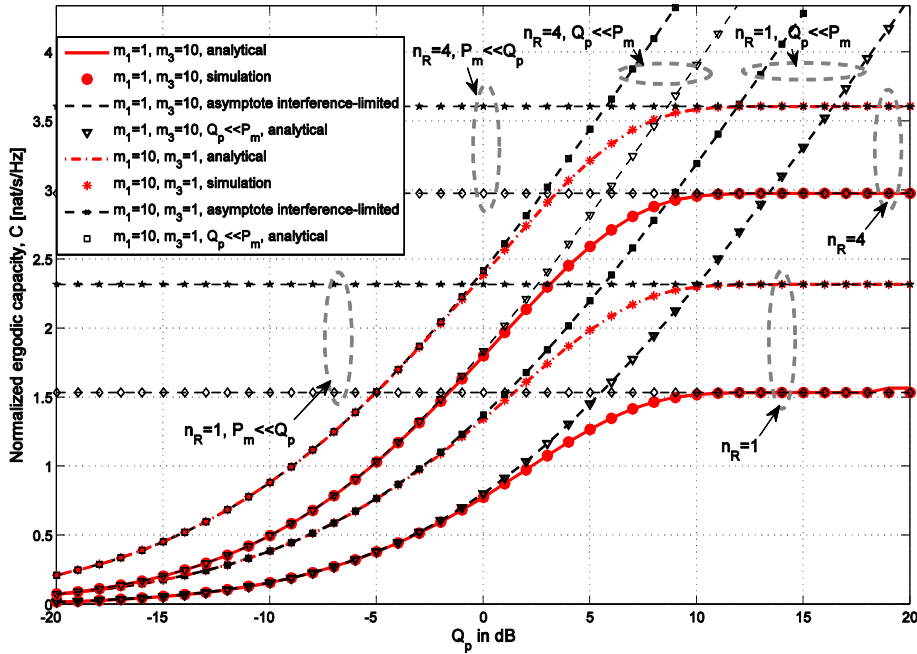


Figure 5.1 – Ergodic capacity vs. Q_p for the case of outdated CSI, MRC diversity with $n_R=1$ or $n_R=4$ antennas, $P_m=5$, $P_{PU}=1$, and $m_2=2$.

Furthermore, it has been shown that the asymptotic expression (5.19) accurately approximates the simulation and analytical ones in the region where peak interference constraint dominates ($Q_p \ll P_m$) for both values of receive antennas applied at the SU-Rx ($n_R=1, 4$). As it was expected, the capacity increases with the rise of the fading parameter in the secondary link, m_1 , and decreases with the increase of the fading

parameter in the interference link, m_3 . When $m_1 < m_3$ the increase of diversity order increases the capacity significantly (when $n_R=4$, the increase is almost 100% for $m_1=1$, $m_3=10$), what corresponds to the effect observed when noise was present instead of the interference that originates from PU [64]. However, in the case $m_1 \geq m_3$ the raise of n_R results in smaller capacity gain (when $n_R=4$, the increase is close to 50% for $m_1=10$, $m_3=1$). This can be explained with the fact that the MRC diversity results in larger performance gain on the SU link for lower Nakagami fading parameter.

Figure 5.2 presents the ergodic capacity vs. the peak interference power constraint Q_p , for the case of outdated CSI ($k_o=0.9$) when $P_{PU}=1$, $P_m=5$, $m_1=2$, $m_2=3$, and $m_3=5$ ($m_i \lambda_i=1$, $i=1, 2, 3$). Ergodic capacity is studied for two cases $n_R=1$, and $n_R=5$ for different values of noise power at the receiver.

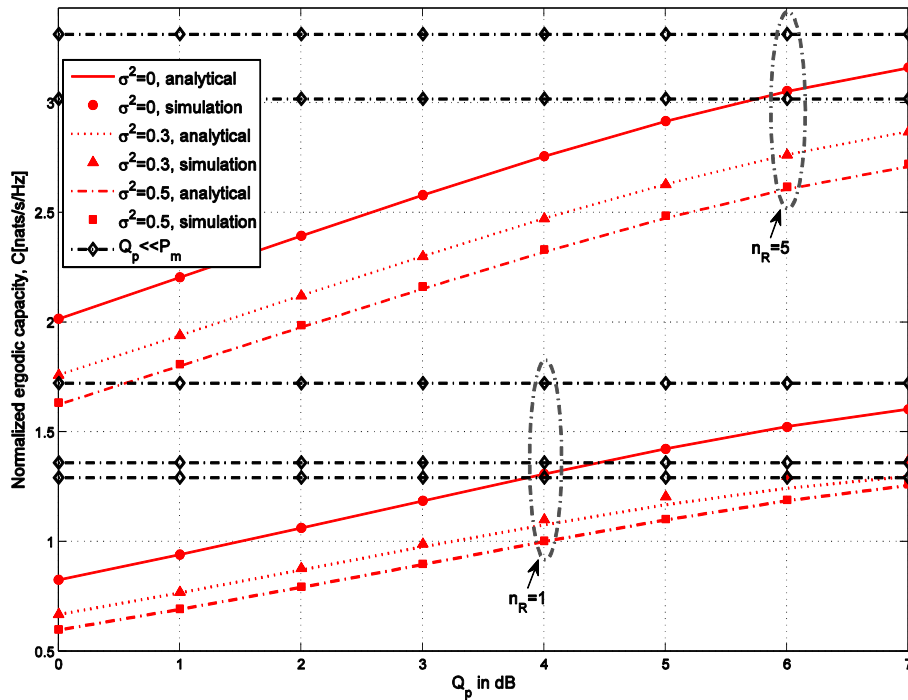


Figure 5.2 – Impact of noise on ergodic capacity for outdated CSI with MRC diversity $n_R=1$, and $n_R=5$, when $P_{PU}=1$, $P_m=5$, $m_1=2$, $m_2=3$, and $m_3=5$.

The results confirm that the increased noise power decreases the capacity for any number of antennas at the secondary receiver. It can be noticed that for the larger number of receive antennas, the relative change of capacity values due to effect of noise is less significant (for $Q_p=5$, the capacity has been decreased about 22.47% when noise

increases from $\sigma^2 = 0$ to $\sigma^2 = 0.5$ for $n_R=1$, while for $n_R=5$ it has been decreased for 14.8%). The analytical results are confirmed by using simulation method. As expected, ergodic capacity is increasing with the raise of peak interference constraint Q_p , and in the region where transmit power constraint dominates ($P_m \ll Q_p$) it asymptotically approaches values obtained by using expression (5.9).

A comparison between ergodic capacity values in the interference-limited and noise-limited cases is presented in Figure 5.3. The scenario when only outdated CSI ($k_o=0.9$) is available at SU-Tx is considered for fading parameter values $m_i=2$, $m_i\lambda_i=1$ (where $i=1, 2, 3$) when MRC diversity is applied at SU-Rx for $n_R=1, 2$ and 4. In the interference-limited case, the noise power is $\sigma^2 = 0.01$ and transmit power of PU is $P_{pU} = 1$, while in the noise-limited case the corresponding parameters are $\sigma^2 = 1$ and $P_{pU} = 0.01$.

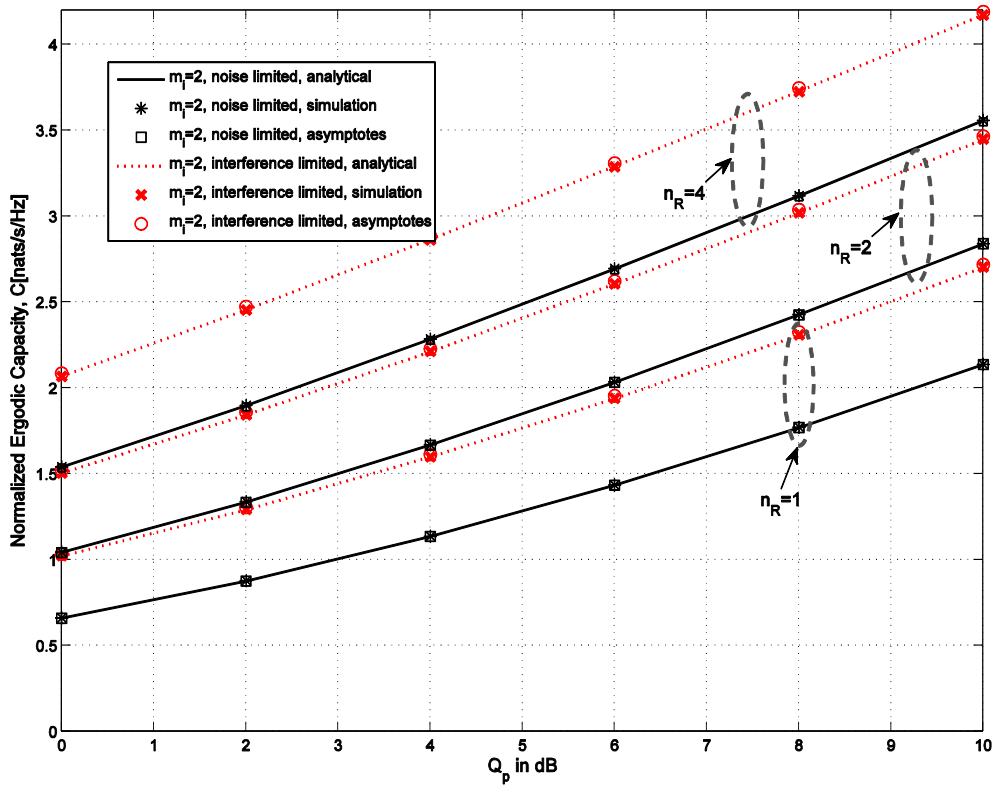


Figure 5.3 – Comparison of ergodic capacities for noise-limited and interference-limited cases with MRC diversity with $n_R=1, 2, 4$ receive antennas for the case of outdated CSI.

As it is previously noticed, the capacity values increase with the raise of the number of applied antennas at the secondary user. Furthermore, for all values of the receive antennas number; the interference-limited system achieves a higher capacity than the noise-limited one. Analytical results are obtained by using the expressions (5.3)-(5.8) and they are confirmed by simulation results. In both noise and interference-limited cases, asymptotic lines obtained by using the expressions (5.15) and (5.19), respectively, show high level of agreement with analytical and simulation ones.

5.1.1 Ergodic Capacity for Interference-limited System with OSTBC for Perfect CSI

A special case is analysed in this paragraph, where the available CSI is assumed to be perfect which means that $k_o = 1$ then the transmission power allocation is given by (3.10). Furthermore, OSTBC codes are applied at the interference-limited secondary user ($\sigma^2 \ll P_i$); in this case the SINR will be simplified to SIR given in (4.11). The probability density function of SIR is given in (4.18) which can be expressed by the special Meijer-G functions following the same applied procedure in deriving (5.18), taking into account that $m_1 n_R = m_1 n_R n_T = s$, $m_2 = m_2 n_T = p$ and $m_3 = m_3 n_R = w$.

The closed-form expression of ergodic capacity for interference-limited system applying OSTBC is given as

$$C_{OSTBC}^{IL} = \left(\frac{\lambda_1 Q_p}{R \lambda_2 \lambda_3 P_{PU}} \right)^w \frac{1}{\Gamma(s) \Gamma(p) \Gamma(w)} G_{4,3}^{3,3} \left(\frac{R \lambda_2 \lambda_3 P_{PU}}{\lambda_1 Q_p} \middle| \begin{matrix} 1, 1-p+w, w, w+1 \\ s+w, w, w \end{matrix} \right). \quad (5.20)$$

Ergodic capacity for the interference limited system applying OSTBC is presented in Figure 5.4 as a function of the peak interference power constraint to interference signal power ratio, when the channels are not unit in power, $\lambda_1=1/6$, $\lambda_2=2$, $\lambda_3=3$. Alamouti code scheme as a special case of OSTBC when ($n_T=n_R=2$, $R=1$) is compared when MRC diversity is applied at the secondary receiver for different values of fading parameters.

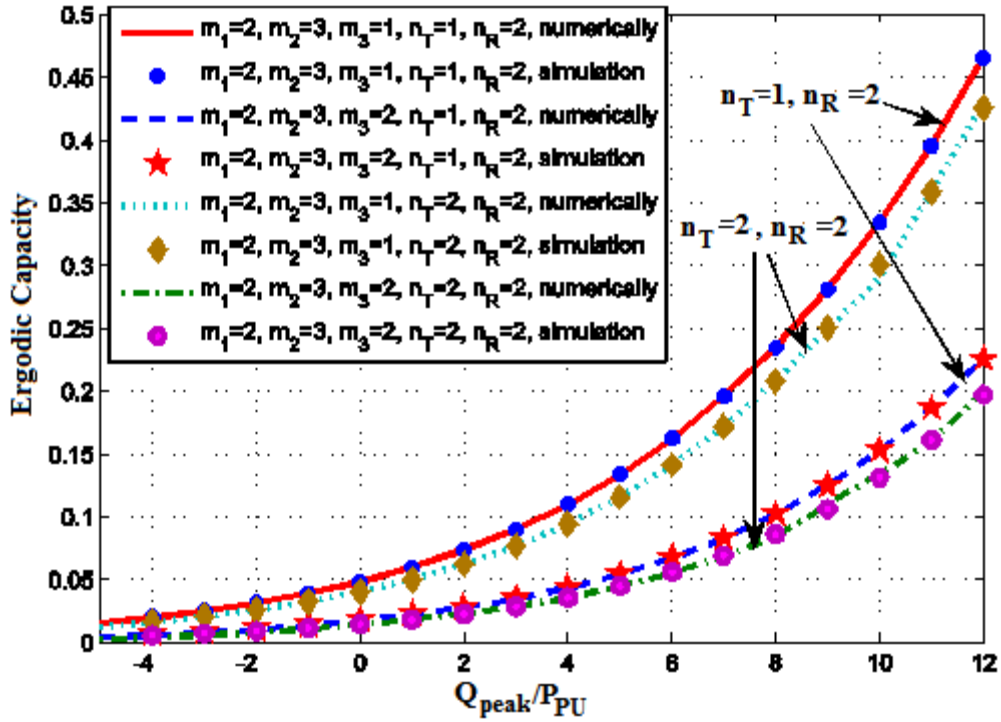


Figure 5.4 – Comparison of ergodic capacity for Alamouti and MRC for interference-limited case.

Ergodic capacity values are greater for the case when $n_T=1, n_R=2$ than for the case $n_T=2, n_R=2$, which means that applying MRC as a diversity technique achieves higher capacities than Alamouti scheme. The increase of the fading parameter in the interference link, m_3 , decreases the ergodic capacity values, since SIR will be smaller as the interference will be larger in this case at the secondary receiver.

5.2 Ergodic Capacity of Cognitive Radio System with MRC Diversity for Statistical CSI

When only statistical CSI for channel power gain of the link from secondary transmitter to primary receiver is available to the secondary user, which is the worst and the most reality case of the available channel state information, the ergodic capacity expression can be obtained by substituting expression (4.39) in definition (5.1).

Following a similar procedure as in the case of outdated CSI, the capacity can be obtained in its closed-form as

$$C = \frac{e^{\sigma^2/\lambda_3 P_{PU}}}{\Gamma(m_1 n_R) \Gamma(m_3)} \sum_{k=0}^{m_3-1} \binom{m_3-1}{k} \left(-\frac{\sigma^2}{\lambda_3 P_{PU}} \right)^{m_3-1-k} \times \left\{ G_{3.3}^{3.2} \left(\begin{matrix} -k, 0, 1 \\ m_1 n_R, 0, 0 \end{matrix} \middle| \frac{1}{c} \right) \right. \\ \left. - \sum_{l=0}^{+\infty} \frac{(-1)^l}{l!} \left(\frac{\sigma^2}{\lambda_3 P_{PU}} \right)^{l+k+1} G_{3.4}^{3.2} \left(\begin{matrix} -l-k, 0, 1 \\ m_1 n_R, 0, 0, -l-k-1 \end{matrix} \middle| \frac{\sigma^2}{c \lambda_3 P_{PU}} \right) \right\}, \quad (5.21)$$

where $c = \lambda_1 \min(k_s Q_p / m_2 \lambda_2, P_m) / \lambda_3 P_{PU}$.

In order to simplify and verify the expressions of capacity, interference-limited scenario as an asymptotic case is derived where SIR can be calculated as

$$\gamma = \frac{\left(\frac{k_s Q_p}{m_2 \lambda_2} \right)^{y_1}}{P_{PU} y_3 + \sigma^2} \approx \frac{P_T y_1}{P_{PU} y_3} \approx \frac{P_T}{P_{PU}} \frac{y_1}{y_3}, \quad (5.22)$$

then the probability density function of SIR can be obtained using the PDF of RV $x = y_1/y_3$ which is the same as (5.13) to get

$$f_{\gamma}^{IL}(\gamma) = \frac{(\gamma)^{m_1 n_R - 1}}{c^{m_1 n_R} \Gamma(m_1 n_R) \Gamma(m_3)} G_{1.1}^{1.1} \left(\frac{\gamma}{c} \middle| \begin{matrix} -m_1 n_R - m_3 + 1 \\ 0 \end{matrix} \right). \quad (5.23)$$

Using definition in (5.1) and transformations given in [109, eqs. (01.02.26.0007.01), (01.04.26.0003.01) and (07.34.21.0011.01)], the capacity in the simple closed-form is obtained

$$C^{IL} = \left(\frac{m_2 \lambda_2 \lambda_3 P_{PU}}{\lambda_1 k_s Q_p} \right)^{m_1 n_R} \frac{1}{\Gamma(m_1 n_R) \Gamma(m_3)} G_{3.3}^{3.2} \left(\frac{m_2 \lambda_2 \lambda_3 P_{PU}}{\lambda_1 k_s Q_p} \middle| \begin{matrix} -m_1 n_R - m_3 + 1, -m_1 n_R, 1 - m_1 n_R \\ 0, -m_1 n_R, -m_1 n_R \end{matrix} \right). \quad (5.24)$$

The ergodic capacity is presented in Figure 5.5, for $m_1=m_3=2$, $m_2=10$ ($m_i \lambda_i=1$, $i=1, 2, 3$), maximal permitted power $P_m=10$ for both cases when noise is present ($\sigma^2 = 0.5$) and when there is no effect of noise ($\sigma^2 = 0$). The scenario with the available statistical

CSI is considered and compared to the case when transmit power is allocated in accordance to the perfect CSI.

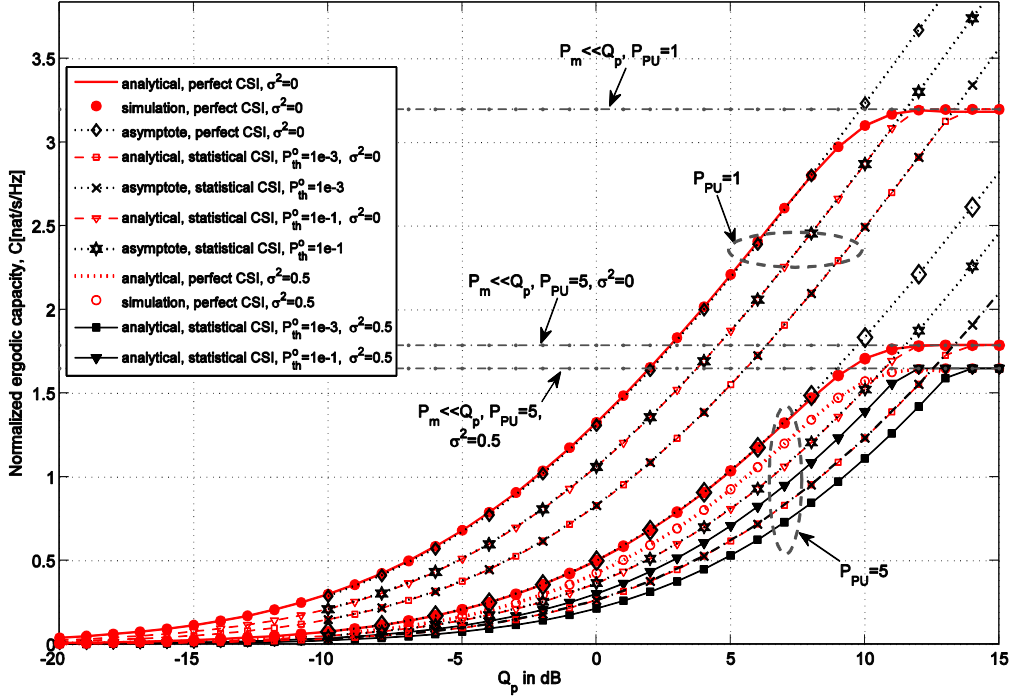


Figure 5.5 – Impact of statistical CSI on the ergodic capacity of the spectrum sharing system, $n_R=2$, $P_m=10$, $P_{PU}=1$ when $\sigma^2=0$, and $P_{PU}=5$ for both cases of presence and absence of noise, $m_1=m_3=2$ and $m_2=10$.

For the interference-limited case ($\sigma^2 = 0$), asymptotes obtained by using the expression (5.24) have been plotted along with the analytical and simulation curves. We can notice that the asymptotic expressions are highly accurate and approximate the analytical results when $Q_p \ll P_m$. When statistical CSI is available, the increased power of co-channel interference P_{PU} results in a decreased capacity in the both regions (for $Q_p \ll P_m$ as well as for $P_m \ll Q_p$). In accordance with the expectations, the higher capacity is obtained if larger values of interference outage probability P_o^{th} can be tolerated for the case when statistical CSI is available. As it is well known that the noise affects negatively the capacity, we can see that the capacity decreases when noise increases for $P_{PU}=5$. Furthermore, as it was noticed for the case of no noise, the larger interference outage probability, the higher capacity can be obtained.

Appendix 5 – A

In order to derive the final form for the first part of ergodic capacity when the available CSI is outdated, we start from (5.5) by writing it as follows

$$C_1 = \frac{(P_{PU} / \lambda_1 P_m)^{m_1 n_R}}{\lambda_3^{m_3} \Gamma(m_1 n_R) \Gamma(m_3)} \left[1 - \frac{\Gamma(m_2, k_o Q_p / (\lambda_2 P_m))}{\Gamma(m_2)} \right]^{+\infty} \int_0^{\infty} (y_3 + \sigma^2 / P_{PU})^{m_1 n_R} y_3^{m_3 - 1} e^{-y_3 / \lambda_3} \times \left[\int_0^{\infty} \gamma^{-(1-m_1 n_R)} e^{-\gamma \frac{y_3 P_{PU} + \sigma^2}{\lambda_1 P_m}} G_{2,2}^{1,2} \left(\begin{matrix} 1, 1 \\ 1, 0 \end{matrix} \middle| \gamma \right) d\gamma \right] dy_3, \quad (5A.1)$$

where

$$\log(1 + \gamma) = G_{2,2}^{1,2} \left(\begin{matrix} 1, 1 \\ 1, 0 \end{matrix} \middle| \gamma \right). \quad (5A.2)$$

Using the conventional integral of Meijer-G function given in [109, eq. (07.34.21.0088.01)] as

$$\int_0^{\infty} x^{-\alpha} e^{-wx} G_{p,q}^{m,n} \left(\begin{matrix} a_p \\ b_q \end{matrix} \middle| \eta x \right) dx = w^{\alpha-1} G_{p+1,q}^{m,n+1} \left(\begin{matrix} \alpha, a_p \\ b_q \end{matrix} \middle| \frac{\eta}{w} \right), \quad (5A.3)$$

then the expression in (5A.1) is written as

$$C_1 = \frac{(P_{PU} / \lambda_1 P_m)^{m_1 n_R}}{\lambda_3^{m_3} \Gamma(m_1 n_R) \Gamma(m_3)} \left[1 - \frac{\Gamma(m_2, k_o Q_p / (\lambda_2 P_m))}{\Gamma(m_2)} \right] \times \int_0^{\infty} \left(y_3 + \frac{\sigma^2}{P_{PU}} \right)^{m_1 n_R} y_3^{m_3 - 1} e^{-\frac{y_3}{\lambda_3} \left(\frac{y_3 P_{PU} + \sigma^2}{\lambda_1 P_m} \right)^{-m_1 n_R}} G_{3,2}^{1,3} \left(\begin{matrix} 1 - m_1 n_R, 1, 1 \\ 1, 0 \end{matrix} \middle| \frac{\lambda_1 P_m}{y_3 P_{PU} + \sigma^2} \right) dy_3. \quad (5A.4)$$

Now using the following expression of the specific function Meijer-G given in [109, eq. (07.34.16.0002.01)]

$$G_{p,q}^{m,n} \left(\begin{matrix} a_p \\ b_q \end{matrix} \middle| z \right) = G_{q,p}^{n,m} \left(\begin{matrix} 1 - b_q \\ 1 - a_p \end{matrix} \middle| z^{-1} \right), \quad (5A.5)$$

and the substitution for $y_3 + \sigma^2 / P_{PU} = t$ with the binomial expansion [88, eq. (1.111)] to get

$$C_1 = \frac{e^{\sigma^2/\lambda_3 P_{PU}}}{\lambda_3^{m_3} \Gamma(m_1 n_R) \Gamma(m_3)} \left[1 - \frac{\Gamma(m_2, k_o Q_p / (\lambda_2 P_m))}{\Gamma(m_2)} \right] \sum_{l=0}^{m_3-1} \binom{m_3-1}{l} \left(-\frac{\sigma^2}{P_{PU}} \right)^{m_3-1-l} \quad (5A.6)$$

$$\times \int_0^{\sigma^2/P_{PU}} t^{-(-l)} e^{-t/\lambda_3} G_{3,2}^{1,3} \left(\begin{matrix} 1 - m_1 n_R, 1, 1 \\ 1, 0 \end{matrix} \middle| \frac{\lambda_1 P_m}{P_{PU} t} \right) dt.$$

If the integral in the previous expression is I , in order to solve it, the integral is expressed by a summation of two integrals as follows

$$I = \int_0^{\sigma^2/P_{PU}} t^{-(-l)} e^{-t/\lambda_3} G_{3,2}^{1,3} \left(\begin{matrix} 1 - m_1 n_R, 1, 1 \\ 1, 0 \end{matrix} \middle| \frac{\lambda_1 P_m}{P_{PU} t} \right) dt - \int_0^{\sigma^2/P_{PU}} t^l e^{-t/\lambda_3} G_{3,2}^{1,3} \left(\begin{matrix} 1 - m_1 n_R, 1, 1 \\ 1, 0 \end{matrix} \middle| \frac{\lambda_1 P_m}{P_{PU} t} \right) dt. \quad (5A.7)$$

Applying the expression (5A.5) and representing the exponential function with power series and applying [109, eq. (07.34.21.0088.01)], the integral I is given in its final solution as

$$I = \left(\frac{1}{\lambda_3} \right)^{-l-1} G_{3,3}^{2,3} \left(\begin{matrix} 1 - m_1 n_R, 1, 1 \\ 1 + l, 1, 0 \end{matrix} \middle| \frac{\lambda_1 P_m}{\lambda_3 P_{PU}} \right) - \sum_{k=0}^{+\infty} \frac{(-1)^k}{\lambda_3^k k!} \left(\frac{\sigma^2}{P_{PU}} \right)^{l+k+1} G_{3,4}^{3,2} \left(\begin{matrix} -l - k, 0, 1 \\ m_1 n_R, 0, 0, -l - k - 1 \end{matrix} \middle| \frac{\sigma^2}{\lambda_1 P_m} \right). \quad (5A.8)$$

Substituting (5A.8) in (5A.6), the final form of first part of ergodic capacity is obtained as it is given in (5.6).

Appendix 5 – B

Starting from (5.7) the closed-form for the second part of the capacity is derived. First, the logarithm is substituted by the special function Meijer-G given in (5A.2), then (5A.3) is applied to get the following expression

$$C_2 = \frac{1}{\Gamma(m_1 n_R) \lambda_3^{m_3} \Gamma(m_3) \lambda_2^{m_2} \Gamma(m_2)} \int_{k_o Q_p / P_m}^{+\infty} \hat{y}_2^{m_2-1} e^{-\hat{y}_2 / \lambda_2} \int_0^{+\infty} y_3^{m_3-1} e^{-y_3 / \lambda_3} \times G_{2,3}^{3,1} \left(\begin{matrix} 0.1 \\ m_1 n_R, 0, 0 \end{matrix} \middle| \hat{y}_2 \frac{P_{PU}}{\lambda_1 k_o Q_p} \left(y_3 + \frac{\sigma^2}{P_{PU}} \right) \right) dy_3 d\hat{y}_2. \quad (5B.1)$$

Using the substitution $y_3 + \sigma^2 / P_{PU} = t$ then the binomial expansion

$$C_2 = \frac{e^{\sigma^2 / \lambda_3 P_{PU}}}{\Gamma(m_1 n_R) \lambda_3^{m_3} \Gamma(m_3) \lambda_2^{m_2} \Gamma(m_2)} \sum_{l=0}^{m_3-1} \binom{m_3-1}{l} \left(-\frac{\sigma^2}{P_{PU}} \right)^{m_3-1-l} \int_{k_o Q_p / P_m}^{+\infty} \hat{y}_2^{m_2-1} e^{-\hat{y}_2 / \lambda_2} d\hat{y}_2 \times I, \quad (5B.2)$$

where

$$I = \int_{\sigma^2 / P_{PU}}^{+\infty} t^l e^{-t / \lambda_3} G_{2,3}^{3,1} \left(\begin{matrix} 0.1 \\ m_1 n_R, 0, 0 \end{matrix} \middle| \frac{\hat{y}_2 P_{PU}}{\lambda_1 k_o Q_p} t \right) dt, \quad (5B.3)$$

and this can be solved following the same procedure for solving (5A.7) get

$$I = \left(\frac{1}{\lambda_3} \right)^{-l-1} G_{3,3}^{3,2} \left(\begin{matrix} -l, 0, 1 \\ m_1 n_R, 0, 0 \end{matrix} \middle| \frac{\hat{y}_2 \lambda_3 P_{PU}}{\lambda_1 k_o Q_p} \right) - \sum_{k=0}^{+\infty} \frac{(-1)^k}{\lambda_3^k k!} \left(\frac{\sigma^2}{P_{PU}} \right)^{l+k+1} \times G_{3,4}^{3,2} \left(\begin{matrix} -l-k, 0, 1 \\ m_1 n_R, 0, 0, -l-k-1 \end{matrix} \middle| \frac{\hat{y}_2 \sigma^2}{\lambda_1 k_o Q_p} \right). \quad (5B.4)$$

Substituting I solution in (5B.2), C_2 can be written as

$$C_2 = \frac{e^{\sigma^2 / \lambda_3 P_{PU}}}{\Gamma(m_1 n_R) \Gamma(m_2) \Gamma(m_3) \lambda_2^{m_2} \lambda_3^{m_3}} \sum_{l=0}^{m_3-1} \binom{m_3-1}{l} \times \left(-\frac{\sigma^2}{P_{PU}} \right)^{m_3-1-l} \left[\lambda_3^{l+1} I_1 - \sum_{k_2=0}^{+\infty} \frac{(-1)^{k_2}}{\lambda_3^{k_2} k_2!} \left(\frac{\sigma^2}{P_{PU}} \right)^{l+k_2+1} I_2 \right], \quad (5B.5)$$

where

$$\begin{aligned}
I_1 &= \int_{k_o Q_p / P_m}^{+\infty} \hat{y}_2^{m_2-1} e^{-\hat{y}_2/\lambda_2} G_{3,3}^{3,2} \left(\begin{matrix} -l, 0, 1 \\ m_1 n_R, 0, 0 \end{matrix} \middle| \hat{y}_2 \frac{\lambda_3 P_{PU}}{\lambda_1 k_o Q_p} \right) d\hat{y}_2, \\
&= \left(\frac{1}{\lambda_2} \right)^{-m_2} G_{4,3}^{3,3} \left(\begin{matrix} 1-m_2, -l, 0, 1 \\ m_1 n_R, 0, 0 \end{matrix} \middle| \frac{\lambda_2 \lambda_3 P_{PU}}{\lambda_1 k_o Q_p} \right) \\
&\quad - \sum_{k=0}^{+\infty} \frac{(-1)^k}{\lambda_2^k k!} \left(\frac{k_o Q_p}{P_m} \right)^{m_2+k} G_{4,4}^{3,3} \left(\begin{matrix} 1-m_2-k, -l, 0, 1 \\ m_1 n_R, 0, 0, -m_2-k \end{matrix} \middle| \frac{\lambda_3 P_{PU}}{\lambda_1 P_m} \right),
\end{aligned} \tag{5B.6}$$

and

$$\begin{aligned}
I_2 &= \int_{k_o Q_p / P_m}^{+\infty} \hat{y}_2^{m_2-1} e^{-\hat{y}_2/\lambda_2} G_{3,4}^{3,2} \left(\begin{matrix} -l-k_2, 0, 1 \\ m_1 n_R, 0, 0, -l-k_2-1 \end{matrix} \middle| \frac{\hat{y}_2 \sigma^2}{\lambda_1 k_o Q_p} \right) d\hat{y}_2 \\
&= \left(\frac{1}{\lambda_2} \right)^{-m_2} G_{4,4}^{3,3} \left(\begin{matrix} 1-m_2, -l-k_2, 0, 1 \\ m_1 n_R, 0, 0, -l-k_2-1 \end{matrix} \middle| \frac{\lambda_2 \sigma^2}{\lambda_1 k_o Q_p} \right) \\
&\quad - \sum_{k_3=0}^{+\infty} \frac{(-1)^{k_3}}{\lambda_2^{k_3} k_3!} \left(\frac{k_o Q_p}{P_m} \right)^{m_2+k_3} G_{4,5}^{3,3} \left(\begin{matrix} 1-m_2-k_3, -l-k_2, 0, 1 \\ m_1 n_R, 0, 0, -l-k_2-1, -m_2-k_3 \end{matrix} \middle| \frac{\sigma^2}{\lambda_1 P_m} \right).
\end{aligned} \tag{5B.7}$$

Finally, substituting (5B.7) and (5B.6) in (5B.5), the final closed form of the second part of ergodic capacity, C_2 , is obtained in (5.8).

6. Experimental results for OFDM-based cognitive radio

Orthogonal frequency division multiplexing (OFDM) is one of the most used modulation techniques for the current wireless communication systems, which can provide large data rates with sufficient robustness to radio channel impairments.

OFDM systems divide the input high-rate data stream into many low-rate streams transmitted in parallel [110], which increases the symbol duration and reduces the Inter Symbol Interference (ISI). These features were the basic motivation to make OFDM the standard for digital transmission systems, such as digital audio broadcasting (DAB) system [111], digital video broadcasting TV (DVB-T) system [112], and wireless local area networks (WLAN) [113]. Furthermore and due to OFDM's high transmission capacity, it has been applied to asymmetric digital subscriber line (ADSL), IEEE 802.11a/g standard, IEEE 802.16 Worldwide Interoperability for Microwave Access (WiMax) systems and Ultra-Wideband (UWB) system [114].

OFDM with the advantages that can provide, from high spectral efficiency, robustness against narrow-band interference to the easy implementation using Fast Fourier Transform (FFT), has been suggested as one of the best candidates for modulation in cognitive radio, where in [115] OFDM is provided as an enhancement of the spectrum efficiency. The advantages of OFDM technology and challenges to a practical OFDM-based cognitive radio system are discussed in [116].

OFDM modulation technique based secondary link has been studied in many works such as [117] where the primary user in each sub-band is limited by allowable interference threshold. Interference detection and cancellation for the OFDM-based cognitive radio system is studied in [118] and [119]. The OFDM system when perfect or only partial information about the intensification of channel to the primary user with a controlled level of interference is discussed in [120] under peak or average interference power constraint. The authors in [121] presented channel estimation algorithms for estimating OFDM wireless channels in the presence of synchronous interference.

Furthermore, the authors in [122] have shown that using OFDM modulation causes mutual interference between the primary and secondary users, even if they have different access technologies, due to the non-orthogonality of the transmitted signals. Hence, designing efficient resource allocation algorithms that work well in OFDM-based cognitive radio networks is a major challenge. The optimal solution for power allocation problem of OFDM can be obtained by using water filling technique where in [123] is employed for single user system without mutual interference. Fast algorithm in [124] is used to tackle the power allocation problem for multiuser OFDM-based cognitive radio networks. While in [125] the total amount of the mutual interference or the mutual interference on each sub channel of PUs are used for power allocation by considering the total power constraint and the transmit power constraint on each sub-channel. Moreover, resource allocation for the OFDM-based cognitive radio system is studied also in [126] and [127].

Since the basic challenge in OFDM-based cognitive radio is the spectrum sensing, many works have pointed to some solutions as [128] where the frequency synchronization in the OFDM-based cognitive radio system is considered. New spectrum sensing methods based on the characteristics of the OFDM signal were proposed using either energy detection, optimal Neyman-Pearson detection, autocorrelation detection or cyclostationarity feature detection, respectively, in [129], [130], [131] and [132]. The effect of spectrum sensing errors on the performance of orthogonal frequency division multiplexing based cognitive radio transmission can be evaluated by deriving the expression for the average bit error rate.

Although the primary user performance is an important issue to be analysed, it does not get the proper attention in recent works about cognitive radio networks.

Therefore, in this chapter, some results from practical study about the coexistence of primary and secondary users employing OFDM are provided in order to analyse the effect of the secondary user transmission at the performance of the primary user.

6.1 OFDM Characteristics

OFDM offers several advantages over other transmission technologies such as high spectral efficiency, robustness to fading channel, immunity to impulse interference, capability of handling very strong multi-path fading and frequency selective fading without having to provide powerful channel equalization.

OFDM is a frequency-division multiplexing (FDM) scheme utilized as a digital multi-carrier modulation method, where the concept of using parallel data transmission by means of FDM was published in mid 60s [133] and [134]. Multi-carrier modulation method is the concept of splitting a wideband signal into a number of narrowband signals modulating each of these new signals to several frequency channels of f_k , $k = 0, 1, 2, \dots, N-1$, where N is the number of multi frequency channels illustrated in Figure 6.1, and combining the data received on the multiple channels at the receiver [135].

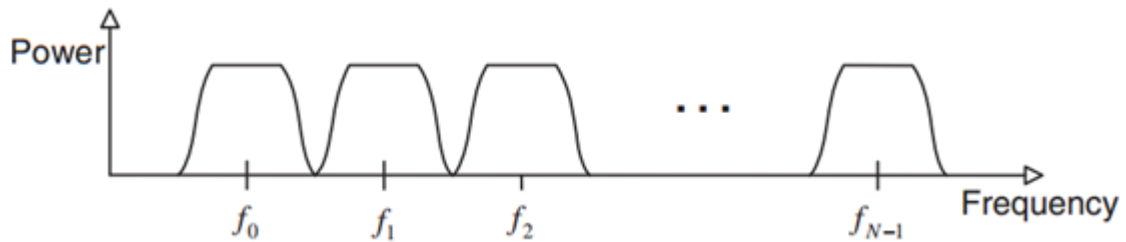


Figure 6.1 – multi-carrier signal spectrum.

Hence, the basic principle of OFDM is to split a high-rate data stream (R) from a data source into N parallel lower rate streams, one for each sub-carrier, where the number of subcarriers can be determined based on the channel bandwidth, data throughput and useful symbol duration. Each subcarrier is modulated with a conventional modulation scheme (such as Quadrature Amplitude Modulation, QAM, or Phase Shift Keying, PSK) at a low symbol rate (R/N), maintaining total data rates similar to conventional single-carrier modulation schemes in the same bandwidth. By

this lowering of the bitrate per carrier, the influence of inter-symbol interference is significantly reduced. Due to the serial to parallel conversion, the duration of transmission time for N symbols is extended to NT_s , which forms a single OFDM symbol with a length of T_{sym} ($T_{sym} = NT_s$). Computationally efficient FFT (Fast Fourier Transform) and IFFT (inverse FFT) architectures are usually implemented to perform OFDM modulation and demodulation, respectively. OFDM scheme is given in Figure 6.2.

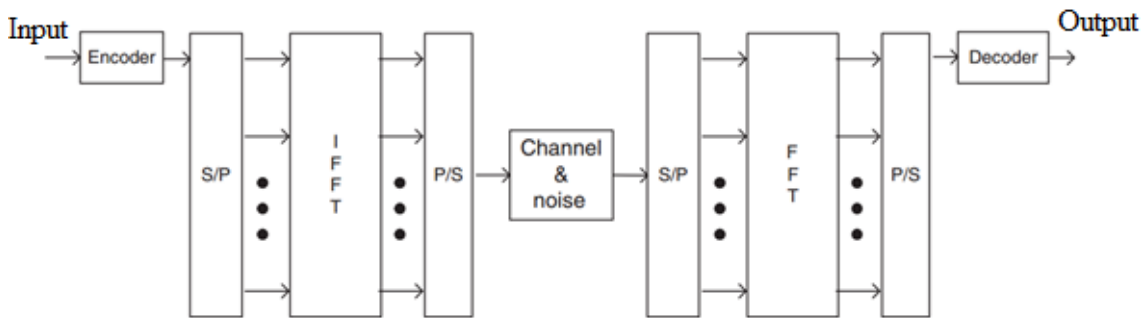


Figure 6.2 – OFDM modulation and demodulation scheme.

The multiple frequency channels, known as sub-carriers, are orthogonal to each other [136] and this differentiates OFDM from original multi-carrier transmission, where it can be seen in Figure 6.3 the efficiency in spectrum due to the orthogonality feature.

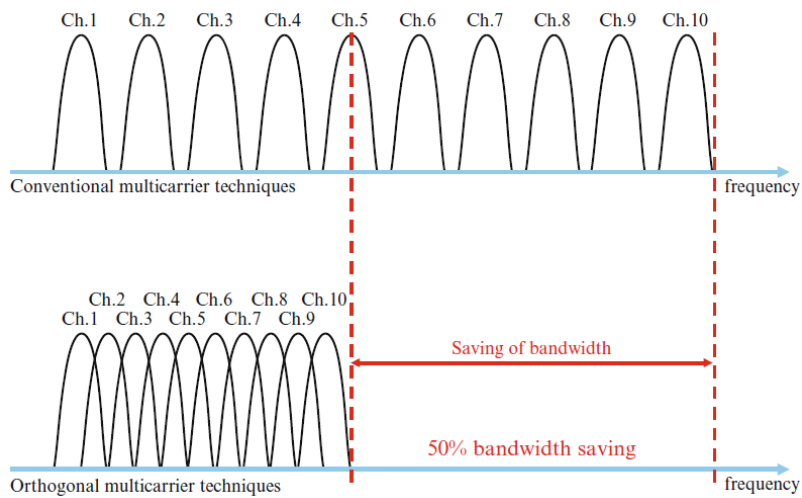


Figure 6.3 – Bandwidth saving in OFDM.

The orthogonality gives the carriers a valid reason to be closely spaced with overlapping without Inter-Carrier Interference (ICI) [137], where orthogonality is a property that allows the signals to be perfectly transmitted over a common channel and detected without interference. It is shown in Figure 6.4 that in OFDM signal, the peak on one sub-carrier coincides with the nulls of the other ones. ICI causes power leakage among subcarriers which degrades the system performance and loss in information, the authors in [138] study OFDM-ICI cancellation scheme which performs better than standard OFDM systems with an easy implementation without increasing the system complexity. More about mathematical deduction of the orthogonal carrier frequencies is given in [133]. As a consequence of keeping the orthogonality property, which implies both orthogonality in time no ISI and in frequency no ICI, equalization in the subcarrier domain becomes particularly simple: the remaining amplitude and phase distortion affecting each subcarrier can be easily corrected by complex division or de-mapping.

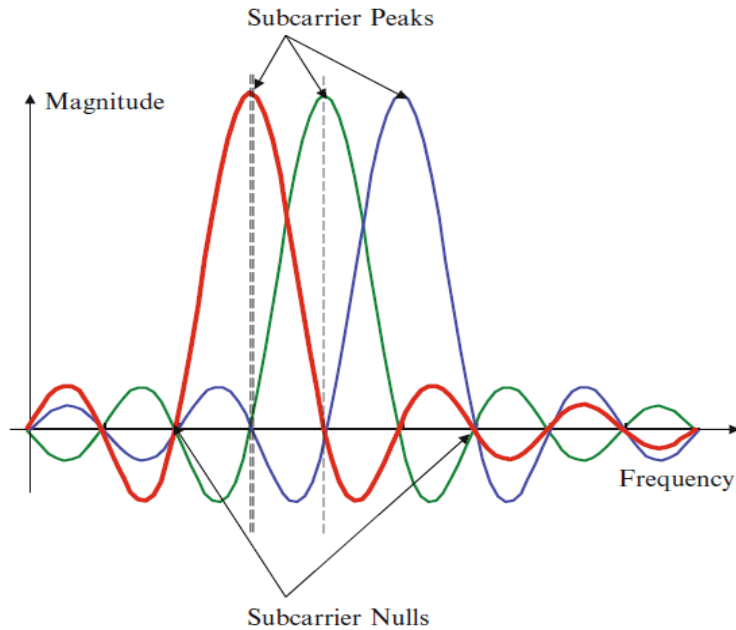


Figure 6.4 – Orthogonality concept in OFDM.

OFDM signal may incur out-of-band radiation, which causes Adjacent Channel Interference (ACI), and in order to reduce the out-of-band power of OFDM symbols, OFDM scheme places a guard band around the frequency band and a guard interval in time domain of length T_g . Guard interval can be inserted in two different ways: Zero

Padding (ZP) that pads the guard interval with zeros, or cyclic extension of the OFDM symbol called Cyclic Prefix (CP) added to the beginning of an OFDM symbol. Cyclic prefix samples are taken from the latter section of the original OFDM symbol and the total OFDM symbol length increases to $T_{sym} = T_{sub} + T_G$, where T_{sub} denotes the duration of effective OFDM symbol without guard interval as it is shown in Figure 6.5.

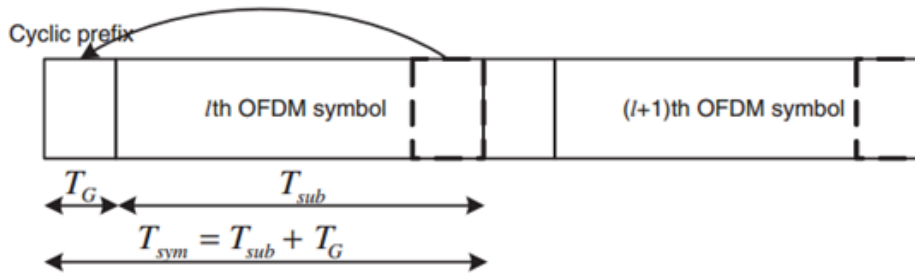


Figure 6.5 – OFDM symbol with guard interval.

Two from the main drawbacks to OFDM are the large dynamic range of the signal (also referred as peak-to average [PAR] ratio) and its sensitivity to frequency errors. When considering a practical system, hardware imperfections such as oscillator phase noise must be taken into account, where modeling the phase noise is covered in [139] and in [140] OFDM sensitivity to phase noise was quantified in terms of SNR loss for different levels of phase noise and frequency offset. Furthermore, BER analysis was covered by Tomba in [141] using a moment method to evaluate the BER analytically. A summary of OFDM theory and practice can be found in [142].

6.2 OFDM-based Cognitive Radio

OFDM has been already mentioned in the literature as a potential transmission technology for cognitive radio systems due to its underlying sensing and spectrum shaping capabilities together with its flexibility. The first important function of cognitive radio system is to sense the environment and see the unused spectrum bands by the licensed users in a fast and efficient way to provide new ways to access spectrum and then organizing the transmission of secondary users through available bands. This function is done by different sensing techniques in cognitive radio, which complexes the

hardware requirements, while in OFDM, scanning the spectrum is done without any extra hardware using FFT. The output of FFT at the receiver tries to detect the presence of the primary user in that band as energy detector [143] and [144]. Furthermore, OFDM can organize and control the transmission through spectrum holes by its ability to disable a set of its sub-carriers introduced in a more detailed scheme called spectrum pooling in [115]. Furthermore, OFDM is not a multiple access technique by itself, but it can be combined with the existed multiple access techniques such as TDMA (Time Division Multiple Access), FDMA (Frequency Division Multiple Access), and CDMA (Code Division Multiple Access) in order to share the available resources to a cognitive system among the users. Many other advantages of OFDM based cognitive radio is given in [116] and many other studies about it is provided in the introduction of this chapter.

Among the OFDM standards that utilize cognitive features are IEEE 802.22 standard, which is known as cognitive radio standard because of the amount of cognitive features that are employed, WLAN standard (IEEE 802.11) in which IEEE 802.11a/g is probably the most commonly known OFDM-based standard. While the main standards that are upgraded to have cognitive features with are: IEEE 802.11h and IEEE 802.11k standards.

To get a closer insight into the problems of practical OFDM system implementation, the authors in [145] presented the FPGA based (802.11a) prototype. Practical implementation of OFDM based cognitive radio links using Universal Software Radio Peripheral (USRP) platforms is provided in few papers in literature such as [146] and [147] which analysis the implementation of cognitive radio with frequency hopping (FH) primary users. In all of these papers GNU radio is used for communication with USRP platforms, where GNU radio is a free open source software development kit that provides signal processing modules to build a software radio in a real-time environment that involves hybrid Python/C++ programming and basic signal processing functions (ex: Filters, FFT, Channel Coding). The advantage is that it provides simulation environment and has extensive library of pre-defined and test-bed functional blocks, but on the other hand it requires a good experience in software. While in [148] Matlab has been used for communicating with USRP instead of GNU.

6.2.1 Hardware: Characteristics of USRP

The Universal Software Radio Peripheral, was developed by Ettus Research LLC, provides the low cost radio systems for commercial and research applications [149]. USRP provides digital baseband and intermediate frequency section within the hardware OFDM based cognitive radio experiment on USRP. The basic philosophy behind the USRP is to provide all waveform specific features like modulation and demodulation in CPU, whereas the high speed operations like interpolation, decimation, digital up and down conversion are provided within FPGA [150] and [151]. The true value of the USRP is in what it enables engineers and designers to create on a low budget and with a minimum of effort.

The basic architecture for USRP version 1 contains USB 2.0, Analog-to-Digital Convertors (ADC) and Digital-to-Analog Convertors (DAC) (Each USRP has 4 ADC and DAC), reprogrammable FPGA and daughter-board interface. The daughter-board interface allows connecting to ADC and DAC components and the USB 2.0 interface provides connection from FPGA to the computer as it is provided in Figure 6.6. It is good to mention that the Maximum effective bandwidth is about 8 MHz, and this limitation is due to the USB 2.0 interface.

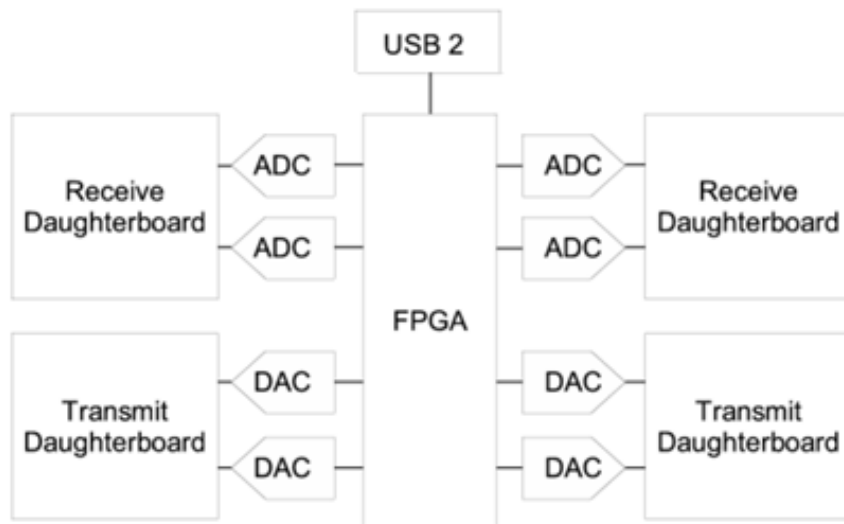


Figure 6.6 – USRP block diagram.

Experimental Study of OFDM implementation USRP – SDR using GNU radio has been provided in [152], while in this work Matlab is used instead as it is in [148].

6.2.2 System Model

The implementation is done using two personal computers (PC) controlling the transmitter and the receiver of USRP platforms as it is provided in Figure 6.7. Experiments are conducted indoor; where the used daughter boards are N210 and the USRP centre frequency is set at 402.5 MHz. Communicating with the USRP by PC is done through Matlab toolbox for USRP using User Datagram Protocol (UDP) protocol. Computer sends baseband signal samples to the USRP which generates signal at a given frequency and bandwidth specified by interpolation factor, signal is then transmitted over antenna or through cable to the receiving end where all operations are reversely executed.



Figure 6.7 – System environment.

The aim of this experiment is to determine the effect of secondary transmission on the primary user performance by analysing the BER of the received signal at the primary receiver. BER is defined as the estimated probability that any transmitted bit will be received in error (a transmitted “one” will be received as a “zero” and vice versa), the ratio of the number of bits received erroneously to the total number of transmitted bits is the BER. It is important to say that the used coding in this experiment is Gray coding instead of the binary one used in [148]. In Gray coding, two adjacent code numbers differ from each other only by one bit. This way, if neighbouring

constellation points are decoded “wrong”, only few bits will be wrong which improves the BER of detection and demodulation.

BER has been analysed for different values of secondary transmission interference, given in the form of signal to interference ratio (SIR), as well as different primary signal strength to noise ratio at the primary receiver. Furthermore, the experiment is done for two different channel type between the USRP transmitter (USRP-Tx) and USRP receiver (USRP-Rx), one when they are communicating wirelessly (through antennas) and the other when they are connecting by a cable.

Primary Signal (OFDM)

Source data for primary user is taken from an 8-bit gray scale (256 gray levels) bitmap image file given in Figure 6.8 [148]. The data is converted to the symbol size determined by the choice of M -PSK, where here the 256PSK modulation is deployed on every subcarrier [153]. The converted data is then separated into multiple frames by the OFDM transmitter scheme given in Figure 6.2 to be modulated frame by frame. During modulation, the symbols are differentially encoded and then the modulated frames are cascaded together along with frame guards inserted in between. Furthermore, a sinusoid signal is added to the beginning of the data stream as a header with a power equals the OFDM stream power. All of this is done before the exit of the transmitter.



Figure 6.8 – Primary transmission data, 256 gray-scale bitmap image.

Secondary Signal (OFDM)

Secondary user signal is generated in Matlab and saved in a file used for simulation of secondary transmission at the location of primary receiver. Secondary signal also employs OFDM and applies 256 PSK modulations. It is assumed that secondary and primary signal bandwidths are equal.

This implementation is extended from the one described in [148], where in this experiment USRP emulates both the primary and secondary transmissions (OFDM). Therefore, the explained schemes for Carrier Frequency Offset (CFO) estimation, time synchronization and channel equalization considered in [148] are the same in this work. The time synchronization process is done using a method based on auto-correlation of two sliding windows of length N , shifted in time [146].

6.2.3 Coexistence of Primary and Secondary Users (OFDM)

It is assumed that the primary and secondary systems are full synchronized in time. Secondary transmitter performs a spectrum sensing in order to obtain information about the used frequencies or subcarriers from the primary user as it is explained in Figure 6.9.

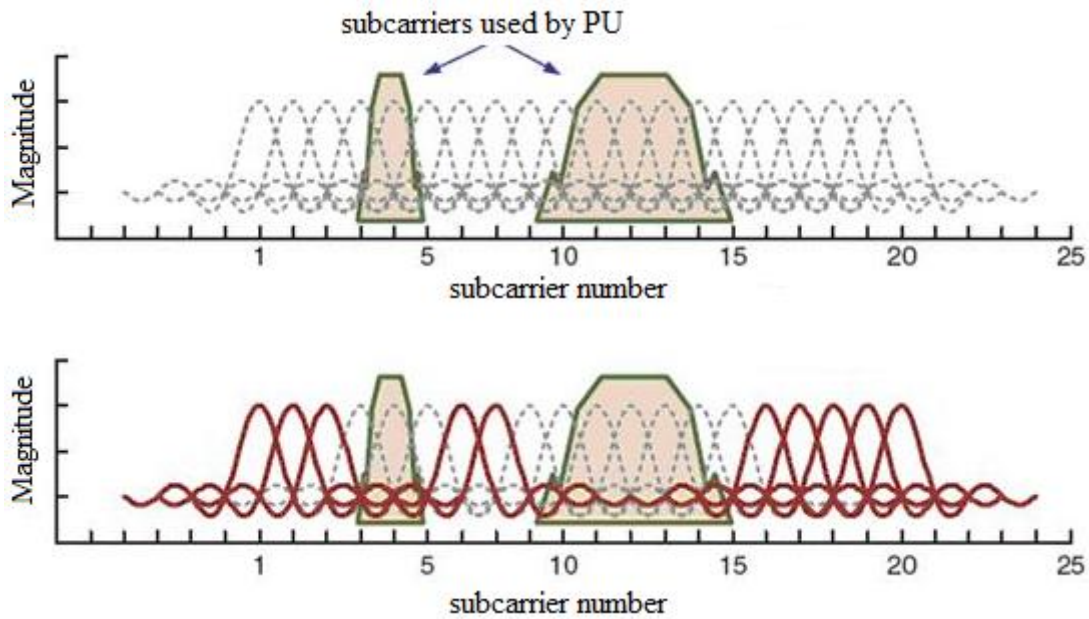


Figure 6.9 – Coexistence between primary and secondary users.

Transmission parameters for primary and secondary signals are given in Table 6.1, whereas the Tables 6.2 and 6.3 give the USRP-Tx and USRP-Rx platform parameters, respectively.

Table 6.1 – Primary and secondary signals’ (OFDM) parameters.

Parameter	Value
Carrier frequency	402.5 MHz
Bandwidth	1 MHz
Number of subcarriers (FFT size)	1024
Modulation on subcarriers	256DPSK
Cyclic prefix length	256 samples
Frame guard interval length	1280 samples
Header length	2560 samples
Data symbols per frame	7
Equalization symbols per frame	2
Frame length (with guard interval)	16640
Number of used subcarriers in a symbol	900

Table 6.2 – USRP-Tx parameters.

Parameter	Value
Carrier Frequency	402.5 MHz
Instantaneous bandwidth	1 MHz
LO offset	10 MHz
Gain	[0-30]

Different values of the USRP-Tx gain, G , is considered in order to perform different values of signal to noise ratio for the primary transmission. Furthermore, Local Oscillator (LO) offset in USRP-Tx as well as in USRP-Rx is used in order to move the signal bandwidth away from the interference generated by the USRP hardware.

Table 6.3 – USRP-Rx parameters.

Parameter	Value
Carrier Frequency	402.5 MHz
Instantaneous bandwidth	1 MHz
LO offset	10 MHz
Gain	0

Bit error rate according to the signal to interference ratio at the primary receiver is presented for different values of signal to noise ratio in Figure 6.10 when the USRP transmitter and receiver communicate wirelessly and in Figure 6.11 when they are connected by a cable. The primary signal SNR is controlled by changing the gain value of USRP transmitter platform, G , where signal to noise ratio values varies from 67 dB which points to $G=30$, to 37 dB which points to $G=0$.

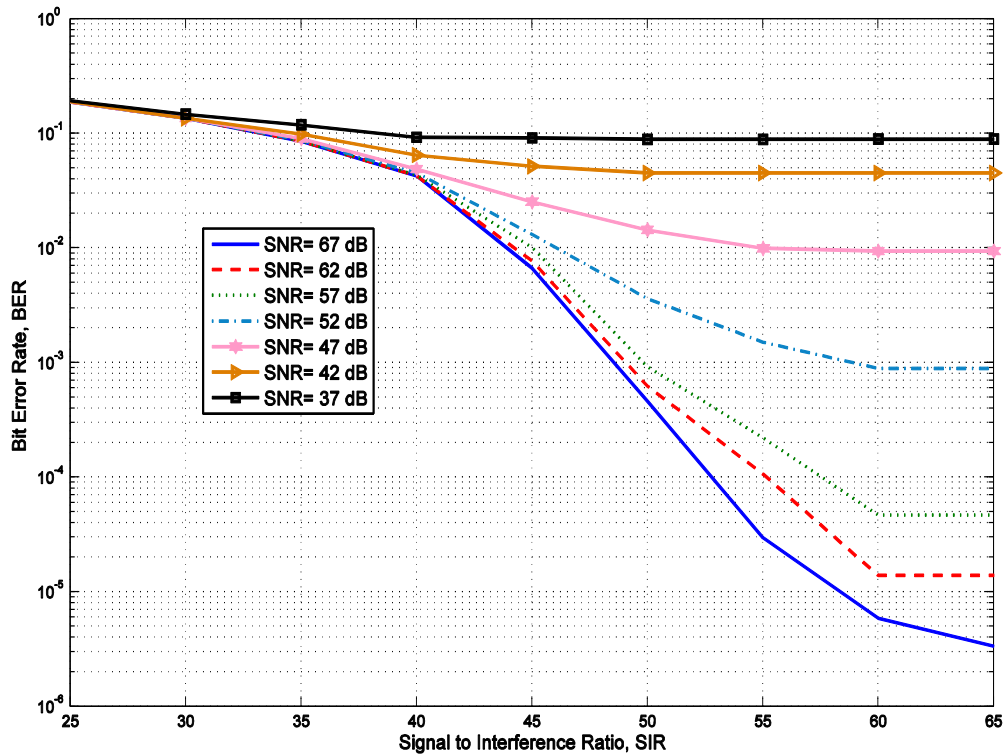


Figure 6.10 – Bit error rate of primary signal for the wireless channel.

It can be noticed that as the signal to interference ratio decreases, which means that the interference generated from the secondary user increases, the bit error rate increases for any value of SNR. On the other hand, for a fixed SIR, the bit error rate increases as the SNR values decrease (the effect of noise increases). Furthermore, it can be seen that the effect of secondary interference on the primary signal at the receiver depends on the value of SNR. As long as $SIR < SNR$ which means that the dominant effect on the primary signal is the interference (interference-limited case), BER increases as the interference increases (SIR decreases) to reach a plateau when $SIR \geq SNR$ where in this range the basic effect belongs to the noise (noise-limited case).

These results are obtained for both cases when the USRP transmitter and receiver are communicating wirelessly or by a cable. On the other hand, comparing the results in Figures 6.10 and 6.11, it can be seen that BER has smaller values when the transmission is done through a cable under the same conditions, this can be explained due to the addition interferers that can be existed in the surrounding environment when the transmission is done through a wireless channel., where the interference value cannot be totally controlled. It had been tried to make the interferers in the surrounding environment through this experiment low as much as it is possible.

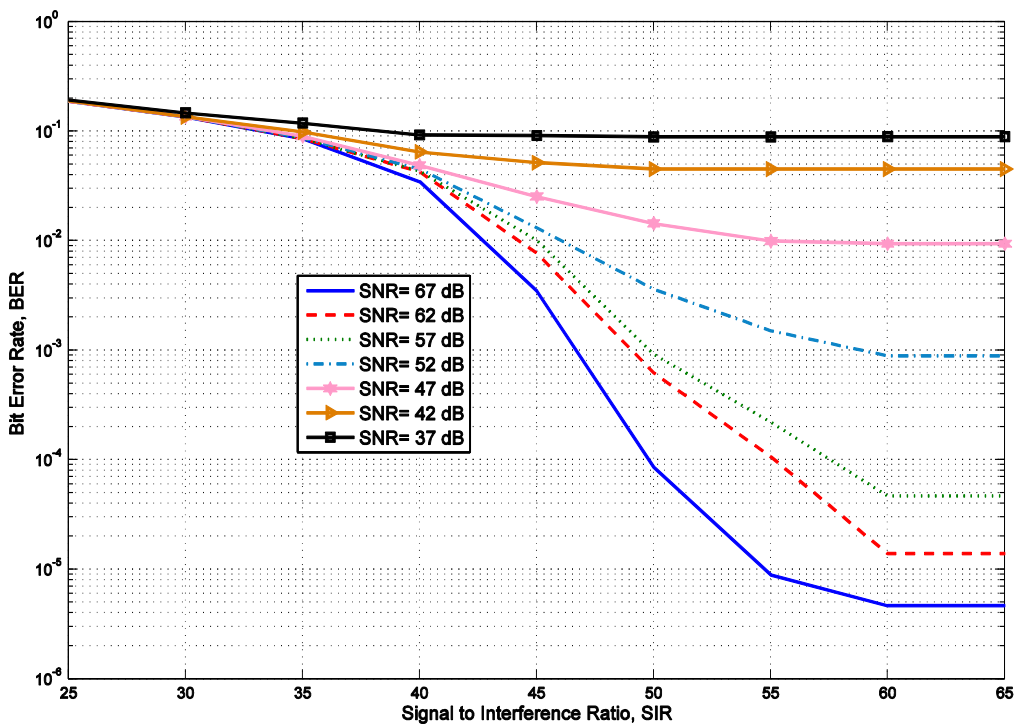


Figure 6.11 – Bit error rate of primary signal for the cable case.

The obtained results can be used in order to define the tolerable interference power at the primary receiver and define the interference power constraint value depending on the strength of the primary signal to the noise and the allowed BER in the system.

7. Conclusion

In this dissertation, the basic goal was to analyze the primary transmission's interference together with the noise at the secondary transmitter when imperfect channel state information of the link between secondary transmitter and primary receiver is imperfect.

In the introduction chapter, the need to cognitive radio and the concept of it are given in details, as well as its main functions. Spectrum access techniques have been explained especially the spectrum underlay access, which is used in this thesis to analyze the performance of cognitive radio system with a controlled interference level. In the second chapter, it has been pointed out to some wireless communication system concepts used in the dissertation, from the wireless channel and the fading models that try to model the channel and different fading effects on the signal through mathematically, especially Nakagami fading propagation which is used in the thesis, to the channel state information forms. Special attention is provided to the power control strategies used in order to protect the primary user, in addition to different diversity techniques used later in studying the secondary link performance.

Cognitive radio system model with controlled interference level under the effect of the co-channel interference signal generated from primary transmitter is described in the third chapter. Maximum transmit power of the secondary transmitter is given depending on the applied interference and transmit power constraints. Signal to interference and noise ratio (SINR) expression and its probability density function, in addition to the outage probability and moments of SINR are derived in closed- form expressions for the case when the channel state information of the channel between

secondary transmitter and primary receiver is perfect in the first half of the chapter. While in the second half of the chapter, the analysis and expressions are derived and given for the case when the CSI is outdated. The concept of outdated CSI and the power control strategy for this case are explained. Outage probability and the moments of SINR have been derived in closed-form expressions for both the perfect and outdated CSI. Asymptotes cases when the interference constraint or the transmit constraint dominates have been provided in both analytical and simulation results.

In the fourth chapter, the performance of cognitive radio system with co-channel interference signal, when MRC is applied at the secondary receiver, is analyzed for the case when perfect CSI is available at the secondary transmitter in the first part of the chapter, outdated CSI in the second part while it is analyzed in the last part of the chapter for the case when only statistical CSI is available. Statistical characteristics of SINR from outage probability to the moments for different number of antennas at the secondary transmitter are derived. Furthermore, For the case when no noise at the receiver, statistical characteristics of SIR when OSTBC is applied at the secondary link is analyzed and compared to the case of MRC when perfect CSI is available for two cases: when the channels have a unit value ($\lambda_i=1/m_i$) and when they do not. It is noticed that the dependence of probability density function of SIR on fading parameters values is less noticeable when the channels have a unit power gain. Transmission power control of the secondary transmitter is provided for the case of statistical CSI and outage probability of SINR is derived in a closed-form when more than one antenna is applied at the secondary receiver. As expected, MRC enhances the performance of the system, where the outage probability values decrease as the number of receive antennas increase; while when the interference power constraint Q_p goes large, the interference is more critical for SU link performance for both cases of MRC diversity and no diversity case. Outage capacity for a defined outage probability is analyzed for the case of statistical CSI where the outage capacity decreases as the tolerated interference outage probability P_o^{th} decreases.

Ergodic capacity in numerical closed-expression when MRC is applied at the secondary receiver for the cases of outdated and statistical CSI is derived for Nakagami fading environment, where it is seen that the MRC diversity results in larger performance gain for the secondary link for lower Nakagami fading parameter. Ergodic

capacity expressions have been derived using special functions explained in the Appendix in the end of the chapter, therefore and in order to simplify the derived analytical expressions, two limiting cases: interference and noise limited cases have been provided as asymptotes for the general case when the interference power constraint dominates ($Q_p \ll P_m$), where it is noticed that for all values of the receive antennas number; the interference-limited system achieves a higher capacity than the noise-limited one, furthermore, it is noticed that for the larger number of receive antennas, the relative change of capacity values due to effect of noise is less significant. For the interference-limited system, ergodic capacity is studied when OSTBC is employed at the secondary link in its special Alamouti scheme when perfect CSI knowledge is available. As a comparison with MRC diversity, the result was that applying MRC as a diversity technique achieves higher capacities than Alamouti scheme.

The correctness of all the obtained numerical results is checked by an independent simulation method. Through the plotted figures, it can be seen that the analytical results match the simulation ones perfectly.

In the last chapter, through experimental work, the performance of primary user under the effect of the secondary transmission is analyzed. The performance is discussed through the value of bit error rate of the received primary signal, where BER is obtained for different values of SIR (primary signal strength to the secondary interference strength ratio) under different values of SNR at the receiver of primary user. The experiment is done using two computers and two USRP platforms to get the results for two cases: first when the transmitter and receiver communicate wirelessly by antennas and second when they are connected by a cable. The obtained results can be used in determining the value of interference power constraint, which is known as the interference temperature, at the primary receiver depending on the strength of the primary signal and the allowed BER in the system.

References

- [1] Y. Deniz. "The Internet of Things will Derive Wireless Connected Devices to 40.9 Billion in 2020." [Online]. Available: <https://cloudcomputing.systems.com/node/3154825> [August 2014].
- [2] P. Cerwall. "Ericsson Mobility Report." Ericsson. [Online]. Available: www.ericsson.com/res/docs/2015/ericsson-mobility-report-june-2015.pdf [June 2015].
- [3] FCC, *Report on The Trend in Wireless Devices*, [Online]. Available: <http://www.fcc.gov/oet/info/documents/reports/wirelessdevices.doc>.
- [4] ITU-R, *Efficient Use of the Radio Spectrum and Frequency Sharing within the Mobile-Satellite Service*, 2009. [Online]. Available: <http://www.itu.int/pub/R-QUE-SG04.83>.
- [5] R. Chiang, G. Rowe, K. Sowerby, "A Quantitative Analysis of Spectral Occupancy Measurement for Cognitive Radio," in *Proc. IEEE Vehicular Technology Conference (VTC)*, Dublin, Ireland, 2007, pp. 3016 – 3020.
- [6] M. Wellens, J. Wu, P. Mahonen, "Evaluation of Spectrum Occupancy in Indoor and Outdoor Scenario in the Context of Cognitive Radio," in *Proc. Second International Conference on Cognitive Radio Oriented Wireless Networks and Communications (CrowCom 2007)*, August 2007, pp. 420 – 427.
- [7] S. Jones, E. Jung, X. Liu, N. Merheb, I. -J. Wang, "Characterization of Spectrum Activities in the U.S. Public Safety Band for Opportunistic Spectrum Access," in

- Proc. Second IEEE International Symposium on New Frontiers*, April 2007, pp. 137 – 146.
- [8] FCC, *Spectrum Policy Task Force (SPTF) Report*, ET Docket Technical Report No. 02-135, 2002.
- [9] M. McHenry, "Frequency Agile Spectrum Access Technologies," in *Proc. FCC Workshop Cognitive Radio*, 2003.
- [10] K. Patil, R. Prasad, K. Skouby, "A Survey of Worldwide Spectrum Occupancy Measurement Campaigns for Cognitive Radio," in *Proc. International Conference on Devices and Communications (ICDeCom)*, 2011, pp. 1 – 5.
- [11] Federal Communications Commission (FCC), *Facilitating Opportunities for Flexible, Efficient, and Reliable Spectrum Use Employing Cognitive Radio Technologies*, ET Docket No. 03 – 108, 2005.
- [12] J. Mitola III, G. Q. Maguire, "Cognitive Radio: Making Software Radio More Personal," *IEEE Personal Communications*, vol. 6, no. 4, pp. 13 – 18, August 1999.
- [13] I. F. Akyildiz, W. Y. Lee, M. C. Vuran, S. Mohanty, "NeXt Generation/ Dynamic Spectrum Access/ Cognitive Radio Wireless Networks: A Survey," *Computer Networks Journal (Elsevier)*, vol. 50, no. 13, pp. 2127 – 2159, September 2006.
- [14] D. Cabric, S. M. Mishra, et al. "Implementation Issues in Spectrum Sensing for Cognitive Radios," in *Proc. 38th. Asilomar Conference on Signals, Systems and Computers*, 2004, pp. 772 – 776.
- [15] S. Haykin, "Cognitive radio: Brain-empowered Wireless Communications," *IEEE Journal on Selected Areas in Communications*, vol. 30, no. 2, pp. 201 – 220, February 2005.
- [16] F. K. Jondral, "Software-defined Radio-basic and Evolution to Cognitive Radio," *EURASIP Journal, Wireless Communication and Networking*, vol. 3, pp. 275 – 283, 2005.
- [17] L. V. Wazer, "Spectrum Access and The Promise of Cognitive Radio Technology," in *Proc. FCC Cognitive Radio Technologies (CRTP)*, ET Docket

No. 03-108, 2003.

- [18] A. Sahai, N. Hoven, R. Tandra, "Some Fundamental Limits on Cognitive Radio," in *Proc. 42nd Allerton Conference on Communication, Control and Computing*, Monticello, IL, 2004.
- [19] C. Stevenson, G. Chouinard, Z. Lei, W. Hu, S. Shellhammer, W. Caldwell, "IEEE 802.22: The First Cognitive Radio Wireless Regional Area Network Standard (WRANs)," *IEEE Communications Magazine*, vol. 47, no. 1, pp. 130 – 138, January 2009.
- [20] WG802.22, Wireless Regional Wireless Regional Area Networks Working Group, Institute of Electrical and Electronics Engineers. Internet:<http://www.ieee802.org/22/>
- [21] C. Cordeiro, K. Challapali, D. Birru, N. Sai Shankar, "IEEE 802.22: The First Worldwide Wireless Standard Based on Cognitive Radios," in *Proc. First IEEE International Symposium on New Frontiers in Dynamic Spectrum Access Networks (DySPAN)*, 2005, pp. 328 – 337.
- [22] A. Goldsmith, S. A. Jafar, I. Maric, S. Srinivasa, "Breaking Spectrum Gridlock with Cognitive Radios: An Information Theoretic Perspective," *Proceedings of the IEEE*, vol. 97, no. 5, pp. 894 – 914, May 2009.
- [23] M. Oner, F. Jondral, "On the Extraction of the Channel Allocation Information in Spectrum Pooling Systems," *IEEE Journal on Selected Areas in Communications JSAC*, vol. 25, no. 3, pp. 558 – 565, April 2007.
- [24] B. Wild, K. Ramchandran, "Detecting Primary Receivers for Cognitive Radio Applications," in *Proc. IEEE DySPAN*, 2005, pp. 124 – 130.
- [25] M. M. Buddhikot, K. Ryan, "Spectrum Management in Coordinated Dynamic Spectrum Access Based Cellular Networks," in *Proc. First International Conference on Dynamic Spectrum Access Networks, IEEE (DySPAN)*, Baltimore, USA, 2005, pp. 299 – 307.
- [26] G. Salami, O. Durowoju, A. Attar, O. Holland, R. Tafazolli, H. Aghvami, "A Comparison Between The Centralized and Distributed Approaches for Spectrum

- Management," *IEEE Communications Surveys & Tutorials*, vol. 13, no. 2, pp. 1 – 17, May 2010.
- [27] C. Peng, H. Zheng, B. Y. Zhao, "Utilization and Fairness in Spectrum Assignment for Opportunistic Spectrum Access," *Journal Mobile Networks and Applications*, vol. 11, no. 2, pp. 555 – 576, August 2006.
- [28] J. Mitola, "Cognitive Radio: An Integrated Agent Architecture for Software Defined Radio," Ph.D. Dissertation, Royal Institute of Technology (KTH), Stockholm, Sweden, 2000.
- [29] P. Kolodzy et al., "Next Generation Communication: Kick off Meeting," in *Proc. DARPA*, 2001.
- [30] Y. C. Liang, Y. Zeng, E. Peh, A. T. Hoang, "Sensing-throughput Trade-off for Cognitive Radio Networks," *IEEE Transactions Wireless Communications*, vol. 7, no. 4, pp. 1326 – 1337, April 2008.
- [31] M. H. M. Costa, "Writing on Dirty Paper," *IEEE Transactions Information Theory*, vol. 29, no. 3, pp. 439 – 441 , May 1983.
- [32] S. I. Gelfand, M. S. Pinsker, "Coding for Channel with Random Parameters," *Problems of Control and Information Theory*, vol. 9, no. 1, pp. 19 – 31, January 1980.
- [33] FCC, *Notice of Proposed Rule Making and Order*, ET Docket Report No. 03 - 322, 2003.
- [34] T. Fryer. "Cognitive Radio Generates Interest from the Military." Internet: <http://www.newelectronics.co.uk/electonics-technology/cognitive-radio-generates-interest-from-the-military/56149>, [September 2013].
- [35] Y. C. Liang, A. T. Hoang, H. H. Chen, "Cognitive Radio on TV Bands: A New Approach to Provide Wireless Connectivity for Rural Areas," *IEEE Wireless Communications*, vol. 15, no. 3, pp. 16 – 22, June 2008.
- [36] C. Cordeiro, K. Challapali, D. Birru, S. N. Shankar, "IEEE 802.22: An Introduction to the First Wireless Standard based on Cognitive Radios," *Journal of Communications*, vol. 1, no. 1, April 2006.

- [37] S. Kim, W. Choi, Y. Choi, J. Lee, Y. Han, "Interference Reduction of Cellular Relay Networks in Multiple-cell Environment by Spectrum Agility," in *Proc. IEEE International Symposium on Personal, Indoor and Mobile Radio Communications (PIMRC)*, Cannes, France, 2008.
- [38] Y. Yu, H. Qingyang, C. S. Bontu, Z. Cai, "Mobile Association and Load Balancing in a Cooperative Relay Cellular Network," *IEEE Communications Magazine*, vol. 49, no. 5, pp. 83 – 89, May 2011.
- [39] V. Chandrasekhar, J. G. Andrews, A. Gatherer, "Femtocell Networks: a Survey," *IEEE Communications Magazine*, vol. 46, no. 9, pp. 59 – 67, September 2008.
- [40] J. Xiang, Y. Zhang, T. Skeie, L. Xie, "Download Spectrum Sharing for Cognitive Radio Femtocell Networks," *IEEE Systems Journal*, vol. 4, no. 4, pp. 524 – 534, December 2010.
- [41] S. Bayhan, F. Alagoandz G. Guandr, "Cognitive Femtocell Networks: an Overlay Architecture for Localized Dynamic Spectrum Access," *IEEE Wireless Communications*, vol. 17, no. 4, pp. 62 – 70, August 2010.
- [42] A. Gorcin, H. Arslan, "Public Safety and Emergency Case Communications: Opportunities from the Aspect of Cognitive Radio," in *Proc. IEEE International Symposium on New Frontier in Dynamic Spectrum Access Networks (DySPAN)*, 2008.
- [43] J. Wang, M. Ghosh, K. Challapali, "Emerging Cognitive Radio Applications: A Survey," *IEEE Communications Magazine*, vol. 49, no. 3, pp. 74 – 81, 2011.
- [44] A. Goldsmith. *Wireless Communications*. Cambridge University Press, 2005.
- [45] M. K. Simon, M. -S. Alouini. *Digital Communication over Fading Channels*, 2nd ed.: Wiley-Interscience, 2005.
- [46] M. Nakagami, "The m-Distribution – A General Formula of Intensity Distribution of Rapid Fading," in *Statistical Methods in Radio Wave Propagation*. W. C. Hoffman, Ed. Los Angeles, 1985, pp. 3 – 6.
- [47] H. Suzuki, "A Statistical Model for Urban Radio Propagation," *IEEE Transactions on Wireless Communications*, vol. 25, no. 7, pp. 472 – 482, July 1977.

- [48] A. U. Sheikh, M. Abdi, M. Handforth, "Indoor Mobile Radio Channel at 946 MHz: Measurements and Modelling," in *Proc. IEEE on Vehicular Technology Conference (VTC)*, vol. 93, Secaucus, 1993, pp. 73 – 76.
- [49] M. D. Yacoub, J. E. V. Bautista, L. G. de R. Guedes, "On Higher Order Statistics of the Nakagami-m Distribution," *IEEE Transactions on Vehicular Technology*, vol. 48, no. 3, pp. 790 – 794, May 1999.
- [50] M. Abramowitz, I. A. Stegun. *Handbook of Mathematical Functions with Formulas Graphs, and Mathematical Tables*. New York: Dover, 1972.
- [51] R. Zhang, "On Active Learning and Supervised Transmission of Spectrum Sharing Based Cognitive Radios by Exploiting Hidden Primary Radio Feedback," *IEEE Transactions on Wireless Communications*, vol. 58, pp. 2960 – 2970, October 2010.
- [52] K. Eswaran, M. Gastpar, K. Ramchandran, "Cognitive Radio through Primary Control Feedback," *IEEE Journal on Selected Areas in Communications JSAC*, vol. 29, pp. 384 – 393, 2011.
- [53] C. Shannon, "Communication in the Presence of Noise," *Institute of Radio Engineers (IRE)*, vol. 37, no. 1, pp. 10 – 21, January 1949.
- [54] M. Gastpar, "On Capacity under Received-signal Constraints," in *Proc. 42nd Annual Allerton Conference Communication, Control Computing*, 2004, pp. 1322 – 1331.
- [55] M. Fogiel. *The Handbook of Electrical Engineering, Research and Education Association*. New Jersey, 1996.
- [56] T. Clancy, "Formalizing the Interference Temperature Model," *Wiley journal Wireless Communications and Mobile Computing*, vol. 7, no. 9, pp. 1077 – 1086, November 2007.
- [57] P. J. Kolodzy, "Interference Temperature: A Metric for Dynamic Spectrum Utilization," *International Journal of Network Management*, vol. 16, no. 2, pp. 103 – 113, March 2006.
- [58] A. Ghasemi, E. Sousa, "Fundamental Limits of Spectrum Sharing in Fading

- Environments," *IEEE Transactions Wireless Communications*, vol. 6, no. 2, pp. 649 – 658, February 2007.
- [59] X. Kang, Y. C. Liang, A. Nallanathan, H. K. Garg, R. Zhang, "Optimal Power Allocation for Fading Channels in Cognitive Radio Networks: Ergodic Capacity and Outage Capacity," *IEEE Transactions on Wireless Communications*, vol. 8, no. 2, pp. 940 – 950, February 2009.
- [60] R. Zhang, "On Peak Versus Average Interference Power Constraints for Protecting Primary Users in Cognitive Radio Networks," *IEEE Transactions on Wireless Communications*, vol. 8, no. 4, pp. 2112 – 2120, May 2009.
- [61] X. Kang, R. Zhang, Y. C. Liang, H. K. Garg, "Optimal Power Allocation Strategies for Fading Cognitive Radio Channels with Primary User Outage Constraint," *IEEE Journal on Selected Areas in Communications*, vol. 29, no. 2, pp. 374 – 383, February 2011.
- [62] P. J. Smith, P. A. Dmochowski, H. A. Suraweera, M. Shafi, "The Effects of Limited Channel Knowledge on Cognitive Radio System Capacity," *IEEE Transactions on Vehicular Technology*, vol. 62, pp. 927 – 933, February 2013.
- [63] S. N. Diggavi, N. Al-Dhahir, A. Stamoulis, A. R. Calderbank, "Great Expectations: The Value of Spatial Diversity in Wireless Network," *Proceeding of the IEEE*, vol. 92, pp. 219 – 270, 2004.
- [64] M. K. Simon, M. -S. Alouini. *Digital Communication over Fading Channel: A Unified Approach to Performance Analysis*: John Wiley & Sohn, 2000.
- [65] T. S. Rappaport. *Wireless Communications: Principles and Practice, First textbook on the subject- Chapter 6*. NJ, Upper Saddle River: Prentice-Hall, 1996.
- [66] E. Al-Hussaini, A. Al-Bassiouni, "Performance of MRC Diversity Systems for the Detection of Signals with Nakagami Fading," *IEEE Transactions on Wireless Communications*, vol. 33, no. 12, pp. 1315 – 1319, December 1985.
- [67] R. Duan, M. Elmusrati, R. Jantti, R. Virrankoski, "Capacity for Spectrum Sharing Cognitive Radios with MRC Diversity at The Secondary Receiver under Asymmetric Fading," in *Proc. IEEE Globecom*, 2010.

- [68] M. -S. Alouini, A. Goldsmith, "Capacity of Nakagami Multipath Fading Channels," in *Proc. IEEE Vehicular Technology Conference (VTC)*, Phoenix, USA, 1997, pp. 358 – 362.
- [69] V. Tarokh, H. Jafarkhani, A. R. Calderbank, "Space-Time Block Codes from Orthogonal Designs," *IEEE Transactions Information Theory*, vol. 45, no. 5, pp. 1456 – 1467, July 1999.
- [70] S. M. Alamouti, "A Simple Transmit Diversity Technique for Wireless Communications," *IEEE Journal on Selected Areas of Communications*, vol. 16, no. 8, pp. 1451 – 1458, October 1998.
- [71] G. Ganesan, P. Stoica, "Space-time Diversity using Orthogonal and Amicable Orthogonal Design," *Wireless Personal Communications*, vol. 18, pp. 165 – 178, 2001.
- [72] R. J. Turyn. *Complex Hadamard Matrices, Structure and their Applications*. New York: Gordon and Breach, 1970.
- [73] H. A. Suraweera, J. Gao, P. J. Smith, M. Shafi, M. Faulkner, "Channel Capacity Limits of Cognitive Radio in Asymmetric Fading Environments," in *Proc. IEEE International Conference on Communications (ICC 2008)*, Beijing, China, 2008, pp. 4048 – 4053.
- [74] R. Zhang, "On Peak versus Average Interference Power Constraints for Spectrum Sharing in Cognitive Radio Networks," in *Proc. IEEE DySPAN*, Chicago, 2008, pp. 1 – 5.
- [75] R. Zhang, "Optimal Power Control over Fading Cognitive Radio Channels by Exploiting Primary User CSI," in *Proc. IEEE Global Communications Conference (Globecom)*, 2008.
- [76] Y. Chen, G. Yu, Z. Zhang, H. H. Chen, P. Qiu, "On Cognitive Radio Networks with Opportunistic Power Control Strategies in Fading Channels," *IEEE Transactions on Wireless Communications*, vol. 7, no. 7, pp. 2752 – 2761, July 2008.
- [77] L. Musavian, S. Aissa, "Fundamental Capacity Limits of Cognitive Radio in

- Fading Environments with Imperfect Channel Knowledge," *IEEE Transactions on Wireless Communications*, vol. 57, no. 11, pp. 3472 – 3480, November 2009.
- [78] H. Yang, M. S. Alounini, "Outage Probabiloty of Dual-branch Diversity Systems in Presence of Co-channel Interference," *IEEE Transactions on Wireless Communications*, vol. 2, no. 2, pp. 310 – 319, March 2003.
- [79] G. T. Đorđević, A. Antić, "Outage Probabilitz of Interference-limited Switch and Stay Diversity System over Generalized-k Fading Channels," *Frequenz*, vol. 67, no. 11 – 12, pp. 387 – 392, October 2013.
- [80] A. Panajotivić, N. Sekulović, D. Drača, M. Stefanović, Č Stefanović, "Average Fade Duraqtion of Dual Selection Diversitz over Correlated Unbalanced Nakagami'm Fading Channels in the Presence of Co-channel Interference," *Frequenz*, vol. 67, no. 11-12, p. 393 – 397, October 2013.
- [81] H. A. Suraweera, P. J. Smith, M. Shafi, "Capacity Limits and Performance Analysis of Cognitive Radio with Imperfect Channel Knowledge," *IEEE Transactions on Wireless Communications*, vol. 59, no. 4, pp. 1811 – 1822, May 2010.
- [82] H. Kim, H. Wang, S. Lim, D. Hong, "On the impact of Outdated Channel Information on the Capacity of Secondary User in Spectrum Sharing Environments," *IEEE Transactions on Wireless Communications*, vol. 11, no. 1, pp. 284 – 295, January 2012.
- [83] Y. Y. He, S. Dey, "Power Allocation for Outage Minimization in Cognitive Radio Networks with Limited Feedback," in *Proc. Communication Theory Workshop (AusCTW)*, Australia, 2012, pp. 84 – 89.
- [84] M. R. Mili, K. A. Hamdi, "Minimum BER Analysis in Interference Channels," *IEEE Transactions on Wireless Communications*, vol. 12, no. 7, pp. 3191 – 3200, July 2013.
- [85] J. Jarrouj, V. Blagojević, P. Ivaniš, "Outage Probability of SINR for Underlay Cognitive Radio Systems in Nakagami Fading," *Frequenz*, vol. 68, no. 11, pp. 563 – 572, November 2014.

- [86] V. Blagojević, P. Ivaniš, "Ergodic Capacity of Spectrum Sharing Cognitive Radio with MRC Diversity and Nakagami Fading," in *Proc. IEEE Wireless Communications and Networking Conference*, 2012.
- [87] A. Papoulis. *Probability, random Variables, and Stochastic Processes*. 2nd ed.: McGraw Hill Companz, 1986.
- [88] I. S. Gradshteyn, I. M. Ryzhik. *Table of Integrals, Series and Products*.: Academic Press Inc., 1994.
- [89] A. Ozgr Yilmaz, "Calculating Outage Probability of Block Fading Channels Based on Moment Generating Functions," *IEEE Transactions on Wireless Communications*, vol. 59, no. 11, pp. 2945 – 2950, July 2011.
- [90] M. -S. Alouini, A. J. Goldsmith, "Adaptive Modulation over Nakagami Fading Channels," *Wireless Personal Communications*, vol. 13, no. 1 - 2, pp. 119 – 143, May 2000.
- [91] D. Brennan, "Linear Diversity Combining Techniques," *IEEE*, vol. 91, no. 2, pp. 331 – 356, February 2003.
- [92] M. -S. Alouini, A. Goldsmith, "Capacity of Rayleigh Fading Channels under Different Adaptive Transmission and Diversity Combining," *IEEE Transactions on Vehicular Technology*, vol. 48, no. 4, pp. 1165 –1181, July 1999.
- [93] D. Li, "Performance Analysis of MRC Diversity for Cognitive Radio Systems," *IEEE Transactions on Vehicular Technology*, vol. 61, no. 2, pp. 849 – 853, February 2012.
- [94] A. H. Y. Kong, "Ergodic and Outage Capacity of Interference Temperature-Limited Cognitive Radio Multi-input Multi-output channel," *IET Communications*, vol. 5, no. 5, pp. 652 – 659, April 2011.
- [95] V. Blagojevic, P. Ivanis, "Ergodic Capacity for TAS/MRC Spectrum Sharing Cognitive Radio," *IEEE Communications Letters*, vol. 16, no. 3, pp. 321 – 323, March 2012.
- [96] V. Blagojevic, P. Ivanis, "Ergodic Capacity of Spectrum Sharing System with OSTBC in Nakagami Fading," *IEEE Communications letters*, vol. 16, no. 9, pp.

1500 – 1503, September 2012.

- [97] R. Duan, R. Jantti, M. Elmusrati, R. Virrankoski, "Capacity for Spectrum Sharing Cognitive Radios with MRC Diversity and Imperfect Channel Information from Primary User," in *Proc. IEEE Global Telecommunications Conference (GLOBECOM)*, 2010, pp. 1 – 5.
- [98] A. Shah, A. M. Haimovich, "Performance Analysis of Maximal Ratio Combining and Comparison with Optimum Combining for Mobile Radio Communications with Co-channel Interference," *IEEE Transactions on Vehicular Technology*, vol. 49, no. 4, pp. 1454 – 1463, July 2000.
- [99] J. Cui, A. U. H. Sheikh, "Outage Probability of Cellular Radio Systems Using Maximal Ratio Combining in the Presence of Multiple Interferers," *IEEE Transactions on Wireless Communications*, vol. 47, no. 8, August 2002.
- [100] V. A. Aalo, J. Zhang, "Performance Analysis of Maximal Ratio Combining in the Presence of Multiple Equal-Power Co-channel Interferers in a Nakagami Fading Channel," *IEEE Transactions on Vehicular Technology*, vol. 50, no. 2, pp. 497 – 503, March 2001.
- [101] J. M. Romero-Jerez, J. P. Peña-Martin, A. J. Goldsmith, "Outage Probability of MRC with Arbitrary Power Co-channel Interferers in Nakagami Fading," *IEEE Transactions on Communications*, vol. 55, no. 7, pp. 1283 – 1286, July 2007.
- [102] K. Tourki, K. A. Qaraqe, M. S. Alouini, "Mean Value-Based Power Allocation and Ratio Selection for MIMO Cognitive Radio Systems," in *Proc. IEEE ICC 2013 – Cognitive Radio and Networks Symposium*, Budapest, 2013.
- [103] A. J. Goldsmith, P. P. Varaiya, "Capacity of Fading Channels with Channel Side Information," *IEEE Transactions on Information Theory*, vol. 43, no. 6, pp. 1986 – 1992, September 1997.
- [104] C. –X. Wang, X. Hong, H. –H. Chen, J. Thompson, "On Capacity of Cognitive Radio Networks with Average Interference Power Constraints," *IEEE Transactions on Wireless Communications*, vol. 8, no. 4, pp. 1620 – 1625, April 2009.

- [105] Z. Rezki, M.-S. Alouini, "On the Capacity of Cognitive Radio under Limited Channel State Information," in *Proc. 7th International Symposium on Wireless Communication Systems (ISWCS)*, 2010, pp. 1066 –1070.
- [106] Z. Rezki, M.-S. Alouini, "On the Capacity of Cognitive Radio under Limited Channel State Information over Fading Channels," in *Proc. IEEE International Conference on Communications (ICC)*, 2011, pp. 1 – 5.
- [107] L. Musavian, S. Aissa, "Fundamental Capacity Limits of Spectrum Sharing Channels with Imperfect Feedback," in *Proc. IEEE GLOBECOM*, 2007, pp. 1385 – 1389.
- [108] J. Jarrouj, V. Blagojevic, P. Ivanis, "Outage Probability and Ergodic Capacity of Spectrum-Sharing Systems with MRC Diversity," *Frequenz*, vol.70, no. 11 – 12, pp. 157 – 171, March 2016.
- [109] The Wolfram Functions Site. Internet: <http://functions.wolfram.com>,2008.
- [110] S. B. Weinstein, P. M. Ebert, "Data Transmission by Frequency-Division Multiplexing using the Discrete Fourier Transform," *IEEE Transactions on Wireless Communications*, vol. Com-19, pp. 628 – 634, October 1971.
- [111] ETSI, "Radio Broadcasting System; Audio Broadcasting (DAB) to Mobile, Portable and Fixed Receivers." ETS 300 401, European Telecommunication Standard Institute, Sophia- Antapolis, Valbonne, France, 1995 – 1997.
- [112] ETSI, "Digital Broadcasting System Television, Sound and Data Services Framing Structure, Channel Coding, and Modulation Digital Terrestrial Television," EN 300 744, European Telecommunication Standard Institute, Sophia-Antapolis, Valbonne, France, 1997.
- [113] ETSI-TR, "Broadband Radio Access Networks (BRAN); High Performance Radio Local Area Networks (HIPERLAN) Type 2;System Overview," ETSI-TR 101 683, European Telecommunication Standard Institute, Sophia-Antapolis, Valbonne, France, 1999.
- [114] Y. -H. Peng, Y. -C. Kuo, G. -R. Lee, J. -H. Wen, "Performance Analysis of a New ICI Self-Cancellation-Scheme in OFDM Systems," *IEEE Transactions on*

- Consumer Electronics*, vol. 53, no. 4, pp. 1333 – 1338, December 2007.
- [115] T. A. Weiss, F. K. Jondral, "Spectrum Pooling: an Innovative Strategy for The Enhancement of Spectrum Efficiency," *IEEE Communications Magazine*, vol. 42, no. 3, pp. 8 – 14, March 2004.
- [116] H. Mahmoud, T. Yücek, H. Arslan, "OFDM for Cognitive Radio: Merits and Challenges," *IEEE Wireless Communication*, vol. 16, no. 2, pp. 6 – 14, April 2009.
- [117] S. Ekin, M. M. Abdallah, K. A. Qaraqe, E. Serpedin, "Random Subcarrier Allocation in OFDM-Based Cognitive Radio Networks," *IEEE Transactions on Signal Processing*, vol. 60, no. 9, pp. 4758 – 4774, September 2012.
- [118] L. Tao, H. M. Wai, V. K. N. Lau, S. Manhung, R. S. Cheng, R. D. Murch, "Robust Joint Interference Detection and Decoding for OFDM Based Cognitive Radio Systems with Unknown Interference," *IEEE Journal Selection Areas Communications*, vol. 25, pp. 566 – 575, March 2007.
- [119] S. -G. Huang, C. -H. Hwang, "Improvement of Active Interference Cancellation: Avoidance Technique for OFDM Cognitive Radio," *IEEE Transactions on Wireless Communications*, vol. 8, pp. 5928 – 5937, December 2009.
- [120] K. Son, B. C. Jung, S. Chong, D. K. Sung, "Power Allocation Policies with Full and Partial Inter-System Channel State Information for Cognitive Radio Networks," *Wireless Networks*, vol. 19, no. 1, pp. 99 – 113, January 2013.
- [121] A. Jeremic, T. A. Thomas, "OFDM Channel Estimation in the Presence of Interference," *IEEE Transactions on Signal Processing*, vol. 52, no. 12, December 2004.
- [122] T. Weiss, J. Hillenbrand, A. Krohn, F. Jondral, "Mutual Interference in OFDM-based Spectrum Pooling Systems," in *Proc. Vehicular Technology Conference Spring*, Milan, Italy, 2004, pp. 1873 – 1877.
- [123] FCC, *Report of Spectrum Efficiency Working Group*, DC, USA, Spectrum Policy Task Force, 2002.
- [124] I. F. Akyildiz, W. -Y. Lee, S. Mohanty, "A Survey on Spectrum Management in Cognitive Radio Networks," *IEEE Communication Magazine*, vol. 46, no. 4, pp.

40 – 48, April 2008.

- [125] K. Krishna, "Optimal Power Allocation in OFDM Based Cognitive Radio System," *International Journal of Communication and Media Science (SSRG-IJCMS)*, vol. 1, no. 2, pp. 14 – 18, October 2014.
- [126] Y. Zhang, C. Leung, "Resource Allocation in an OFDM-Based Cognitive Radio System," *IEEE Transactions on Wireless Communications*, vol. 57, pp. 1928 – 1931, July 2009.
- [127] C. Zhao, K. Kwak, "Power/bit Loading in OFDM-Based Cognitive Networks with Comprehensive Interference Considerations: the Single-SU Case," *IEEE Transactions on Vehical Technology*, vol. 59, p. 1910 –1922, April 2010.
- [128] M. Morelli, M. Moretti, "Robust Frequency Synchronization for OFDM-based Cognitive Radio Systems," *IEEE Transactions on Wireless Communications*, vol. 7, pp. 5346 – 5355, December 2008.
- [129] C.-H. Hwang, G.-L. Lai, S.-C. Chen, "Spectrum Sensing in Wideband OFDM Cognitive Radios," *IEEE Transactions on Signal Processing*, vol. 58, pp. 709 - 719, February 2010.
- [130] E. Axell, E. G. Larsson, "Optimal and Sub-optimal Spectrum Sensing of OFDM Signals in Known and Unknown Noise Variance," *IEEE Journal Selection Areas Communications*, vol. 29, pp. 290 – 304, February 2011.
- [131] S. Chaudhari, V. Koivunen, H. V. Poor, "Autocorrelation-based Decentralized Sequential Detection of OFDM Signals in Cognitive Radios," *IEEE Transactions on Signal Process*, vol. 57, pp. 2690 – 2700, July 2009.
- [132] J. Lundén, V. Koivunen, A. Huttunen, H. V. Poor, "Collaborative Cyclostationary Spectrum Sensing for Cognitive Radio Systems," *IEEE Transactions on Signal Process*, vol. 13, pp. 4182 – 4195, November 2009.
- [133] R. W. Chang, "Synthesis of Band-Limited Orthogonal Signals for Multichannel Data Transmission," *Bell System Technology Journal*, vol. 45, pp. 1775 – 1796, December 1966.
- [134] B. R. Salzberg, "Performance of an Efficient Parallel Data Transmission," *IEEE*

Transactions on Communication Technology, vol. Com-15, pp. 805 – 813, December 1967.

- [135] White Paper: High-speed Wireless OFDM Communication Systems, Wi-LAN Inc., February 2001.
- [136] CommsDesign. "Enabling Fast Wireless Networks with OFDM." Internet: <http://www.commsdesign.com/story/OEG20010122S0078>, May 2003.
- [137] M. Rawat, S. Aggarwal, K. S. Gaur, "ICI Self Cancellation Scheme for OFDM System," in *Proc. International Conference on Advanced Computing, Communication and Networks*, 2011.
- [138] S. Kaur, C. Singh, A. S. Sappal, "Inter Carrier Interference Cancellation in OFDM System," *International Journal of Engineering Research and Applications (IJERA)*, vol. 2, no. 3, pp. 2272 – 2275, June 2012.
- [139] G. Foschini, G. Vannucci, "Characterizing Filtered Light Waves Corrupted by Phase Noise," *IEEE Transactions on Information Theory*, vol. 34, pp. 1437 – 1448, November 1988.
- [140] M. V. B. T. Pollet, M. Moeneclaey, "BER Sensitivity of OFDM Systems to Carrier Frequency Offset and Wiener Phase Noise," *IEEE Transactions on Communications*, vol. 43, pp. 192 – 193, February 1995.
- [141] L. Tomba, "On the Effect of Wiener Phase Noise in OFDM Systems," *IEEE Transactions on Communications*, vol. 46, pp. 580 – 583, May 1988.
- [142] A. Bahai, B. Saltzberg. *Multi-carrier Digital Communications, Theory and Application of OFDM*. Kluwer Academic: Plenum Publisher, 1999.
- [143] M. W. Green, "Dynamic Spectrum Sensing by Multiband OFDM Radio for Interference Mitigation," in *Proc. First IEEE International Symposium on DySPAN 2005*, 2005, pp. 619 – 625.
- [144] T. Weiss, J. Hillenbrand, F. Jondral, "A Diversity Approach for The Detection of Idle Spectral Resources in Spectrum Pooling Systems," in *Proc. 48th International Scientific Colloquium*, Ilmenau, Germany, 2003.

- [145] D. M. Dramicanin, D. Rakic, S. Denic, V. Vlahovic, "FPGA-based Prototyping of IEEE 802.11a Baseband Processor," *Serbian Journal Electrical Engineering*, vol. 1, no. 3, pp. 125 – 136, November 2004.
- [146] V. V. Patcha. "Experimental Study of Cognitive Radio Test-bed using USRP." Thesis, B. TECH in Electronics and Communication Engineering Padmasri Institute of Technology, India, 2011.
- [147] A. Jain, V. Sharma, B. Amrutur, "Soft Real Time Implementation of a Cognitive Radio Testbed for Frequency Hopping Primary Satisfying QoS Requirements," in *Proc. Twentieth National Conference on Communications*, Kanpur, India, 2014.
- [148] M. Janjic, M. Brkovic, M. Eric, "Development of OFDM based Secondary Link: Some Experimental Results on USRP N210 Platform," *TELFOR Journal*, vol. 6, no. 1, pp. 30 – 35, 2014.
- [149] Open source gnu-radio. [Online]. <http://gnuradio.org/>
- [150] M. Ettus, *USRP User's and Developer's Guide.*: Ettus Research.
- [151] F. A. Hamza, "The USRP under 1.5X Magnifying lens," in *Proc. GNU Radio Community*, 2008.
- [152] M. A. Marwanto, M. A. Sarijari, N. Fisal, S. K. S. Yusof, R. A. Rashid, "Experimental Study of OFDM Implementation Utilizing GNU Radio and USRP - SDR," in *Proc. IEEE 9th Malaysia International Conference on Communications*, Kuala Lumpur, Malaysia, 2009, pp. 15 – 19.
- [153] P. G. Lin, "OFDM Simulation in Matlab," Bachelor, California Polytechnic State University, San Luis Obispo, 2010.